A Comparative Study of Different Redox Additive Based Gel Polymer Electrolyte for Supercapacitor Application

A thesis submitted towards partial fulfilment

of the requirements for the degree of

Master of Technology in

Nano Science and Technology

Submitted by

Ankita Saha

Roll No: 002230701013

Exam Roll No: M4NST24011

Registration No.: 163814 of 2022-2023

Under the guidance of

Prof. (Dr.) Kalyan Kumar Chattopadhyay

Department of Physics &

School of Materials Science and Nanotechnology

Jadavpur University

Jadavpur University

Kolkata-700032

India

2024

CERTIFICATE OF RECOMMENDATION

This is to clarify that the thesis entitled **"A Comparative Study of Different Redox Additive based Gel Polymer Electrolyte for Supercapacitor Application"** is a bonafide work carried out by ANKITA SAHA under our supervision and guidance for partial fulfilment of the requirement of Master of Technology (Nano Science and Technology) in School of Materials Science and Nanotechnology, during the academic session 2022-2024.

SUPERVISOR
Prof. (Dr.) Kalyan Kumar Chattopadhyay
Department of Physics
Jadavpur University, Kolkata-700032

DIRECTOR
Dr. Mahua Ghosh Chaudhuri
School of Materials Science and
Nanotechnology Jadavpur University,
Kolkata-700032

DEAN
Faculty Council of Interdisciplinary Studies,
Law and Management (FISLM)
Jadavpur University, Kolkata-700032

CERTIFICATE OF APPROVAL **

This forgoing thesis is hereby approved as a credible study of an engineering subject carried out and presented in a manner satisfactorily to warranty its acceptance as a prerequisite to the degree for which it has been submitted. It is understood that by this approval the undersigned do not endorse or approve any statement made or opinion expressed or conclusion drawn therein but approve the thesis only for purpose for which it has been submitted.

Committee of final examination for evaluation of thesis

** Only in case the thesis is approved.

ACKNOWLEDGEMENT

In the first place, I would like to express my profound gratitude to my supervisor **Prof (Dr). Kalyan Kumar Chattopadhyay** for his advice and guidance from the very early stage of this research as well as giving me extraordinary experiences throughout the work. Above all and the most needed, he provided me constant encouragement and support in various ways. Thankyou also for the amicable environment conducive to extensive research work at Thin Film and Nanoscience Lab, in which you have welcomed me. All these provided me great support, helping me to confront the difficult periods of my project, which I do not think I would have completed it otherwise.

I want to extend my gratitude to my co-supervisor **Dr. Pulak Pal** (SERB-National Postdoctoral fellow, Jadavpur University) for his advices, guidance, and crucial contribution throughout my work. His involvement with his originality has triggered and nurtured my scholarly development that I will benefit from, for along time to come. I really cannot value his support and generous cooperation. He has been like an elder brother to me always by my side whenever needed him.

I would also like to express my sincere thanks to Dr. Mahua Ghosh Chowdhury, Prof. C.K. Ghosh, Prof. Sourav Sarkar for their help, support, encouragement, suggestion and advice during the course of the research. Their enthusiasm provided me a helpful and effective way of learning which in turn inspired me to follow the research project with great enthusiasm.

I would also really like to thank all the staff members of School of Materials Science and Nanotechnology and Department of Physics for carrying out the critical characterization parts of the synthesized samples that composed a very important part of the thesis.

I extend my heartiest thanks to all my seniors of 'Thin Film & Nano Science' lab especially, Suvankar da, Manash da, Nabanita di, Moumita di, Souvik da, Riaz da, Dimitra di, Ratna di, and everyone in this lab for extending their helping hands. I would also like to thank all my friends Aritra Mukherjee, Kingshuk Chakrabarty, Prasenjit Sarkar, and all of them for their encouragement and cooperation. Finally, I express my special gratitude to my parents and all my well-wishers for their wholehearted support, love and encouragement.

ABSTRACT

This study describes the fabrication oh high energy density supercapacitors (SCs) employing activated carbon (AC) electrodes and gel polymer electrolytes (GPEs) based on redox additives. Adiponitrile was used as a plasticizer, 1-Butyl-3-methylimidazolium bis-(trifluoromethylsulfonyl)imide (BMIMTFSI) as an ionic liquid (IL), potassium Iodide (KI), Caesium Iodide (CsI), and rubidium iodide (RbI) as redox additives, and poly(vinylidene fluoride-co-hexafluoropropylene) as the host polymer to create the GPEs.

The amorphous character of the host polymer matrix was increased by plasticizers, redox additives, and ILs, according to the microstructural studies. Up to about 200 °C, the GPEs remained thermally stable. The redox additive-based GPE-KI has an electrochemical potential window of 6.38 V and an electrical conductivity of 3.3×10^{-3} S cm^{-1} at ambient temperature. Electrochemical impedance spectroscopy, galvanostatic charge-discharge, and cyclic voltammetry were used to examine the electrochemical performance of the SCs made with the dual redox additive-based GPEs and AC electrodes. Good cyclic performance was also demonstrated by the redox additive-based GPEs in specific capacitance, with an initial 34% fading and a about 100% sustained Coulombic efficiency over 5000 cycles.

CONTENTS

Topic	Page Number
Introduction and Objective	7-31
Review of Past work	32-42
Instruments and Apparatus	43-64
Sample Preparation and Fabrication	65-70
Characterization Results and Discussion	71-101
Conclusion & Future scope of work	102-104

CHAPTER 1:

INTRODUCTION AND OBJECTIVE

INTRODUCTION

The study of energy storage materials is a burgeoning area of research with significant implications for the development of electrochemical charge storage devices, including batteries and supercapacitors (SCs). While it has been observed that batteries typically have lower output power and shorter cycling times, SCs are known for their high-power density, long cycle life, and excellent intrinsic safety, among other advantages. SCs can store charge through electrostatic means (capacitive, non-Faradaic) or through electrochemical charge transfer mechanisms (Faradaic). The low energy density of SCs (<10 W h kg^{-1}) is one of its main disadvantages. The charge storage process is dependent on the electrolytes and electrode materials, and the specific capacity is one of those factors. Numerous scientists worked with a variety of electrode materials, including conducting polymers, transition-metal oxides and sulfurides, carbon nanotubes and graphene, activated carbon (AC), and so on. The huge surface area, regulated porosity, chemical inertness, and high charge-discharge rate of the AC-based electrode are its numerous advantages. Selecting appropriate electrolytes is crucial for creating supercapacitors with elevated energy densities. Because of their benefits, including high ionic conductivity and superior interfacial stability, liquid electrolytes are employed in SCs. These electrolytes do, however, have a number of drawbacks, including corrosion, leakage, hefty weight, and a small electrochemical stability window. Ionic liquids (ILs) are getting a lot of interest these days as novel electrolytes or electrolyte components because of their large potential stability window, nonvolatility, and high ionic conductivity. A good substitute for the liquid electrolyte is an IL-incorporated solid or gel polymer electrolyte (GPE). Similar to this, adiponitrile (ADN), a significant member of the aliphatic dinitrile group, has drawn a lot of interest lately as a plasticizer for lithium-ion batteries and SC electrolytes because of its unique electrochemical properties, high boiling point, low vapor pressure, strong ion salvation power, superior thermal stability, and low cost. The GPEs possess several significant attributes, including excellent thermal stability, strong electrochemical stability, high ionic conductivity (>10−3 S cm−1), flexibility, and so forth. Nevertheless, poor specific capacitance and low energy density are problems for the GPE-based SCs. A variety of techniques have been used to produce SCs with a high energy density. The successful technique of adding redox materials to GPEs is one that has been used recently. Both the specific capacitance and the energy density of the SCs are increased by the ion dissociation of redox additives at the electrode-electrolyte interface. Within the working potential ranges, the appropriate redox additives also improve the cathodic and anodic capacitance of the SCs. Several redox additives, such as potassium iodide (KI), rubidium iodide (RbI), and caesium iodide (CsI), are utilized in both aqueous and nonaqueous systems. Some improvements have been made to the redox added electrolytes previously stated, such as improved heat stability and an expanded electrochemical stability window of 6.8 V. Additionally, it has been stated that the main

components of the SCs are improved by the addition of ionic liquid (BMIMTFSI). Redox additives' ability to increase the electrochemical stability of electrolytes is therefore a current area of study.

In order to create symmetrical SCs with a high energy density, we have prepared highly ion conductive GPEs incorporating redox actives in this paper. The host polymer matrix for the GPEs was poly(vinylidene fluoride-co-hexafluoropropylene) P(Vdf-HFP), with ADN serving as a plasticizer, 1-Butyl-3-methylimidazolium bis(trifluoromethylsulfonyl)imide (BMIMTFSI) as an IL, and redox additives such as potassium, caesium, and rubidium. These electrolytes' ionic conductivity, thermal, structural, and microstructural characteristics, as well as their electrochemical stability and comparative analysis of various redox additives, were examined. The synthetic electrolytes and AC electrodes used to create the SCs gave them a long cycle life, high specific capacitance, and energy density.

NANOSCIENCE AND TECHNOLOGY

The study, engineering, and manipulation of matter, particles, and structures at the nanoscale—one millionth of a millimetre, or the scale of atoms and molecules—is referred to as nanoscience. The way that molecules and atoms come together to form larger structures on the nanoscale determines important features of materials, including their electrical, optical, thermal, and mechanical properties. Furthermore, because quantum mechanical effects become significant, these features are frequently different in nanoscale size structures than they are on the macroscale.
The application of nanoscience to create novel nanomaterials and nanoscale components for practical goods is known as nanotechnology. In the future, nanotechnology will enable us to create novel, upgraded materials and goods, as well as new nanoelectronics components, "smart" medications, sensors, and even interfaces between biological systems and electronics.

These relatively emerging fields of study are at the crossroads of materials science, biochemistry, microelectronics, physics, and biotechnology. A scientific education that is both academic and multidisciplinary is thus necessary for control over various areas.

In contemporary research, nanoscience and nanotechnology are at the forefront. Experts with exceptional knowledge of nanoscience and the ability to apply that knowledge to new products are needed in this rapidly expanding field due to the economy. In order to supply industry and research institutions with top-notch experts who are both specialists in their own field and have a general background in various subdisciplines like electronics, physics, chemistry, material science, and

biotechnology, a multidisciplinary scientific education is essential. This is what the master's program has to offer.

The Master of Nanoscience and Nanotechnology program teaches you the fundamentals of physics, biology, and chemistry at the nanoscale scale. To help you grasp real-world applications, we will also take courses in technology and engineering. Additionally, you will have the option to specialize in a particular field of nanoscience within the curriculum. The philosophy of the EMM-Nano+ program is based on the combination of a strong multidisciplinary scientific foundation with an individual high-level specialization in a particular area of nanoscience.

Electrochemical Storage Devices

The study of energy storage devices is a dynamic area that includes research on capacitors, supercapacitors, and batteries, among other technologies. Researchers study materials, structures, and workings to improve energy density, longevity, and effectiveness. Studies look into developments in solid state batteries, lithium-ion batteries, EDLC, etc. Reactants are enclosed within containers for energy storage devices, while oxidant and reductant are supplied into electrochemical cells for energy conversion devices to produce a continuous electrical flow. Supercapacitors and rechargeable lithium-ion batteries are two types of energy storage devices.

To get a broad understanding of these devices, it is necessary to analyze the mapping of power density as a function of energy density (Ragone plot). Electrochemical double layer supercapacitors allow the user to achieve very high output current in a very short amount of time. To have a better grasp of these devices' capabilities, a brief explanation of their construction and operation is necessary.

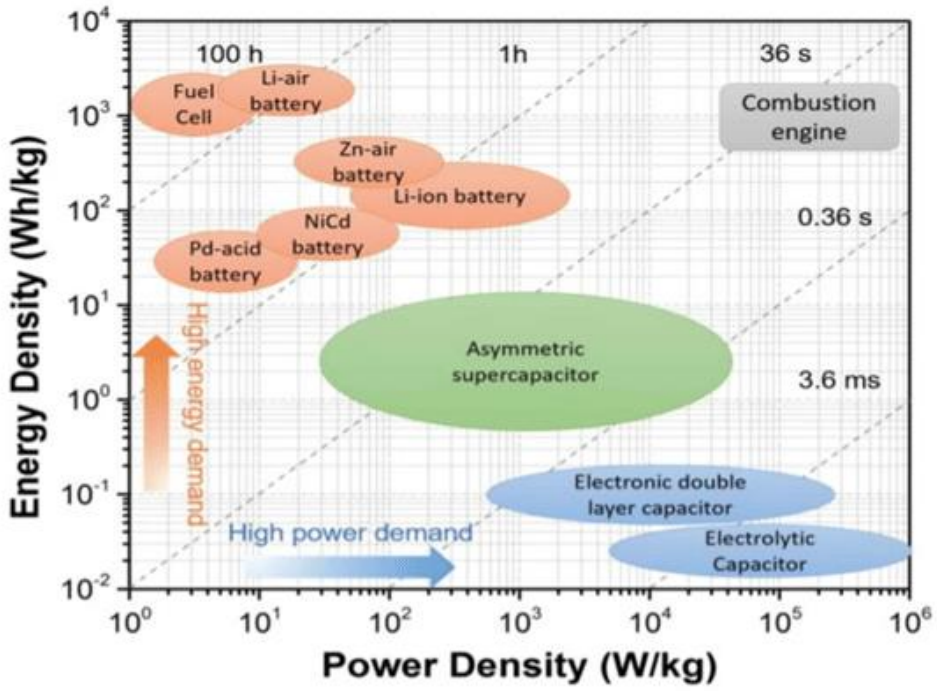


Fig 1.1 A comparison of the power and energy densities of several electrochemical energy storage and conversion systems is shown by a Ragone plot.

Supercapacitor

Supercapacitors, also known as ultracapacitors or electrochemical capacitors, are advanced energy storage devices that store electrical energy via electrostatic charge accumulation at the electrode-electrolyte interface. Unlike conventional capacitors, which store energy through the separation of electric charges on opposing electrodes, supercapacitors utilize a high-surface-area porous electrode material and an electrolyte to achieve a large electrochemical interface area, allowing for the rapid storage and release of energy. Supercapacitors offer several advantages over traditional energy storage technologies, including high power density, rapid charge and discharge rates, long cycle life, and wide operating temperature ranges. These characteristics make them well-suited for applications requiring frequent cycling, high-power bursts, and fast response times, such as regenerative braking systems in vehicles, peak power shaving in industrial applications, and grid stabilization in renewable energy systems.

However, supercapacitors typically have lower energy density than batteries, limiting their use in applications requiring long-term energy storage. Research in the field focuses on improving energy density, enhancing cycling stability, reducing internal resistance, and exploring new materials and fabrication techniques to further advance the performance and versatility of supercapacitors.

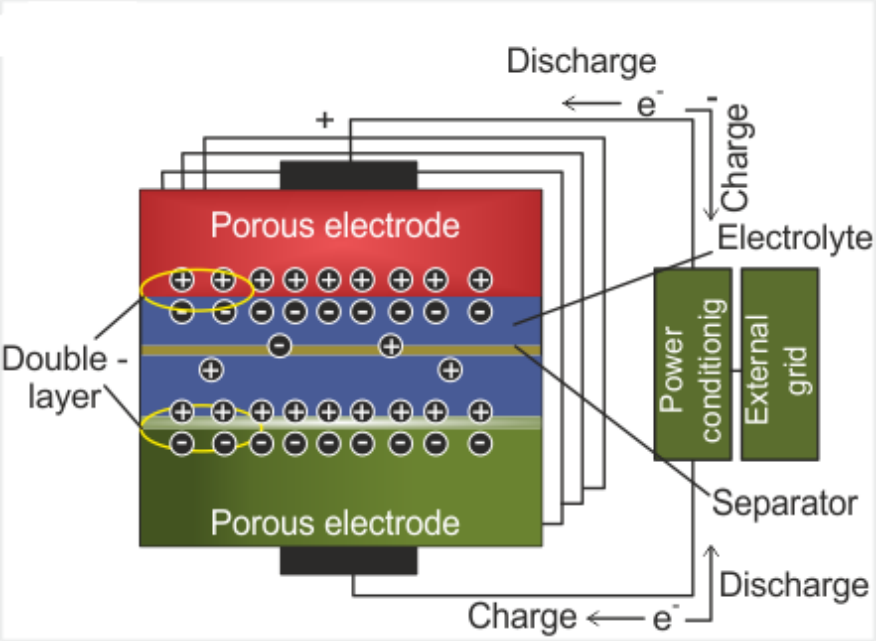


Fig 1.2 Supercapacitor

Electrochemical Double-Layer Capacitor (EDLC)

This capacitor employs the charge storage mechanism, which involves physically storing a charge on the surface of the electrodes without causing any irreversible chemical processes by establishing an electrical double layer. Carbon-based electrodes are often used in supercapacitors; they are separated by a dielectric substance that acts as an insulator and has electrical properties that affect the supercapacitor's performance. Charges are retained electrostatically in supercapacitors. When a voltage is applied to the terminals of each electrolyte, an electric field is created, causing the electrolyte to polarize. As a result, ions with opposing charges seep through the dielectric and into the porous electrodes. As a result, each electrode creates an electric double layer. This enhances each electrode's surface area while minimizing their distance.

Some properties of Supercapacitors are Listed in the points below:

- Supercapacitors have a lengthy cycling duration and a high cycle efficiency (84-97%), which is one of its most essential qualities.
- Supercapacitors have capacitance ranging from 1 mF over 10 kF
- Supercapacitors offer an impressive energy density of up to 10 Wh/kg.
- Supercapacitors have a lower potential for pollution because no heavy metals are employed in their creation.
- Supercapacitors have charge/discharge times that range from milliseconds to many seconds.
- Supercapacitors have a service life of around 10-15 years.

- Supercapacitors are chosen over batteries and regular capacitors due to their larger capacitance and lower voltage restrictions.

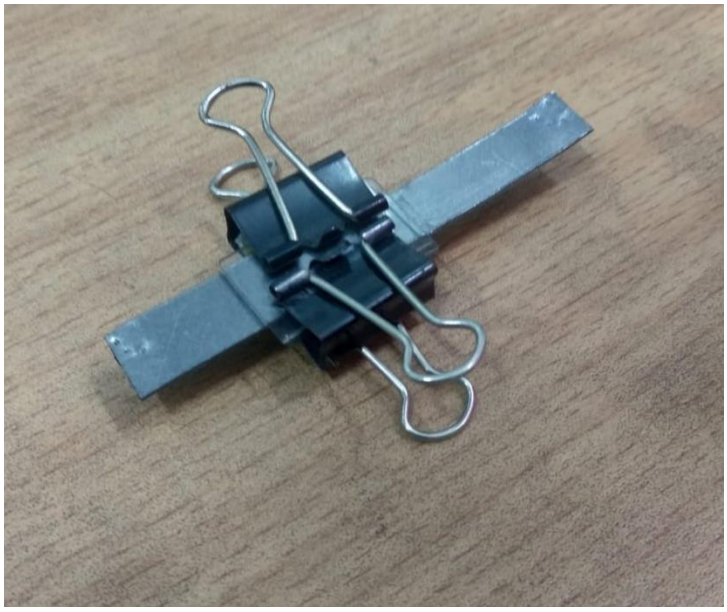


Fig 1.3 EDL Capacitor

Working Principle of Supercapacitor

A supercapacitor stores electrical energy between two electrostatic double layers formed by tiny charge layers at the electrolyte-electrode interface. A supercapacitor can store a large amount of charge value because its capacitance value is always directly proportional to the surface area of its conduction plates, which in this case is quite large. Furthermore, the amount of capacitance is inversely related to the distance between the plates, which is substantially less in supercapacitors than in conventional capacitors.

The porous materials or nanomaterials used to coat the metal plates of a supercapacitor are commonly activated charcoal. Static electricity, or electrostatics, is utilized to store energy in capacitors. The electrolyte solution between the supercapacitor's two plates produces both positively and negatively charged ions.

When a voltage is applied to the supercapacitor's plates, one plate produces a positive charge while the other plate develops a negative charge. This draws negatively charged ions in the electrolyte to the positively charged plate, and positively charged ions to the negatively charged plate. On the inner surface of both plates, a thin layer of ions is formed. This causes the formation of an electrostatic double layer, comparable to connecting two capacitors in series. Each charge has a high capacitance because the distance between the resulting capacitors is very small and the electrode surface is large.

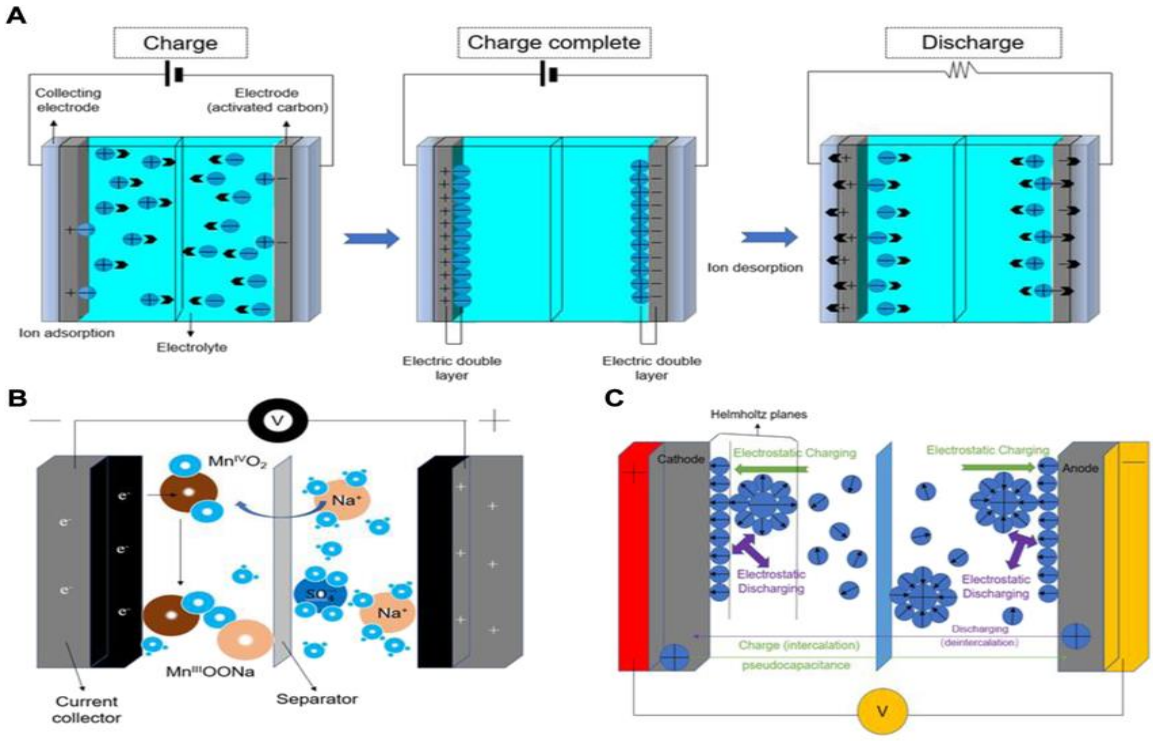
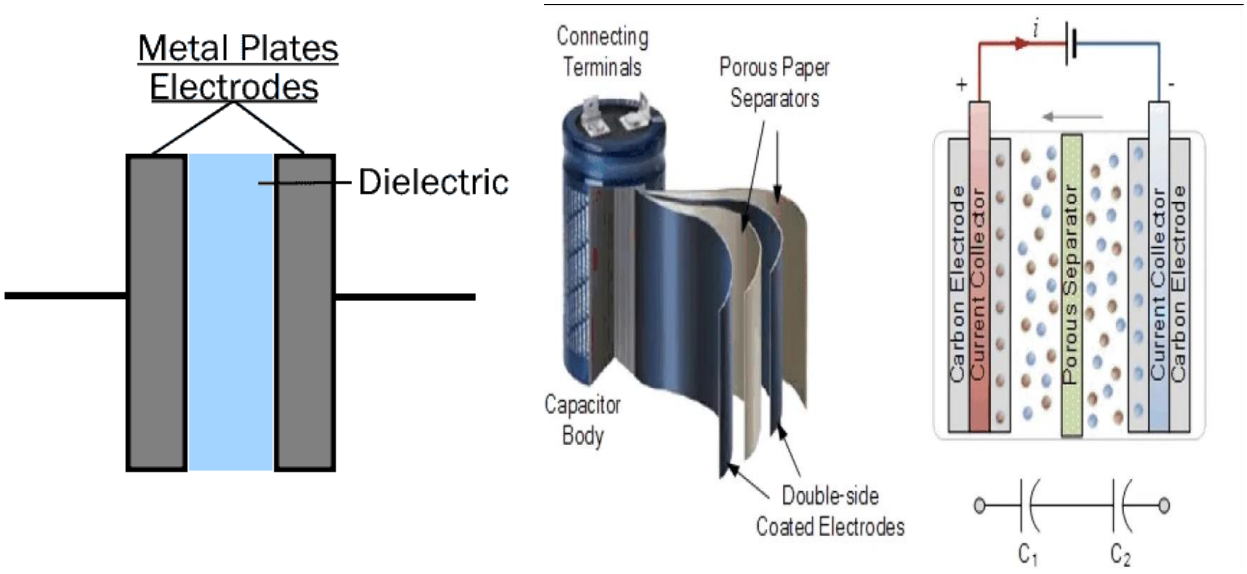


Fig 1.4 Taxonomy of Supercapacitor

Capacitor and Supercapacitor

A supercapacitor, also referred to as an ultracapacitor or double-layer capacitor, stands out from conventional capacitors with significantly increased capacity, energy density, and power density. These qualities make it an ideal power source for high-power devices requiring robust energy storage. Unlike regular capacitors, supercapacitors store energy in the electric field between two conductive electrodes. They can store and release electrical charge as needed, allowing the passage of AC while blocking DC. Thanks to carbon technology, supercapacitors boast a vast surface area even with minimal electrode separation, enabling continuous charging and discharging.



(i) Capacitor *(ii) Supercapacitor*

Fig 1.5(i) Capacitor (ii) Supercapacitor

Advantages of Supercapacitor

- High Efficiency
- High energy and power density because it employs activated carbon material, which enhances the capacitance value.
- High-performance dependability with faster charging rates
- Supercapacitors may readily be coupled in series, like batteries, to give higher voltages utilized in power-demanding equipment.
- Supercapacitors have high specific power and low resistance, allowing them to generate large load currents.
- Supercapacitors are produced in tiny sizes and lightweight, making them easy to install in limited places.
- Supercapacitors have a longer cycle time than batteries and a better service life.

Disadvantages of Supercapacitor

- Supercapacitors have significant self-discharge rates.
- Supercapacitors have limited voltage limitations and require serial connections to generate high voltage.
- Supercapacitors have the greatest dielectric absorption rate of any capacitor.
- The entire energy spectrum cannot be exploited due to the linear discharge of voltage.

Uses Of Supercapacitor

- Supercapacitors are utilized in hybrid buses to extend battery life while reducing size.
- Supercapacitors are becoming increasingly popular in energy-efficient applications, and they are being used in automobiles to offer stored energy in a matter of seconds.
- Supercapacitors are used in the development of memory devices such as laptop computers, cell phones, and tablets. These are also utilized in LED Flash devices.
- Supercapacitors are also employed in renewable energy applications, such as wind energy, to power blade pitch control.
- Supercapacitors are widely employed in a variety of applications, including industry, military, medicine, transportation, and music.

Polymer Electrolytes

Polymer electrolytes play a crucial role in various electrochemical devices, including batteries, fuel cells, and supercapacitors. These materials typically consist of a polymer matrix, a lithium salt as the electrolyte, and sometimes additives like plasticizers or fillers. They serve as ion-conducting mediums that enable the transport of ions between the electrodes while preventing electronic conduction. One common type of polymer electrolyte is the gel polymer electrolyte (GPE), which combines the advantages of both solid and liquid electrolytes. GPEs offer flexibility, ease of processing, and improved safety compared to traditional liquid electrolytes, while maintaining sufficient ionic conductivity for practical applications. The polymer matrix in GPEs is often a polymer such as polyethylene oxide (PEO), polyvinylidene fluoride (PVDF), or polyacrylonitrile (PAN). These polymers provide mechanical support and help retain the electrolyte within the device. The lithium salt, such as lithium perchlorate ($LiClO_4$) or lithium hexafluorophosphate ($LiPF_6$), dissociates into lithium ions (Li+) and counterions when dissolved in the polymer matrix, facilitating ion conduction. Additives like plasticizers are sometimes incorporated into GPEs to improve flexibility, enhance ion mobility, and increase the overall performance of the electrolyte. Plasticizers, such as nitrile group-containing compounds, can help reduce the crystallinity of the polymer matrix, thereby improving ion transport properties. The development of efficient polymer electrolytes, including GPEs, is crucial for advancing the performance and safety of electrochemical devices, particularly in emerging technologies such as electric vehicles and grid-scale energy storage systems. Researchers continue to explore new polymer compositions, electrolyte formulations, and processing techniques to further optimize the properties of polymer electrolytes for various applications.

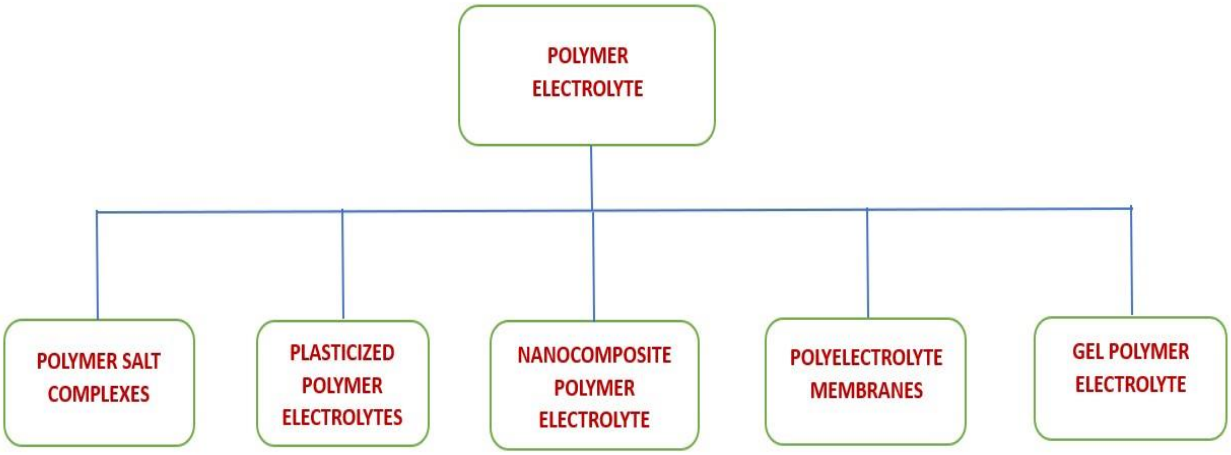


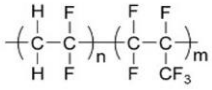
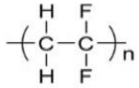
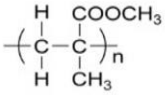
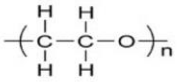
Fig 1.6 Polymer Electrolyte Classification according to Component and Structure

Polymer Matrix

A polymer matrix refers to the continuous phase in a composite material where one or more types of polymers serve as the binding or structural component. In composite materials, the polymer matrix acts as a host or medium in which reinforcing materials, such as fibres or particles, are dispersed. Polymer matrix composites are widely used in various industries due to their desirable properties, including high strength-to-weight ratio, corrosion resistance, and tailored mechanical properties. The choice of polymer matrix depends on factors such as the intended application, required mechanical properties, processing methods, and environmental considerations. Common polymers used as matrices in composite materials include epoxy resins, polyester resins, vinyl ester resins, thermoplastics like polyethylene, polypropylene, and engineering thermoplastics such as polyetheretherketone (PEEK) and polyphenylene sulphide (PPS). The properties of the polymer matrix, such as its stiffness, toughness, thermal stability, and chemical resistance, significantly influence the overall performance and behaviour of the composite material. Therefore, selecting the appropriate polymer matrix is crucial in designing composites with specific functional requirements for various applications ranging from aerospace and automotive to construction and consumer goods.

P(Vdf-HFP) as host polymer matrix - P(Vdf-HFP) copolymer is commonly used to make gel polymer electrolytes due to its high dielectric, mechanical properties supported by P(Vdf) crystalline part, and liquid electrolyte trapping ability assisted by P(HFP) amorphous part.



Molecular Formula	Polymer Matrix
	**P(VdF-HFP)** Poly (vinylidene-fluoride- hexafluoropropylene)
	**PVdF** Poly(vinylidene-fluoride)
	**PMMA** Poly (methyl methacrylate)
	**PEO** Poly (ethylene oxide)

(i) P(Vdf – HFP) *(ii) Polymer matrix and its composition*

Fig 1.7(i) P(Vdf – HFP) (ii) Polymer matrix and its composition

Poly(vinylidene fluoride-co-hexafluoropropylene) P(VDF-HFP)

P(VDF-HFP) stands for poly (vinylidene fluoride-co-hexafluoropropylene), which is a copolymer composed of vinylidene fluoride (VDF) and hexafluoropropylene (HFP) monomer units. This copolymer is widely used in various applications, including membranes for lithium-ion batteries, piezoelectric devices, sensors, coatings, and biomedical materials.

The incorporation of hexafluoropropylene into the vinylidene fluoride backbone alters the properties of the resulting copolymer compared to pure polyvinylidene fluoride (PVDF). Specifically, P(VDF-HFP) copolymers typically exhibit improved flexibility, thermal stability, and processability, making them suitable for applications where these properties are desirable.

In the context of Supercapacitor & lithium-ion batteries, P(VDF-HFP) is often used as a binder material in the electrode fabrication process and as a polymer matrix in gel polymer electrolytes (GPEs). In GPEs, P(VDF-HFP) provides mechanical support to retain the liquid electrolyte while enabling ion conduction through the polymer matrix. The presence of hexafluoropropylene units enhances the compatibility of the copolymer with lithium salts and electrolyte solvents, resulting in improved electrolyte stability and ion transport properties.

Overall, P(VDF-HFP) copolymers offer a balance of properties that make them valuable materials in various technological applications, particularly in energy storage and conversion devices like Supercapacitor and lithium-ion batteries.

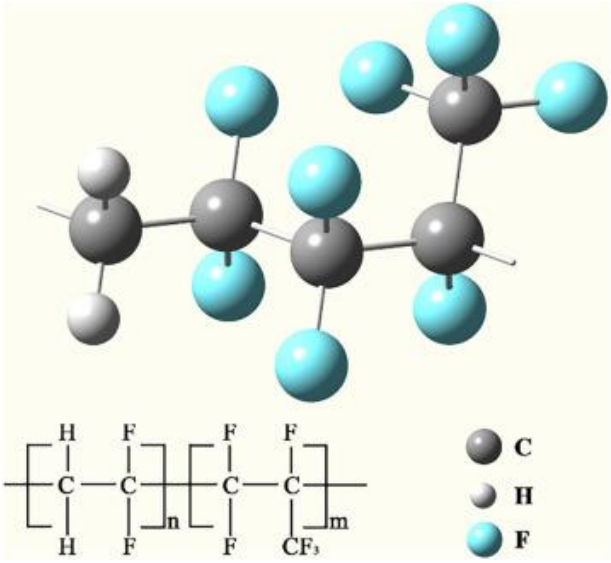


Fig 1.8 3D Structure of P(Vdf – HFP)

Poly(vinylidene fluoride) P(VDF)

P(VDF) refers to polyvinylidene fluoride, a thermoplastic polymer known for its exceptional properties. It's extensively utilized in various applications due to its chemical resistance, thermal stability, and piezoelectric behaviour. P(VDF) finds use in diverse fields such as sensors, filtration membranes, battery separators, coatings, and biomedical materials.

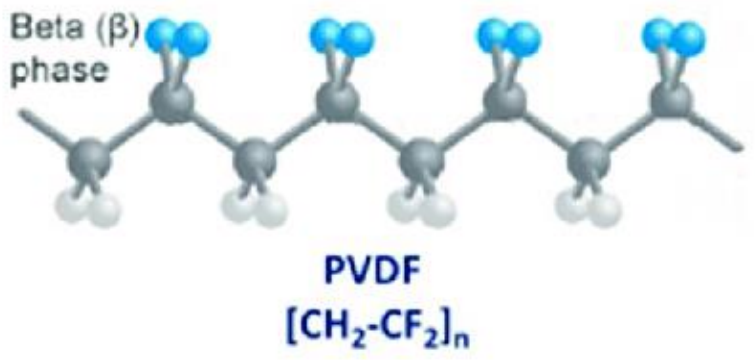


Fig 1.9 Structural Configuration of PVDF

Solvents

Solvents are substances capable of dissolving other substances to form a solution. They are typically liquids, although some gases and solids can also act as solvents under certain conditions. Solvents play a crucial role in a wide range of applications, including chemical synthesis, industrial processes, cleaning, and extraction.

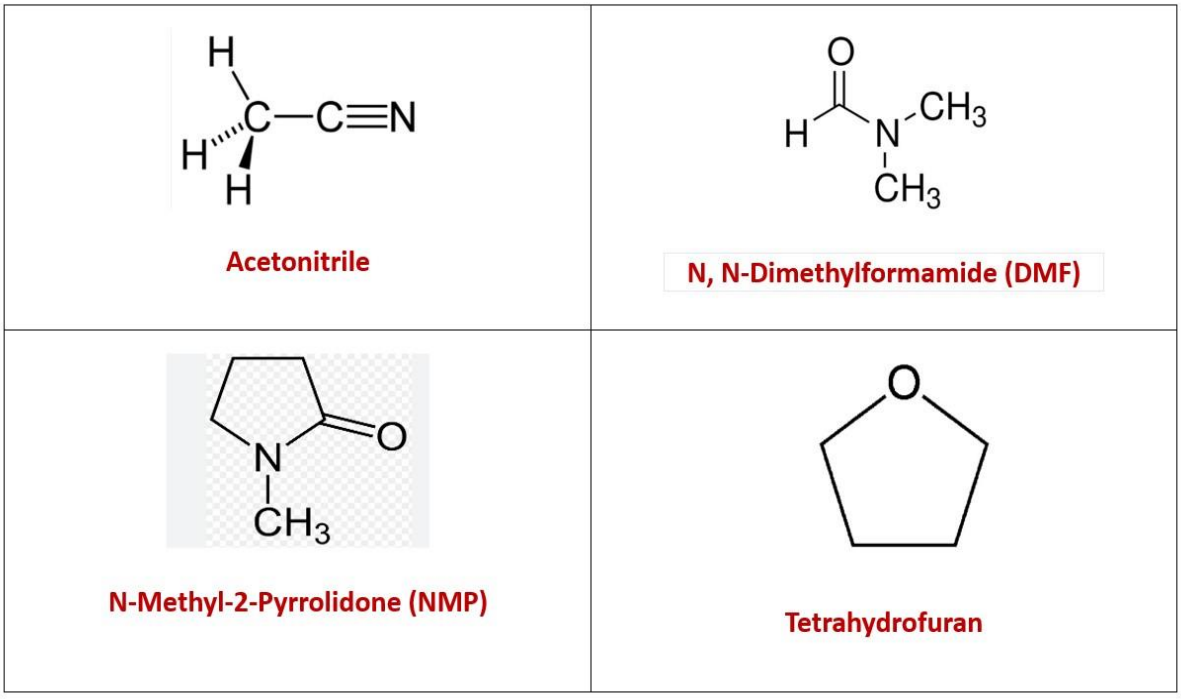


Fig 1.10 Structure of a few typical solvents.

In a solvent, molecules are in constant motion and interact with solute molecules, surrounding and dispersing them evenly throughout the solvent volume. This process occurs due to the attractive forces between solvent and solute molecules, which overcome the intermolecular forces holding solute molecules together. The ability of a solvent to dissolve a particular solute depends on factors such as the polarity, size, and chemical compatibility of the solvent and solute molecules.

Solvents can be classified based on various criteria, including polarity, volatility, and chemical composition. Polar solvents, such as water, ethanol, and acetone, have molecules with uneven distributions of charge and can dissolve polar solutes like salts and sugars. Nonpolar solvents, such as hexane and benzene, have molecules with relatively uniform charge distributions and are effective at dissolving nonpolar solutes like oils and greases. Commonly used solvents are organic solvents such as acetonitrile (ACN), tetrahydrofuran (THF), acetone, chloroform, toluene, N, N-Dimethyl

methanamide (DMF), N-Methyl-2 pyrrolidone (NMP), etc. Solvents depend on the host polymer matrix.

Some solvents are considered universal solvents because they can dissolve a wide range of solutes, while others are more specialized and suitable for specific applications. The choice of solvent depends on factors such as the nature of the solute, desired solubility, reaction conditions, and environmental considerations.

Solvents can also influence the rate and outcome of chemical reactions by facilitating the mixing of reactants, stabilizing reaction intermediates, and controlling reaction kinetics. However, solvents may pose health and environmental risks, leading to the development of safer alternatives and sustainable solvent practices in many industries.

Ionic Liquid

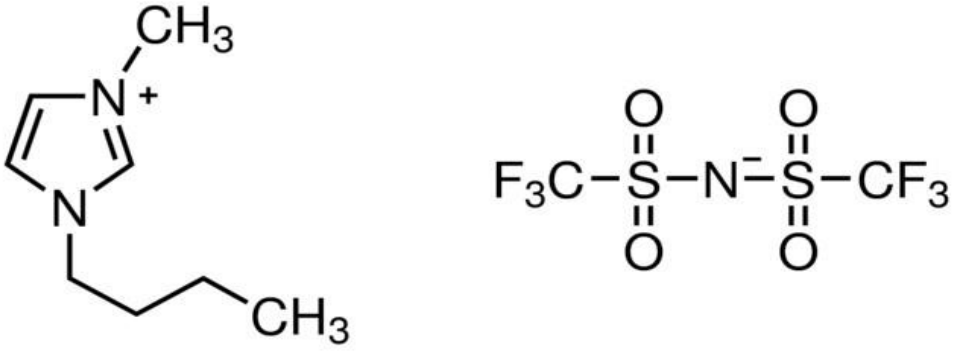


Fig 1.11 Structure of BMIMTFSI Ionic Liquid

Ionic liquids are a unique type of liquid salts composed entirely of ions, typically featuring organic cations and inorganic or organic anions. One key characteristic that sets them apart is their notably low melting points, often falling below 100°C, distinguishing them from conventional salts. These liquids have attracted considerable interest across various fields due to their adjustable properties like viscosity, conductivity, and solubility. They're being investigated for diverse applications such as chemical synthesis, catalysis, electrochemistry, separations, and as eco-friendly solvents due to their low volatility and potential for reuse.

Table 1.12 The ionic liquids' physiochemical characteristics

Ionic Liquids	T_g (°C)	T_m (°C)	ρ (g/cm^3)	η (cP)	σ_{dc} (mS/cm)	ESW (V)
BMIMTFSI	-87	-3	1.43	40	4.6	4.1
$BMIMBF_4$	-83	…	1.20	75	4.5	6.1
$EMIMBF_4$	-94	15	1.29	42	15.4	4.3
BMIMTf	-82	17	1.29	64	3.6	…
$BMIMPF_6$	-77	10	1.37	182	1.9	3.7
$BDMIMBF_4$	-68	37	1.19	243	1.2	4.6
BMPTFSI	-83	15	1.39	60	3.4	5.7
PMIMTFSI	…	…	…	40	7.4	…
EMIMTFSI	-87	16	1.28	…	…	4.3

Their array of properties makes them appealing for a wide range of uses. For instance, their robust thermal stability renders them valuable in high-temperature processes, while their minimal vapor pressure makes them suitable for vacuum applications. Moreover, their capacity to dissolve a broad spectrum of compounds positions them as promising options for sustainable chemistry.

Nevertheless, despite their numerous advantages, challenges persist, especially concerning their environmental footprint and scalability in industrial settings. Ongoing research aims to devise more sustainable and cost-efficient synthesis methods while also uncovering novel applications for these intriguing liquids.

Using them as electrochemical devices such as electrochemical capacitors.

To Study –

- Cationic Size
- Dielectric constant of the ionic liquids on the physiochemical properties
- Electrochemical stability of gels
- Electrochemical performance of the electrochemical capacitor fabricated with these gel electrolytes

Benefits of Ionic Liquids:

- Flame retardance
- Negligible Vapour Pressure
- Negligible Volatility

- Solubility with several compounds
- High electrochemical stability
- Low melting temperature
- Low viscosity
- High ionic conductivity

Which make them potential candidates for good electrochemical performance in electrochemical devices. The physical properties of ionic liquids such as relative size of ions and viscosity strongly influence the ionic conductivity which is a fundamental parameter to design electrochemical devices.

Difference Between Ionic Liquid and Normal Salt

Ionic liquids are composed entirely of ions, which are charged particles, while normal salts consist of ions as well, but in a solid crystalline structure. Ionic liquids typically have low melting points and can exist as liquids at room temperature, whereas normal salts are solid at room temperature. Additionally, ionic liquids often possess unique properties such as low volatility, high thermal stability, and high conductivity compared to conventional salts.

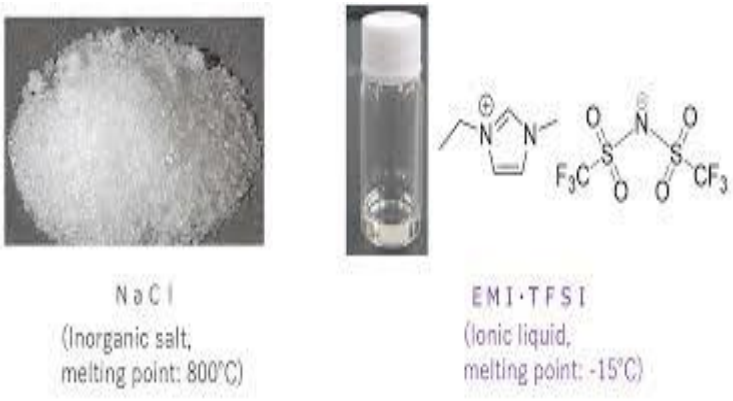
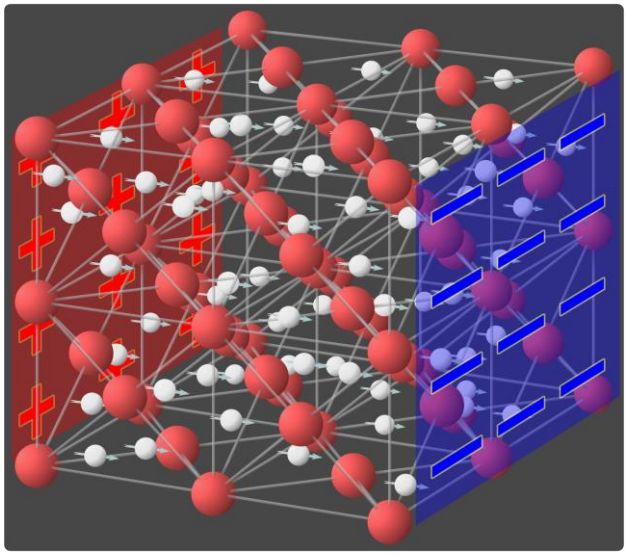


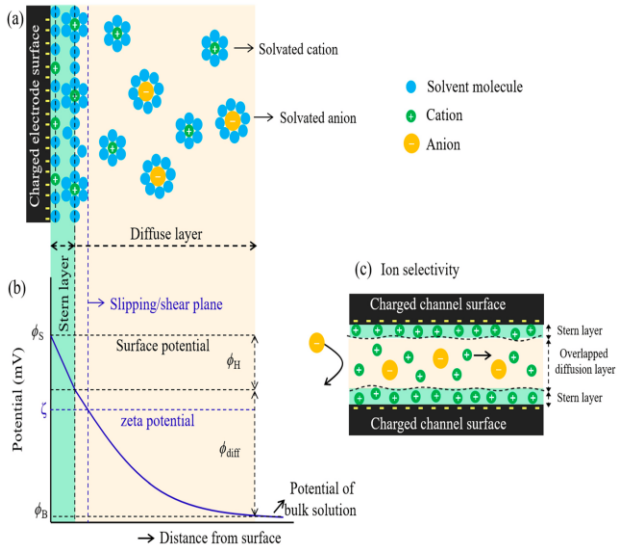
Fig 1.13 Comparison of Ionic liquid and Normal salt

Ionic Transport & Ionic Conductivity

Ion transport refers to the movement of ions from one location to another within a medium. This movement can occur in solids, liquids, or gases and is driven by various factors such as concentration gradients, electrical fields, and temperature gradients. Ion transport plays a crucial role in numerous natural and technological processes, including biological signalling, electrochemical reactions, and energy storage.

Ion conductivity, on the other hand, is a measure of how easily ions can move through a medium in response to an applied electric field. It is a physical property that quantifies the ability of a material to conduct electric current carried by ions. Materials with high ion conductivity allow ions to move rapidly, resulting in efficient electrical conduction. Ion conductivity is influenced by factors such as the concentration and mobility of ions, as well as the structure and properties of the medium through which they are moving. It is a key parameter in the design and optimization of various electrochemical devices, including batteries, fuel cells, and sensors.





(i) Ionic Conductivity *(ii) Ionic Transport*

Fig. 1.14 (i) Ionic Conductivity (ii) Ionic Transport

Plasticizer

A plasticizer is a substance added to a polymer material to increase its flexibility, workability, and processability. These additives are commonly used in the production of plastics, rubber, adhesives, and coatings to modify various properties of the final product. The primary function of plasticizers is to reduce the glass transition temperature (T_g) of the polymer, thereby lowering its stiffness and making it more pliable. This allows the polymer to be molded, shaped, or extruded more easily during manufacturing processes.

Common types of plasticizers include phthalates, adipates, trimellitates, and epoxidized oils. Phthalates, in particular, have been widely used in various applications due to their low cost and effectiveness. However, concerns have been raised about their potential health and environmental effects, leading to increased scrutiny and the development of alternative plasticizers. Plasticizers are used in a wide range of industries, including construction, automotive, packaging, and consumer

goods. They play a crucial role in improving the performance and versatility of polymer materials, enabling the production of flexible and durable products for numerous applications.

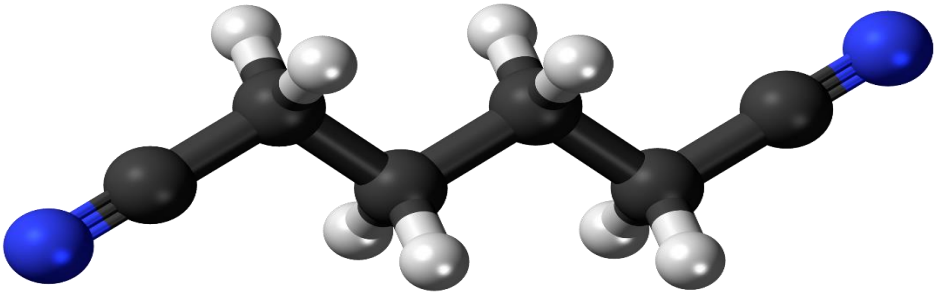


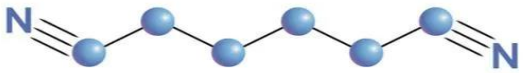
Fig 1.15 Structure of Adiponitrile (ADN) as plasticizer

Why Nitrile group containing compounds in Adiponitrile (ADN) are often chosen as plasticizers for gel polymer electrolyte not the carboxyl group?

Nitrile group-containing compounds are often preferred as plasticizers for gel polymer electrolytes over carboxyl group-containing compounds due to several reasons. First, nitrile groups possess higher compatibility with polymer matrices commonly used in gel polymer electrolytes, such as polyethylene oxide (PEO), due to their similar chemical structures and intermolecular interactions. This compatibility ensures better miscibility and dispersion of the plasticizer within the polymer matrix, leading to improved mechanical properties and electrolyte stability. Second, nitrile groups exhibit favourable solvation characteristics with lithium salts commonly employed as electrolytes in battery applications. This solvation ability enhances ion transport properties within the gel polymer electrolyte, resulting in improved conductivity and electrochemical performance.

Additionally, nitrile group-containing compounds often offer enhanced thermal and chemical stability compared to carboxyl group-containing compounds, making them more suitable for demanding operating conditions in battery systems. Furthermore, the presence of nitrile groups can contribute to reducing the crystallinity of the polymer matrix, which is beneficial for maintaining flexibility and enhancing ion mobility within the gel electrolyte.

Overall, the unique combination of compatibility, solvation characteristics, stability, and effects on polymer structure makes nitrile group-containing compounds preferable choices as plasticizers for gel polymer electrolytes in comparison to carboxyl group-containing compounds.



Adiponitrile

Fig 1.16 Adiponitrile (ADN)

Gel Polymer Electrolyte (GPEs)

Gel Polymer Electrolytes (GPEs) are solid-state electrolytes that consist of a polymer matrix, typically in a gel-like form, containing a liquid electrolyte. They offer a unique combination of properties from both liquid and solid electrolytes. The polymer matrix provides mechanical stability, while the liquid electrolyte facilitates ion conduction. GPEs are used in various electrochemical devices, including lithium-ion batteries, fuel cells, and supercapacitors. They offer advantages such as improved safety, flexibility, and potential for higher energy density. Additionally, GPEs can be tailored to enhance specific properties like ion transport and thermal stability, making them promising candidates for next-generation energy storage technologies.

The essential components of GPEs are host polymer matrix, salt and solvents (solvents are low molecular weight plasticizers or organic liquids such as Ionic liquids)

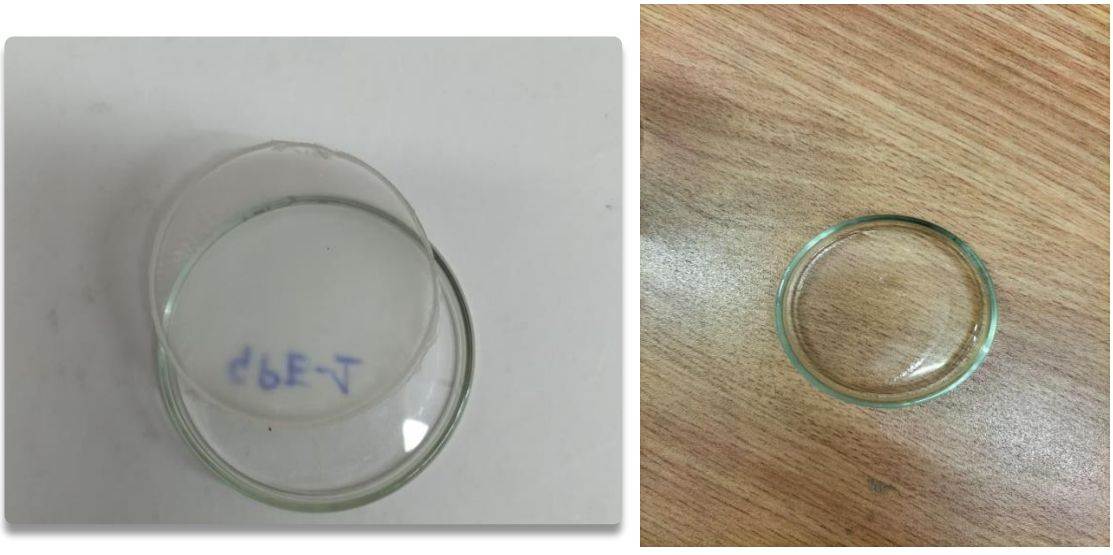


Fig 1.17 Gel Polymer Electrolyte

Gel polymer electrolytes and liquid electrolytes are both types of electrolytes used in various electrochemical devices such as batteries, fuel cells, and supercapacitors. The key difference between them lies in their physical state and structure.

Liquid electrolytes are solutions composed of dissolved salts in a liquid solvent, typically an organic solvent like ethylene carbonate or a mixture of solvents. In liquid electrolytes, ions are free to move and conduct electricity within the solution. Liquid electrolytes are widely used in many battery chemistries due to their high ion conductivity and compatibility with a variety of electrode materials. However, they can suffer from issues such as leakage, flammability, and volatility.

On the other hand, gel polymer electrolytes are composed of a solid polymer matrix containing a liquid electrolyte immobilized within it. The polymer matrix provides mechanical support and retains the liquid electrolyte, preventing leakage and improving safety. Gel polymer electrolytes offer advantages such as improved mechanical stability, reduced risk of electrolyte leakage, and enhanced safety compared to liquid electrolytes. They are commonly used in lithium-ion batteries and other advanced battery technologies.

Overall, the choice between gel polymer electrolytes and liquid electrolytes depends on factors such as the specific application requirements, desired performance characteristics, and safety considerations. Gel polymer electrolytes are favoured in applications where safety and stability are paramount, while liquid electrolytes may be preferred when high ion conductivity and flexibility are needed.

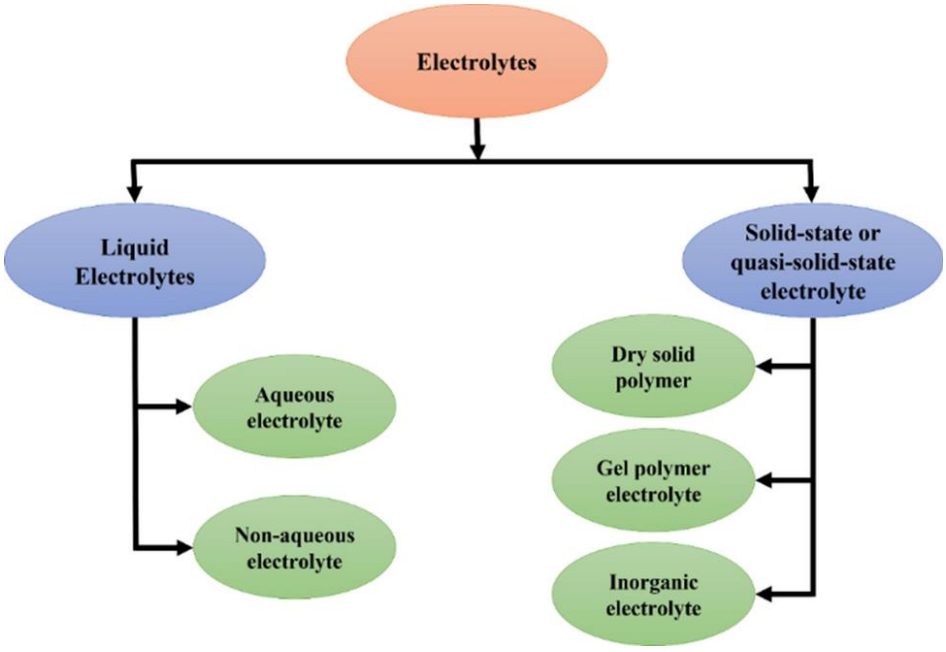


Fig 1.18 Comparison of Liquid Electrolyte and Gel Polymer Electrolyte

REDOX ADDITIVES

Redox additives are compounds added to battery electrolytes to enhance their performance. They undergo reversible redox reactions during charging and discharging, providing additional electroactive species to improve capacity, efficiency, and stability. These additives can mitigate side reactions, reduce overpotential, improve cycle life, enhance voltage stability, and offer temperature-dependent behaviours. Research aims to optimize redox additives for various battery systems, contributing to the development of high-performance and durable energy storage technologies.

Using gel polymer electrolytes with redox additives can enhance the performance of both supercapacitors and lithium-ion batteries. These additives can improve ion conductivity, increase the stability of the electrolyte, and enhance the overall energy density and cycling stability of the devices. They offer the potential for safer and more efficient energy storage solutions.

Table 1.19 A review of redox electrolytes for Supercapacitors

	Redox additives	Supporting electrolyte	Capacitance	Energy density (Wh kg^{-1})	Cycling stability
Redox mediated aqueous electrolytes	KI	H_2SO_4	203–616 F g^{-1} at 1 A g^{-1}	—	77.3% capacitance retention after 5,000 cycles
	$Ce_2(SO_4)_3$	H_2SO_4	408 F g^{-1} at 17.7 mA cm^{-2}	1.24–13.84	94% capacitance retention after 3,000 cycles
	0.8 M Fe^{3+}/Fe^{2+}	H_2SO_4	1,062 F g^{-1} at 2 A g^{-1} (almost tripled)	8.3–22.1	93% capacitance retention after 10,000 cycles
	Catechol	H_2SO_4	429–1,967 F g^{-1} at 1 A g^{-1}	81.8	80% capacitance retention after 5,000 cycles
	$CuCl_2$	HNO_3	440–4,700 F g^{-1} at 5 mVs^{-1}	163	99.4% capacitance retention after 5,000 cycles
	PPD	KOH	119.2–501.4 F g^{-1} at 3 A g^{-1}	—	85.2% capacitance retention after 5,000 cycles
	KI	Li_2SO_4	96–198 F g^{-1} at 1 A g^{-1}	65	85.3% capacitance retention after 3,000 cycles
Redox mediated organic electrolytes	HQ	PMMA	0.2–7.1 mF cm^{-2} at 0.1 mA cm^{-2}	—	97% capacitance retention after 10,000 cycles
	PPD	$LiClO_4$+AC	25–69 F g^{-1} at 0.5 A g^{-1}	18–54	93% capacitance retention after 5,000 cycles
	DmFc	TBAP+THF	8.3–61.3 F g^{-1} at 10 A g^{-1}	36.8	88.4% capacitance retention after 10,000 cycles
Redox mediated ionic electrolytes	HQ	TEATFSI	72 F g^{-1} at 0.57 mA cm^{-2}	18.4–31.22	84.1% capacitance retention after 1,000 cycles
	p-BQ	$PYR_{14}TFSI$	20–70 F g^{-1} at 5 mA cm^{-2}	3.5–10.3	50% capacitance retention after 1,000 cycles
	Ferrocene	[EMIM] [NTf_2]	—	7.2–13.2	—
Redox mediated gel electrolytes	$FeBr_3$	H_2SO_4+PVA	204–885 F g^{-1}	33.9	100% capacitance retention after 10,000 cycles
	BMIMI	Li_2SO_4+PVA	139.1–384 F g^{-1} at 0.25 A g^{-1}	10.4–29.3	80.9% capacitance retention after 10,000 cycles
	[EMIM]BF_4	H_3PO_4+ PVA	103–271 F g^{-1} at 0.5 A g^{-1}	20.7–54.3	70% capacitance retention after 3,000 cycles

EVD, ethyl viologen dibromide; AQDS, anthraquinone-2,7-disulphonate; PMMA, poly (methyl methacrylate); DmFc, decamethylferrocene; TBAP, tetrabutylammonium perchlorate; THF, tetrahydrofuran; TEATFSI, triethylammonium bis(trifluoromethane)sulfonamide; p-BQ, para-benzoquinone; $PYR_{14}TFSI$, N-butyl-N-methyl pyrro lidinium bis(trifluoromethanesulfonyl) imide; [EMIM][NTf_2], 1-ethyl-3-methylimidazolium bis(trifluoromethanesulfonyl)imide.

Objectives

The main goals of this thesis are to prepare energy storage devices, such as lithium-ion batteries and supercapacitors, and to investigate the material's numerous structural, morphological, electrochemical, and electrical properties.

The following are the thesis's precise goals:

- To create supercapacitors using gel polymer electrolyte
- Gel Polymer Electrolyte preparation utilizing P(VDF-HFP) as the host polymer matrix and several redox additives.
- The electrode being ready for the fabrication procedure.
- X-ray diffraction (XRD), field emission scanning electron microscopy (FESEM), Fourier transform infrared spectroscopy (FTIR), Thermogravimetric analysis (TGA), Differential Scanning Calorimetry (DSC), Cyclic Voltammetry (CV), Galvanostatic Charge Discharge Analysis (GCD), Calculating Specific Capacitance, and comparative study of the performance of various samples made for fabricating the energy storage devices are some of the sophisticated techniques used to characterize the synthesized samples.
- The ultimate goal of this thesis is to use various materials to create an energy storage device with improved electrical properties, which will open the door for energy storage devices to overcome their current limitations

References:

1. G.P. Pandey, S.A. Hashmi, Ionic liquid 1-ethyl-3-methylimidazolium tetracyanoborate-based gel polymer electrolyte for electrochemical capacitors, J. Mater. Chem. A 1 (2013) 3372–3378.
2. J. Tian, C. Cui, Q. Xie, W. Qian, C. Xue, Y. Miao, Y. Jin, G. Zhang, B. Guo, EMIMBF4-GBL binary electrolyte working at -70 [degree]C and 3.7 V for a high performance graphene-based capacitor, J. Mater. Chem. A 6 (2018) 3593–3601.
3. E. Frackowiak, F. Béguin, Carbon materials for the electrochemical storage of energy in capacitors, Carbon 39 (2001) 937–950.
4. W. Deng, T. Kang, H. Liu, J. Zhang, N. Wang, N. Lu, Y. Ma, A. Umar, Z. Guo, Potassium hydroxide activated and nitrogen doped graphene with enhanced supercapacitive behaviour, Sci. Adv. Mater. 10 (2018) 937–949.
5. M. Brachet, T. Brousse, J. Le Bideau, All solid-state symmetrical activated carbon electrochemical double layer capacitors designed with ionogel electrolyte, ECS Electrochem. Lett. 3 (2014) A112–A115.
6. C. Lin, L. Hu, C. Cheng, K. Sun, X. Guo, Q. Shao, J. Li, N. Wang, Z. Guo, NanoTiNb2O7/carbon nanotubes composite anode for enhanced lithium-ion storage, Electrochim. Acta 260 (2018) 65–72.
7. Y. Guo, Y. Li, X. Lou, J. Guan, Y. Li, X. Mai, H. Liu, C.X. Zhao, N. Wang, C. Yan, G. Gao, H. Yuan, J. Dai, R. Su, Z. Guo, Improved extraction of cobalt and lithium by reductive acid from spent lithium-ion batteries via mechanical activation process, J. Mater. Sci. 53 (2018) 13790–13800.
8. T. Liu, K. Yu, L. Gao, H. Chen, N. Wang, L. Hao, T. Li, H. He, Z. Guo, A graphene quantum dot decorated SrRuO3 mesoporous film as an efficient counter electrode for high-performance dye-sensitized solar cells, J. Mater. Chem. A 5 (2017) 17848–17855.
9. Q. Luo, H. Ma, Q. Hou, Y. Li, J. Ren, X. Dai, Z. Yao, Y. Zhou, L. Xiang, H. Du, H. He, N. Wang, K. Jiang, H. Lin, H. Zhang, Z. Guo, All-carbon-electrode-based endurable flexible perovskite solar cells, Adv. Funct. Mater. 28 (2018) 1706777.
10. Q. Luo, H. Ma, F. Hao, Q. Hou, J. Ren, L. Wu, Z. Yao, Y. Zhou, N. Wang, K. Jiang, H. Lin, Z. Guo, Carbon nanotube based inverted flexible perovskite solar cells with all-inorganic charge contacts, Adv. Funct. Mater. 27 (2017) 1703068.
11. C. Wang, B. Mo, Z. He, Q. Shao, D. Pan, E. Wujick, J. Guo, X. Xie, X. Xie, Z. Guo, Crosslinked norbornene copolymer anion exchange membrane for fuel cells, J. Membr. Sci. 556 (2018) 118–125.

12. J.-G. Wang, H. Liu, H. Sun, W. Hua, H. Wang, X. Liu, B. Wei, One-pot synthesis of nitrogen-doped ordered mesoporous carbon spheres for high-rate and long-cycle life supercapacitors, Carbon 127 (2018) 85–92.
13. J.-G. Wang, H. Liu, X. Zhang, X. Li, X. Liu, F. Kang, Green synthesis of hierarchically porous carbon nanotubes as advanced materials for high-efficient energy storage, Small 14 (2018) 1703950.

CHAPTER-2

REVIEW OF PAST WORK

Literature Review of Past Work

A novel redox-mediated gel polymer (PVA-KOH-PPD) is employed as both the electrolyte and separator in a supercapacitor, with activated carbon serving as the electrodes. Through investigation using cyclic voltammetry, galvanostatic charge-discharge, and electrochemical impedance spectroscopy, it is observed that the supercapacitor demonstrates remarkable properties: high ionic conductivity (25 mS cm $^{-1}$), a large electrode specific capacitance (611 F g $^{-1}$), and a high energy density (82.56 Wh kg^{-1}). This exceptional performance is attributed to the rapid redox reactions occurring at the interface between the electrolyte and the electrode, facilitated by PPD undergoing a two-proton/two-electron reduction and oxidation during cycling. Moreover, the supercapacitor featuring the PVA-KOH-PPD gel polymer exhibits outstanding charge-discharge stability, maintaining a high electrode specific capacitance of 470 F g^{-1} even after 1000 charge-discharge cycles. This suggests that employing a redox mediator holds promise for enhancing the performance of supercapacitors.

A novel strategy to boost the specific energy of carbon supercapacitors involves augmenting redox activity at the electrode-electrolyte interfaces by dispersing redox additives within the electrolytes. In this study, we developed a non-aqueous gel polymer electrolyte (GPE) containing an ionic liquid (IL) 1-butyl-3-methylimidazolium bis(trifluoromethane sulfonyl)imide, along with dual redox additives (KI and diphenylamine, DPA), encapsulated within a host polymer poly(vinylidenefluoride-co-hexafluoropropylene). The resulting free-standing film of the GPE, incorporating dual redox additives, demonstrated outstanding flexibility, thermal stability (up to ~320 °C), high ionic conductivity (σRT ~ 4.52 mS cm^{-1}), and a wide electrochemical stability window (~6.2 V versus Ag), indicating its suitability for use as an electrolyte in quasi-solid-state supercapacitors.

When utilized in a supercapacitor alongside biomass-derived activated carbon electrodes, the redox-active GPE (comprising KI and DPA) yielded superior performance compared to devices employing GPEs containing a pure IL or its mixture with a single additive (DPA or KI). This improvement can be attributed to the synergistic effect of dual redox activity at the interfaces, resulting in optimal specific energy (~73.2 W h kg^{-1}) and maximum power (~34.8 kW kg^{-1}), driven by enhanced specific capacitance (~337 F g^{-1}) and reasonably high operating voltage (2.5 V). The optimized capacitor demonstrated robust performance over ~6000 charge-discharge cycles, experiencing only a 20% decrease in capacitance, while maintaining a coulombic efficiency as high as 98–100%.

Gel Polymer Electrolytes (GPEs) are favoured for use in energy storage devices like flexible supercapacitors due to their enhanced safety and flexibility. Introducing a small amount of redox

additives into GPEs significantly boosts their conductivity, representing an innovative approach to increasing the capacitance of supercapacitors, as both the electrolyte and electrode materials contribute to capacitance. This study explores the performance of Flexible Supercapacitors (FSCs) utilizing symmetrical Laser Induced Graphene (LIG) as electrodes and the ionic liquid 1-Ethyl-3-Methylimidazolium Ethyl Sulfate [EMIM] [$EtSO_4$] incorporated into Gel Polymer Electrolyte (GPE), both with and without the redox additive Hydroquinone (HQ).

This study focuses on fabricating supercapacitors (SCs) with high energy density utilizing dual redox additive-based gel polymer electrolytes (GPEs) and activated carbon (AC) electrodes. The GPEs were formulated using poly(vinylidene fluoride-co-hexafluoropropylene) as the host polymer, adiponitrile as a plasticizer, 1-ethyl-3-methylimidazolium bis(trifluoromethyl sulfonyl)imide as the ionic liquid (IL), and diphenylamine (DPA) and copper iodide (CuI) as dual redox additives. Microstructural analysis revealed that the inclusion of plasticizers, ILs, and redox additives augmented the amorphous characteristics of the host polymer matrix. The thermal stability of the GPEs was demonstrated up to ∼200 °C. The electrical conductivity at room temperature and the electrochemical potential window of the dual redox additive-based GPE-IL + DPA + CuI were measured at 3.3×10^{-3} S cm^{-1} and 6.4 V, respectively.

To evaluate the electrochemical performance of the SCs, cyclic voltammetry, galvanostatic charge–discharge, and electrochemical impedance spectroscopic techniques were employed. It was noted that the incorporation of dual redox additives significantly increased the specific capacitance of the SCs from 108.3 to 243.4 F g^{-1} and the specific energy from 5.1 to 11.5 W h kg^{-1}. Moreover, the dual redox additive-based GPEs exhibited favourable cyclic performance in specific capacitance, with an initial 34% decrease, while maintaining a Coulombic efficiency of ∼100% over 5000 cycles.

Electrochemical characterization through Galvanostatic Charge Discharge (GCD) revealed that the FSC with the redox additive exhibited the highest areal capacitance and energy density, reaching 15.1 $mFcm^{-2}$ and 1.54 $\mu Whcm^{-2}$ respectively, while the FSC without the redox additive showed lower values of 1.94 $mFcm^{-2}$ and 0.14 $\mu Whcm^{-2}$ respectively, at 2 $mAcm^{-2}$. The device with the redox additive also maintained 100% columbic efficiency after 50 cycles and retained 80% capacitance over 5000 charge-discharge cycles. Furthermore, the electrolyte containing the redox additive demonstrated superior conductivity of 10.8 $mScm^{-1}$, underscoring how modifying the electrolyte with redox additives proves to be a straightforward yet effective approach in enhancing the overall performance of FSCs. Additionally, the synthesized LIG underwent characterization using X-ray Diffraction (XRD), Raman spectroscopy, and Scanning Electron Microscopy techniques, confirming the formation of a bi-layer porous graphene structure.

Supercapacitors (SCs) have garnered considerable attention owing to their rapid charging/discharging rates, extended cycle longevity, and stable performance across varying

temperatures. Among the crucial factors influencing SC performance, electrolytes play a pivotal role. They dictate both the energy density, determined by their decomposition voltage, and the power density, reliant on their ionic conductivity. In recent times, there has been a burgeoning interest in redox electrolytes due to their capacity to augment charge storage capabilities in SCs through additional redox activity. This review article provides an overview of the recent advancements in redox electrolyte research, emphasizing their properties, mechanisms, and applications across different solvent types. Furthermore, it suggests potential strategies to effectively enhance the energy density of SCs while upholding their high-power output and extended lifespan.

A supercapacitor utilizing an innovative redox-mediated gel polymer electrolyte (PVA–H2SO4–P–benzenediol) alongside activated carbon electrodes is constructed. Through assessment using cyclic voltammetry, galvanostatic charge–discharge, and electrochemical impedance spectroscopy methods, it is determined that the supercapacitor showcases notable characteristics: a substantial specific capacitance (474.29 F g^{-1}), high energy density (11.31 W h kg^{-1}), and impressive cyclic stability. This superior performance is attributed to the synergy of the capacity-storage mechanism, combining electrical double layer capacitance with Faradaic pseudo capacitance facilitated by p-benzenediol/p-benzoquinone within the electrolyte.

A supercapacitor is constructed using a novel redox-mediated gel polymer (PVA-KOH-PPD) as both the electrolyte and separator, with activated carbon serving as the electrodes. The performance of the PVA-KOH-PPD gel polymer as a potential electrolyte is evaluated through cyclic voltammetry, galvanostatic charge-discharge, and electrochemical impedance spectroscopy techniques. The results reveal that the supercapacitor demonstrates impressive properties: high ionic conductivity (25 mS cm^{-1}), significant electrode-specific capacitance (611 F g^{-1}), and elevated energy density (82.56 Wh kg^{-1}). This exceptional performance is attributed to the rapid redox reactions occurring at the electrolyte-electrode interface, where PPD undergoes two-proton/two-electron reduction and oxidation during cycling. Additionally, the supercapacitor featuring the PVA-KOH-PPD gel polymer exhibits outstanding charge-discharge stability, retaining a high electrode-specific capacitance of 470 F g^{-1} even after 1000 charge-discharge cycles. The utilization of a redox mediator is believed to hold promising potential for enhancing the performance of supercapacitors.

We have introduced a novel and eco-friendly approach by incorporating phloroglucinol as an additive into polyvinyl alcohol–LiClO4 gel polymer electrolytes for flexible symmetrical solid-state supercapacitors. Adding 10 wt.% phloroglucinol to PVA–LiClO4 gel polymer electrolytes significantly enhance the specific capacitance, reaching 114 F g^{-1} compared to 60 F g^{-1} without phloroglucinol, marking a remarkable 90% increase, attributed to the redox reaction of phloroglucinol within the system.

Utilizing PVA–LiClO4 with 10 wt.% phloroglucinol as the gel polymer electrolyte in conjunction with nitrogen-doped graphene nanosheet-based electrodes, we fabricated a symmetrical solid-state supercapacitor. The resulting supercapacitor, incorporating the phloroglucinol redox additive, achieves an energy density of 2.3 W h kg^{-1} at a power density of 150 W kg^{-1}, surpassing the one without a redox additive, which records 1.9 W h kg−1 at the same power density. Furthermore, the supercapacitor with the redox additive exhibit's excellent stability, maintaining its capacitance at approximately ~94% even after 5000 charge/discharge cycles.

The current research trend focuses on integrating redox characteristics at the electrode-electrolyte interface to enhance both the specific capacity and energy density of carbon supercapacitors. In this study, symmetric carbon supercapacitor cells are fabricated using gel polymer electrolytes (GPEs) with and without the addition of a redox additive (MB), alongside activated carbon (AC) derived from natural bio-waste honeycomb (HCAC). The inclusion of the redox additive in the polymeric electrolyte results in high room temperature ionic conductivity ($\sigma RT \sim 2.3 \times 10^{-3}$ S cm^{-1}) and an electrochemical stability window of ~1.4 V upon adding 0.1 g of MB. The HC-based activated carbon (HCAC) exhibits a high surface area (~ 586 m2 g^{-1}) and predominant mesoporosity.

Performance optimization of the supercapacitor cells is conducted using cyclic voltammetry, charge-discharge (CD), and electrochemical impedance spectroscopy (EIS) techniques. The supercapacitor with the redox-additive GPE demonstrates electric double layer characteristics alongside faradaic reactions at the electrode-electrolyte interface, resulting in a high capacitance of ~114 F g^{-1} and specific energy of ~7.76 Wh kg^{-1} at a power density of 0.49 kW kg−1, nearly ~2.5 times higher than the supercapacitor cell without the redox-additive GPE. Moreover, the supercapacitor cell utilizing 0.1 g of MB redox-additive-based electrolyte maintains almost stable capacitance for up to 10,000 CD cycles with ~36% initial fading.

A solid-state supercapacitor is constructed using a redox-mediated gel polymer as both the electrolyte and separator, with electrodes derived from steam-activated coconut shells. The gel polymer electrolyte (GPE) comprises poly(vinyl alcohol) (PVA)-potassium hydroxide (KOH)-hydroquinone (HQ) and is fabricated via a solution casting technique. XRD analysis confirms the amorphous nature of the GPE, while FTIR spectral analysis confirms the formation of complexes within it. Electrochemical characterization of the GPE films is conducted using impedance analysis, cyclic voltammetry, and galvanostatic charge/discharge tests, along with self-discharge studies of the assembled supercapacitor.

The redox-mediated GPE demonstrates notable advantages such as higher ionic conductivity of approximately 53 mS cm^{-1} and superior flexibility. The supercapacitor exhibits a high electrode-specific capacitance of up to 326.53 F g^{-1} with a capacity retention of 84.2% after 1000 charge-discharge cycles at a current density of 0.8 A g^{-1}. Moreover, the assembled supercapacitors offer a significantly high energy density and power density, approximately 33.15 Wh kg^{-1} and 689.58 W

kg^{-1}, respectively. These flexible, redox-mediated gel polymer electrolytes present a promising avenue for the development of solid-state supercapacitors with high power capabilities for energy storage applications.

As renewable energy sources gain increasing prominence, there's a growing emphasis on exploring innovative energy storage technologies. Carbon-based redox-enhanced supercapacitors (RE-SCs) have emerged as a promising solution, integrating soluble redox electrolytes into conventional devices. This approach leverages the diffusion-controlled faradaic process of the redox electrolyte at carbon electrode surfaces, enhancing energy density while preserving power density. Despite notable progress in designing novel redox electrolytes and configuring new devices, the development of these systems is hindered by significant self-discharge issues.

This overview provides a comprehensive understanding of the fundamentals of RE-SCs, along with a discussion on challenges and future prospects. We emphasize the influence of redox electrolytes on capacitance, energy density, and power output. Additionally, we delve into the self-discharge phenomenon stemming from redox electrolyte introduction and its underlying mechanisms. Strategies ranging from material improvements to system optimization are summarized.

Furthermore, potential avenues for future research in this field are explored, aiming to address current limitations and propel advancements in RE-SC technology.

The paper discusses the critical aspect of energy density in energy storage devices and presents the preparation of a series of gel polymer electrolytes. These electrolytes utilize renewable soy protein isolate (SPI) as the polymer matrix, Li2SO4 as the neutral electrolyte salt to widen the potential window to 1.5 V, and the introduction of the redox mediator KI to enhance the energy density of flexible supercapacitors. The performance of the supercapacitor with optimized SPI-Li2SO4-KI gel polymer electrolytes is evaluated through physical characterization (SEM, FT-IR, XRD, Raman) and electrochemical analysis (CV, GCD, EIS).

The addition of the KI mediator increases the ionic conductivity of the gel polymer electrolyte, reduces the electrochemical series resistance of the supercapacitor, and allows for the observation of pseudo capacitance. The electrode-specific capacitance of the supercapacitor with SPI-Li_2SO_4-100 wt.% KI electrolyte is 224.19 F g^{-1}, marking a 156% increase compared to the SPI-Li_2SO_4 system at the same current density. Moreover, the energy density of the supercapacitor rises from 5.90 to 16.02 Wh kg^{-1}. Additionally, the quasi-solid-state supercapacitor exhibits exceptional flexibility and holds significant potential for practical applications.

We introduce a novel gel polymer electrolyte (GPE) supercapacitor design that enhances pathways for ion transport by creating a coherent and continuous distribution of the electrolyte throughout the electrode. Poly(vinylidene fluoride-co-hexafluoropropylene) (PVDF-HFP) serves as the chosen polymer framework for organic electrolytes. The permeation of GPE into the electrodes, serving as both integrated electrolyte and binder, as well as a thin separator, facilitates ion diffusion and

augments the active electrode–electrolyte interface, resulting in improvements in both capacitance and rate capability. An activation process initiated during the initial charge–discharge cycles was observed, leading to a decrease in charge transfer resistance and Warburg impedance. Optimal capacitance and rate capability were achieved with a GPE thickness of 12 μm.

A novel hybrid nanocomposite material, comprising the tetraethylammonium salt of 1 nm-sized phosphomolybdate cluster and activated carbon (AC/TEAPMo12), was demonstrated to enhance capacitive performance with this gel electrolyte arrangement. The homogeneous dispersion of PMo12 clusters allows for a non-diffusion-controlled energy storage process. In symmetric capacitors, the hybrid nanocomposite material can undergo redox reactions in both positive and negative electrodes in an ambipolar mode. Compared to cells with parent AC electrodes, the volumetric capacitance of a symmetric supercapacitor made with the hybrid electrodes increased by 40%. The synergy between permeating GPE and hybrid electrodes enables the GPE hybrid symmetric capacitor to deliver three times higher energy density at higher power densities and comparable cycle stability to conventional AC symmetric capacitors.

The integration of a redox-active additive, sodium molybdate (Na2MoO4), brings about a notable enhancement in polarization and charge transport at the solid–solid electrode–electrolyte interface. The presence of the electrochemically active oxide centre alongside Na+ ions facilitates hopping-based charge transport of the ionic liquid, resulting in elevated ionic conductivity and a doubling of specific capacitance (0.009 to 0.018 F cm^{-2}). This leads to a 200% increase in energy density (0.76–1.7 μW h cm^{-2}) and a 2.5 times improvement in rate capability (10,000 mV s^{-1}) of the solid-state supercapacitor. Importantly, power density, non-Faradic nature, and cyclability remain unaffected, surpassing the performance of several solid-state and liquid electrolyte-based supercapacitors. Hence, the utilization of redox-active additives demonstrates the robustness of the approach and the practicality of the resulting device, offering transformative opportunities for enhancing the performance of solid-state devices.

The addition of redox additives to electrolytes is currently a prominent method for advancing the electrochemical activity at electrode–electrolyte interfaces to develop high-energy-density supercapacitors. In this study, we investigate a quasi-solid-state supercapacitor constructed with a nonaqueous gel polymer electrolyte (GPE) composed of a blend of succinonitrile, a plastic crystal, and an ionic liquid 1-butyl-1-methylpyrrolidinium bis(trifluoromethyl sulfonyl) imide, supplemented with a redox additive, hydroquinone (HQ), immobilized within a poly(vinylidene fluoride-co-hexafluoropropylene) polymer matrix.

The HQ-incorporated GPE forms a standalone film that is easy to process and reuse, exhibiting remarkable flexibility and thermal stability up to approximately 100 °C. Through linear sweep voltammetry measurements, the GPE with the optimal composition demonstrates high ionic conductivity (~4.2 mS cm^{-1}) and a wide electrochemical stability window (~5.0 V), rendering it a

promising electrolyte for high-energy-density supercapacitors. Symmetric supercapacitor coin cells are assembled using porous carbon electrodes derived from peanut shells and separated by GPE films.

The electrochemical activity stemming from HQ at the carbon electrode–GPE interfaces introduces additional pseudocapacitance beyond the double-layer capacitance, resulting in an enhanced overall specific capacitance (289 F g^{-1}). Consequently, this corresponds to high specific energy (~40 Wh kg^{-1}) and maximum power (~20 kW kg^{-1}). The capacitor cell exhibits extended cyclic stability over approximately 10,000 charge–discharge cycles with a Coulombic efficiency of approximately 85–93%.

Gel Polymer Electrolytes (GPEs) are promising candidates for flexible supercapacitors due to their enhanced safety and flexibility. The incorporation of small amounts of redox additives into GPEs has shown to significantly boost their conductivity, presenting an innovative approach to enhancing supercapacitor capacitance, as both electrolyte and electrode materials contribute to it. This study investigates the performance of Flexible Supercapacitors (FSCs) employing symmetrical Laser Induced Graphene (LIG) electrodes and ionic liquid 1-Ethyl-3-Methylimidazolium Ethyl Sulfate [EMIM][EtSO4] incorporated in Gel Polymer Electrolyte (GPE) with and without the redox additive Hydroquinone (HQ).

Through electrochemical characterization using Galvanostatic Charge Discharge (GCD), it was observed that the FSC with the redox additive exhibited the highest areal capacitance and energy density, measuring 15.1 mFcm^{-2} and 1.54 μWhcm^{-2} respectively, while the FSC without the redox additive showed lower values, with an areal capacitance and energy density of 1.94 mFcm^{-2} and 0.14 μWhcm^{-2} respectively at 2 mAcm^{-2}. Moreover, the device with the redox additive displayed 100% coulombic efficiency after 50 cycles and maintained 80% capacitance over 5000 charge-discharge cycles. Additionally, the electrolyte containing the redox additive exhibited superior conductivity of 10.8 mScm−1, highlighting the effectiveness of modifying the electrolyte through the addition of redox additives in enhancing the overall performance of FSCs. The synthesized LIG was characterized using X-ray Diffraction (XRD), Raman, and Scanning Electron Microscopy techniques, confirming the formation of bi-layer porous graphene.

Recent advancements in quasi-solid-state carbon supercapacitors, renowned for their high-power density, flexibility, and extended cycle life, have positioned them as promising contenders for commercial applications. Efforts in research and development have predominantly aimed at enhancing their energy density. A novel strategy entails augmenting the redox activity at electrode-electrolyte interfaces by introducing suitable redox additives into electrolytes. This study introduces an ionic liquid (IL)-incorporated redox-active gel polymer electrolyte (GPE) composed of a polymer blend comprising poly(vinyl alcohol) (PVA) and poly(vinyl pyrrolidone) (PVP), designed for implementation in carbon supercapacitors.

The GPE, containing the IL 1-ethyl-3-methylimidazolium hydrogen-sulfate (EMIHSO4) and supplemented with the redox additive hydroquinone (HQ), immobilized within the PVA/PVP matrix, exhibits outstanding flexibility, thermal stability, and electrochemical stability, with an optimal ionic conductivity of approximately 9.3 mS cm-1 at room temperature. Quasi-solid-state supercapacitors are constructed using GPEs with symmetrical electrodes comprising multiwalled carbon nanotubes (MWCNTs), graphene nanoplatelets (GNPs), and biomass-derived activated carbon (AC) for comparative analysis.

AC electrodes demonstrate superior capacitive responses compared to other carbon electrodes owing to their well-suited porous texture with hierarchical porosity. The redox activity of the HQ-incorporated GPE at the interfaces with porous AC electrodes yields optimal capacitive parameters for the device (Cs ~485 F g^{-1} and E ~24.3 Wh kg^{-1}), coupled with prolonged cyclic performance for up to 5000 charge-discharge cycles.

Reference

1. Bi, Z.; Kong, Q.; Cao, Y.; Sun, G.; Su, F.; Wei, X.; Li, X.; Ahmad, A.; Xie, L.; Chen, C.-M. Biomass-derived porous carbon materials with different dimensions for supercapacitor electrodes: a review. J. Mater. Chem. A 2019, 7 (27), 16028−16045.
2. Jiang, H. R.; Sun, J.; Wei, L.; Wu, M. C.; Shyy, W.; Zhao, T. S. A high power density and long cycle life vanadium redox flow battery. Energy Storage Mater. 2020, 24, 529−540.
3. Li, K.; Li, J.; Wang, L.; Li, X.; Yang, X.; Lü, W. Flexible Zn-ion hybrid supercapacitor enabled by N-Doped MnO2 cathode with high energy density and ultra
4. Wang, Y.; Shi, Z.; Huang, Y.; Ma, Y.; Wang, C.; Chen, M.; Chen, Y. Supercapacitor Devices Based on Graphene Materials. J. Phys. Chem. C 2009, 113 (30), 13103−13107.
5. Liu, A.; Zhang, H.; Xing, C.; Wang, Y.; Zhang, J.; Zhang, X.; Zhang, S. Intensified Energy Storage in High-Voltage Nanohybrid Supercapacitors via the Efficient Coupling between TiNb2O7/HoleyrGO Nanoarchitectures and Ionic Liquid-Based Electrolytes. ACS Appl. Mater. Interfaces 2021, 13 (18), 21349−21361.
6. Yue, F.; Zhang, Q.; Xu, L.; Zheng, Y.; Yao, C.; Jia, J.; Leng, W.; Hou, S. Porous Reduced Graphene Oxide/Single-Walled Carbon Nanotube Film as Freestanding and Flexible Electrode Materials for Electrosorption of Organic Dye. ACS Appl. Nano Mater. 2019, 2 (10), 6258−6267.
7. Kouchachvili, L.; Yaïci, W.; Entchev, E. Hybrid battery/ supercapacitor energy storage system for the electric vehicles. J. Power Sources 2018, 374, 237−248.
8. Zhang, W.; Liu, F.; Li, Q.; Shou, Q.; Cheng, J.; Zhang, L.; Nelson, B. J.; Zhang, X. Transition metal oxide and graphene nanocomposites for high-performance electrochemical capacitors. Phys. Chem. Chem. Phys. 2012, 14 (47), 16331−16337.
9. Liu, H.; Liu, X.; Wang, S.; Liu, H.-K.; Li, L. Transition metal based battery-type electrodes in hybrid supercapacitors: A review. Energy Storage Mater. 2020, 28, 122−145.
10. Kondawar, S. B. Conducting Polymer Nanocomposites for Supercapacitors; Smithers Rapra, 2015, p 8.
11. Zheng, C.; Zhou, X.; Cao, H.; Wang, G.; Liu, Z. Synthesis of porous graphene/activated carbon composite with high packing density and large specific surface area for supercapacitor electrode material. J. Power Sources 2014, 258, 290−296.
12. Shao, H.; Wu, Y.-C.; Lin, Z.; Taberna, P.-L.; Simon, P. Nanoporous carbon for electrochemical capacitive energy storage. Chem. Soc. Rev. 2020, 49 (10), 3005−3039.
13. Zhao, C.; Zheng, W. A Review for Aqueous Electrochemical Supercapacitors. Front. Energy Res. 2015, 3, 23.

14. Zhong, C.; Deng, Y.; Hu, W.; Qiao, J.; Zhang, L.; Zhang, J. A review of electrolyte materials and compositions for electrochemical supercapacitors. Chem. Soc. Rev. 2015, 44 (21), 7484−7539.
15. Karmakar, A.; Ghosh, A. Charge carrier dynamics and relaxation in (polyethylene oxide-lithium-salt)-based polymer electrolyte containing 1-butyl-1-methylpyrrolidinium bis (trifluoromethylsulfonyl) imide as ionic liquid. Phys. Rev. E 2011, 84 (5), 051802.
16. Jin, M.; Zhang, Y.; Yan, C.; Fu, Y.; Guo, Y.; Ma, X. High Performance Ionic Liquid-Based Gel Polymer Electrolyte Incorporating Anion-Trapping Boron Sites for All-Solid-State Supercapacitor Application. ACS Appl. Mater. Interfaces 2018, 10 (46), 39570−39580.
17. Balducci, A. Electrolytes for high voltage electrochemical double layer capacitors: A perspective article. J. Power Sources 2016, 326, 534− 540.
18. Kerner, M.; Lim, D.-H.; Jeschke, S.; Rydholm, T.; Ahn, J.-H.; Scheers, J. Towards more thermally stable Li-ion battery electrolytes with salts and solvents sharing nitrile functionality. J. Power Sources 2016, 332, 204−212.
19. Bothe, A.; Pourhosseini, S. E. M.; Ratajczak, P.; Beguin, F.; Balducci, A. Towards understanding the impact of operating voltage on the stability of adiponitrile-based electrical double-layer capacitors. J. Power Sources 2021, 496, 229841.
20. Mastragostino, M.; Arbizzani, C.; Soavi, F. Polymer-based supercapacitors. J. Power Sources 2001, 97−98, 812−815.
21. Stettner, T.; Huang, P.; Goktas, M.; Adelhelm, P.; Balducci, A. Mixtures of glyme and aprotic-protic ionic liquids as electrolytes for energy storage devices. J. Chem. Phys. 2018, 148(19). DOI: 10.1063/ 1.5013117.
22. Li, J.; Qiao, J.; Lian, K. Hydroxide ion conducting polymer electrolytes and their applications in solid supercapacitors: A review. Energy Storage Mater. 2020, 24, 6−21.

CHAPTER 3:

INSTRUMENTS AND APPARATUS

Sample characterization Techniques

The produced materials were evaluated using X-ray diffraction (XRD), scanning and tunneling electron microscopy (SEM & TEM), differential scanning calorimetry (DSC), thermogravimetric analysis (TGA), Fourier transform infrared (FT-IR) spectroscopy, electrical and electrochemical tests, and so on. These strategies are briefly described below.

Physiochemical Characterization:

1. X-ray diffraction (XRD)

X-ray diffraction (XRD) is a flexible non-destructive analytical method for determining physical parameters such as phase composition, crystal structure, and orientation of powder, solid, and liquid samples.

Many materials are composed of microscopic crystallites. The chemical content and structural type of these crystals is known as their 'phase'. Materials can be single or multiphase mixtures, including both crystalline and non-crystalline components. In an X-ray diffractometer, various crystalline phases produce distinct diffraction patterns. Phase identification can be accomplished by comparing X-ray diffraction patterns acquired from unknown substances to those found in reference databases. This procedure is similar to comparing fingerprints at a crime scene.

Bragg's Law: According to the rule, an X-ray's angle of incidence will reflect back to the crystal surface at the same angle of scattering. And constructive interference will happen when the path difference, d, equals a full integer, n, of a wavelength. X-rays are impinging at an angle of θ on the surface of a series of crystallographic lattice planes to irradiate them. The path length difference between the ray scattered from the top plane and the ray scattered from the bottom plane is determined by the inter-planar spacing d_{hkl}. The path length difference is $2dSin^{i}$. Nevertheless, positive interference is only possible when the path length difference is equal to Braggs equation was therefore created and can

$$\mathbf{2dSin\theta=n\lambda}$$

where n is the integer and θ is the angle of scattering and d is the interplanar distance.

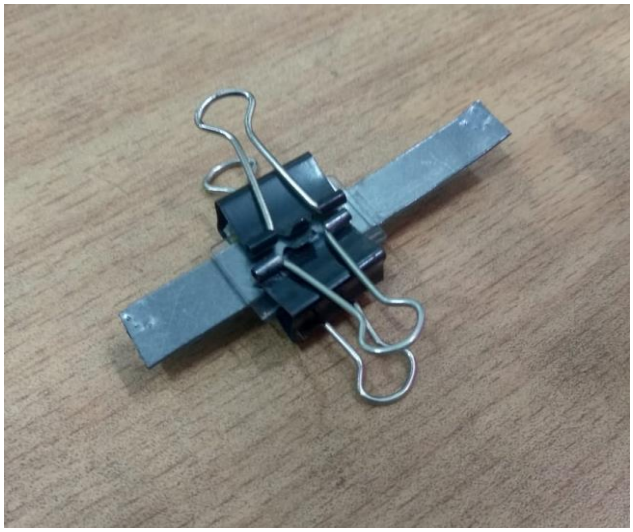


Fig 3.1 EDL Capacitor containing gel polymer Electrolyte

The basic measurement geometry is depicted in Fig 3.2 The angle of both the incoming beam and exciting beam is θ with respect to the specimen surface. The diffraction pattern is collected by varying the incidence angle of the inward X-ray beam by θ and the scattering angle by 2θ while measuring the scattered intensity as a function of 2θ. Therefore, two angles must be varied during a θ/2θ scan in one case X-Ray source remains fixed while the sample is rotated around θ and the detector moves by 2θ. In another case the sample was fixed and both the source and detector were rotated by θ respectively but the sense of rotation was different. The central part of a diffractometer or goniometer performed the rotations. The sample was loaded on to the rotational axis while the detector and the x-ray source moves along the periphery but the axes coincide.

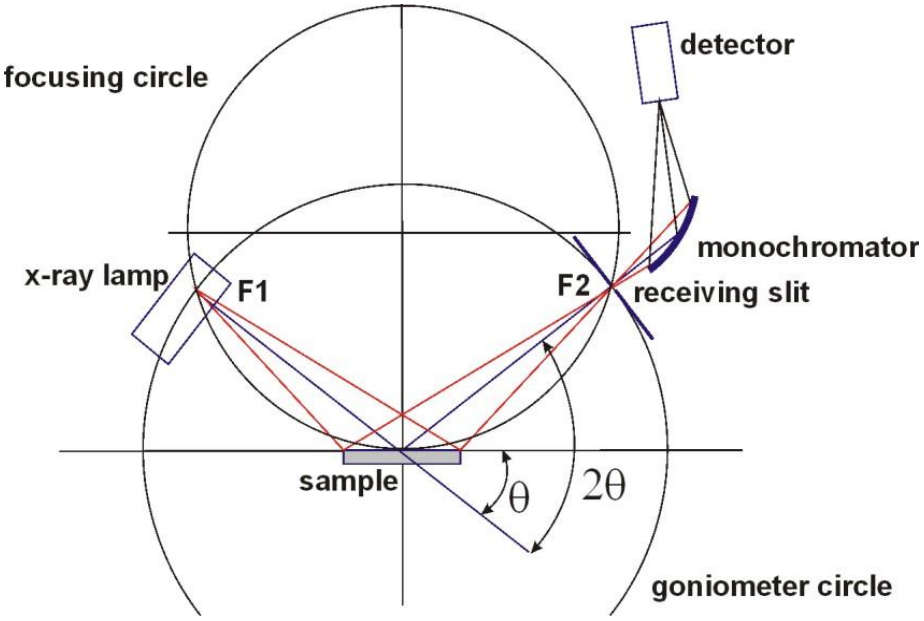


Fig 3.2 Schematic Representation of θ/2θ diffraction in Bragg-Brentano geometry

How does XRD Instrumentation work?

An X-ray instrument contains three main items: an X-ray source, a sample holder and an XRD detector.

The X-ray produced by the source illuminated the sample. It is then diffracted by the sample phase and enters the detector. By moving the tube or sample and detector to change the diffraction angle (2θ, the angle between the incident and diffracted beams), the intensity is measured, and diffraction data are recorded. Depending on the geometry of the diffractometer and the type of sample, the angle between the incident beam and the sample can be either fixed or variable and is usually paired with the diffracted beam angle.



Fig 3.3 XRD Instrument

Applications of XRD

Many researchers, both in commercial and scientific facilities, use X-ray diffraction (XRD) as a method to create novel materials or increase manufacturing efficiency. Innovations in X-ray diffraction are directly related to research on novel materials, such as semiconductor technology or medicinal investigations. Industrial research focuses on boosting the speed and efficiency of industrial operations. Fully automated X-ray diffraction examinations at mining and construction material production facilities lead to more cost-effective production control solutions.

The main uses of X-ray diffraction are:

Pure substances and mixtures are analysed both qualitatively and quantitatively. 'X-ray powder diffraction' (XRPD) is the most frequent technique for phase analysis.

- Analyse phase shifts under non-ambient variables including temperature, humidity, and applied pressure.
- Analyse physical characteristics of polycrystalline materials, including crystallite size (diameter), orientation, and residual stress, to determine their' microstructure'.
- Many of these methods may also be used to polycrystalline layered materials such as coatings and thin films using grazing incidence XRD (GIXRD). Microdiffraction is a technique used to investigate tiny regions in polycrystalline materials.

Other X-ray diffraction techniques for non-polycrystalline materials, such as single crystal semiconductor wafers or epitaxial layers, include high-resolution analysis of heteroepitaxial layers (HR-XRD). These are analysed using Bragg's Law, dynamical diffraction theory, and single crystal orientation for both wafers and ingots.

X-ray scattering

Other methods for studying a material's non-crystalline components using X-ray scattering methods include grazing incidence small-angle X-ray scattering (GISAXS), small-angle X-ray scattering (SAXS), total scattering (also known as Pair Distribution Function (PDF) analysis), and X-ray reflectometry. Each technique uses its own data analysis algorithm based on fundamental scattering theory.

Advantages of XRD

XRD is a quick technique (usually less than 20 minutes) and is frequently the most precise and reliable method for unambiguously identifying unknown materials.

Sample preparation is minimal, which is why this approach is so popular. It may be used in both industrial process applications and materials research.

With the correct analytical tools, data analysis may be relatively simple, and for industrial operations, it can even be automated, so that the operator in QC applications does not need to be an XRD expert.

2. Field Emission Scanning Electron Microscopy (FESEM)

A field emission scanning electron microscope (JEOL JSM-6700F) was used to collect field emission scanning electron micrographs (FE-SEM) of the generated samples to evaluate their microstructure and surface morphology. A scanning electron microscope (SEM) is an electron microscope that takes photographs of materials by scanning them with a high-energy electron beam. Electrons interact with atoms, producing signals that provide important information about the sample's surface structure or composition.

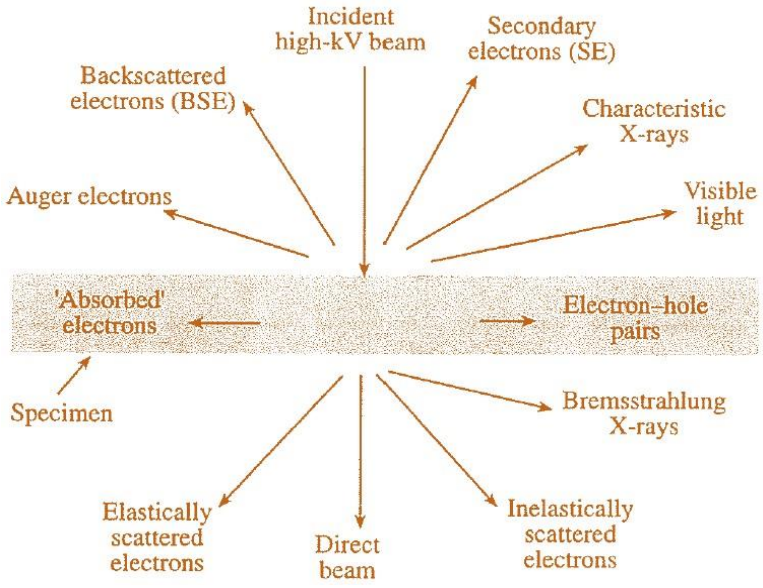


Fig 3.4 Schematic drawing of signals generated when a high-energy beam of electrons interacts with a thin specimen.

When an incoming or primary electron beam interacts with a material, the electrons lose energy due to random scattering and absorption. The energy exchange between the sample and the electron beam produces elastic scattering to reflect high energy electrons (HEE), inelastic scattering to emit electromagnetic radiation, and a variety of other radiations, as seen in Figure 3.5

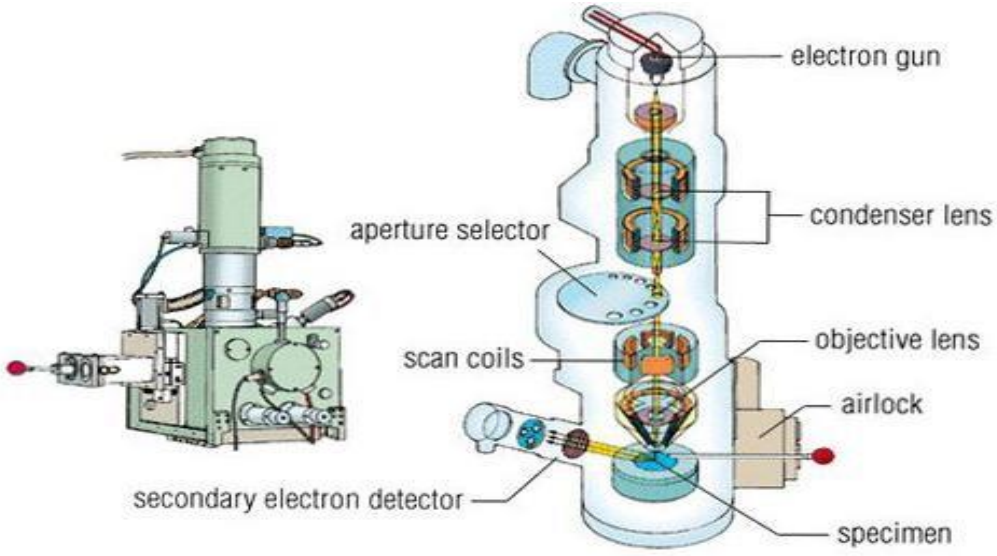


Fig 3.5 Schematic drawing of a conventional scanning electron microscope (SEM).

This Figure depicts a schematic concept for SEM imaging. In a conventional SEM, an electron beam is thermionically emitted from an electron cannon with a tungsten filament cathode. The FESEM generates electron beams using a field emission gun (FEG) rather than a thermionic cannon, allowing the production of an electron probe with a diameter of around 0.50 nm, enabling high resolution imaging and opening up new paths for fascinating surface characterization applications.

The SEM micrographs of the newly prepared samples were then taken with a field-emission SEM (JEOL, model JSM-6700F). For SEM studies, the samples were mounted on a specimen stub and platinum was sputtered on them under vacuum to provide a path to ground for the specimen current, as the specimen's local charge can be a more serious issue, repelling incident electrons and deflecting the scanning probe, resulting in image distortion or fluctuations in image intensity. The sample stub is placed inside the sample chamber under vacuum, and images are taken with a voltage of 5 kV and a current of 10 A.



Fig 3.6 FESEM Instrument

Advantages of Scanning Electron Microscopy

Here are some benefits of using SEM with EDS for materials characterization and failure analysis.

- Resolution

This test generates digital images with resolutions as low as 15 nanometers, giving useful information for analysing microstructures such as fracture, corrosion, grains, and grain boundaries.

- Traceable standard for magnification

Because all imaging is calibrated to a traceable standard, stored pictures may be analyzed for coating thicknesses, grain size estimations, and particle sizing.

- Chemical analysis

SEM using EDS may do qualitative elemental analysis, standardless quantitative analysis, x-ray line scans, and mapping. This information may be utilized to investigate product flaws, detect the elemental makeup of foreign components, measure coating thickness, and calculate grain and particle size.

Disadvantages of Scanning Electron Microscopy

While SEM with EDS is an effective test for surface typography and chemical analysis, it is not appropriate for all materials. Here are some reasons why you should explore various forms of material analysis.

- Vaccum Environment

In most circumstances, SEM samples must be solid and vacuum-safe. However, greater pressures can be employed to image vacuum-sensitive, nonconductive, and volatile materials.

- Artifacts are possible

Strong insulator samples must be coated (typically with gold or carbon) before testing. However, this technique can produce artifacts. However, preparation and analysis by a skilled SEM testing lab guarantees that these artifacts have no effect on test findings.

3. Fourier Transform Infrared (FT-IR) Spectroscopy:

Fourier Transform Infrared Spectroscopy, often known as FTIR Analysis or FTIR Spectroscopy, is an analytical technique for detecting organic, polymeric, and, in certain cases, inorganic materials. FTIR analysis scans test samples using infrared light to identify their chemical properties.

How does FT-IR Works?

The FTIR instrument sends infrared light from 10,000 to 100 cm-1 through a substance, with some being absorbed and some flowing through. The absorbed radiation is converted into rotational and/or vibrational energy by the sample molecules. The resulting signal at the detector is shown as a spectrum spanning 4000 cm-1 to 400 cm-1, revealing the sample's chemical fingerprint. Each molecule or chemical structure produces a distinct spectral fingerprint, making FTIR analysis a valuable tool for chemical identification.

What is FTIR used for?

FTIR spectroscopy is a well-known quality control technique for examining industrially produced materials, and it is commonly employed as the first step in the material analysis process. A change in the characteristic pattern of absorption bands indicates a change in the material's composition or contamination. If defects in the product are discovered by visual inspection, the source is frequently identified using FTIR microanalysis. This approach is ideal for evaluating the chemical composition of both microscopic particles (10-50 microns) and larger areas on the surface.

FTIR analysis is used to:

- Identify and describe unknown materials, such as films, solids, powders, or liquids.
- Detect contamination on or in a substance (such as particles, fibers, powders, or liquids).
- Identify additives extracted from a polymer matrix.
- Identify oxidation, decomposition, or uncured monomers in failure analysis studies.

FTIR Sample Introduction Techniques

Proper FTIR analysis is only as successful as its ability to inject and monitor energy from a specific matrix. Fortunately, we have a range of sample preparation and introduction protocols available in the lab to assure accurate analysis. In the early days of infrared spectroscopy, transmission was the only available method of investigation. To do transmission analysis, the sample must be made transparent to laser and infrared radiation by placing it directly in the optical path, casting a thin coating on a salt crystal, or mixing a powder form of the sample with salt and casting.

Because of technological developments, we now use both transmission and reflectance approaches. We use optics to inject and detect energy, typically using versions of ATR (Attenuated Total Reflectance) approaches. ATR uses internal reflection to transmit incident energy. The energy beam enters a crystal at an angle, allowing it to bounce internally at the bottom and top before leaving on the opposite side. The sample makes contact with the crystal at the top, allowing energy interaction to occur at the interface between the crystal and the sample, which is where the bouncing happens. Typically, having more bounce spots results in more energy transfer and hence improved spectral response. However, single bounce systems are used to analyze relatively tiny regions.

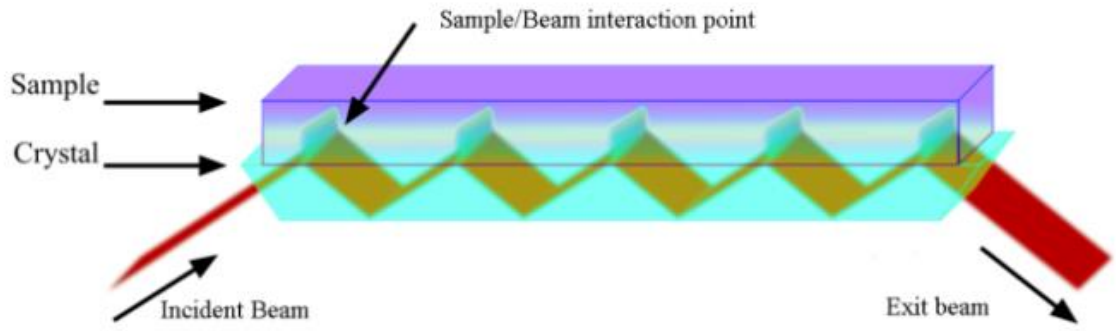


Fig 3.7 Interaction of the infrared beam with the sample when introduced via Attenuated Total Reflectance (multi bounce)

For liquid and paste samples, we often use a HATR (Horizontal Attenuated Total Reflectance) multi bounce technique, which includes putting the sample horizontally over a crystal plate or trough and enabling gravity to make intimate contact with the cell. Different crystals can be used, varying the depth of penetration into the sample. For example, for rubber analysis, we will use a germanium crystal to limit the impact of strong IR absorption chemicals in rubber (namely carbon black), but for daily samples, the zinc selenide crystal is preferable for longevity, moisture resistance, and penetration depth. When we wish to concentrate the beam on specific areas of interest, we'll use the FTIR bench's micro-ATR adaptor to direct it to a single bounce ATR crystal. With optical observation via the ATR cell, we may position the sample in close contact with the ATR crystal, with an irradiating zone of around 0.2mm in diameter. When precise positioning is necessary to characterize a sample area, layer, or micro-fine particle, we move the investigation to a microscopic FTIR system with a positioning precision of 10 microns in diameter. The microscopic FTIR in reflectance mode allows us to use small optics in conjunction with a concentrated infrared beam to send an ATR probe directly to the region of interest. This method also allows us to spatially resolve differential chemistry in very small regions. In addition to the ATR reflectance techniques listed above, there are other reflectance There are several methodologies available, including specular reflectance, which measures the energy from a genuine surface reflectance at a single angle of measurement, and diffuse reflectance, which measures the energy from a true surface reflectance at numerous angles. Your consultant analyst may advise you on which technique is best for your application, matrix, and measurement objectives.

Advantages and Disadvantages of FTIR Spectroscopy

Advantages of FTIR:

- Fourier Transform Infrared Spectroscopy (FTIR) is a sensitive and rapid approach for obtaining high-quality spectra.
- This spectroscopy provides a higher signal-to-noise ratio than the dispersive instrument.
- FTIR allows for rapid spectrum analysis, saving time.
- FTIR may be used to analyse gases, solids, and liquids.
- Using FTIR, no external calibration is necessary and produces reliable findings.
- FTIR is a non-destructive method.
- Fourier transform infrared spectroscopy can easily identify both organic and inorganic substances.
- Mechanical breakdown is smaller than in other instruments since the mirror coupled to the interferometer is the sole moving portion in FTIR.
- Multiple gaseous chemicals can be analysed simultaneously.
- FTIR can detect even low levels of contamination.
- The FTIR instrument uses a laser beam for reliable calibration.
- Scans typically take 1–2 seconds to complete.
- High Resolution

Disadvantages of FTIR are:

- FTIR instruments have a single beam, whereas dispersive instruments often have two beams.

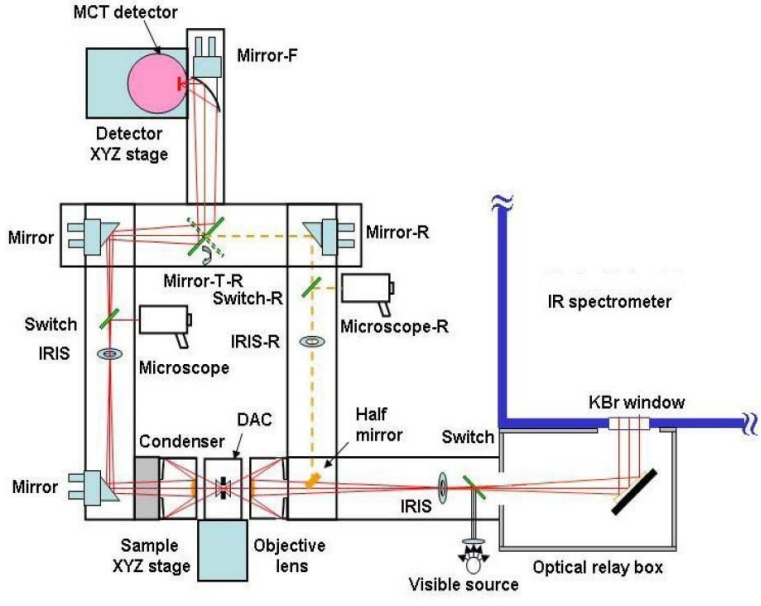


Fig 3.8 Schematic diagram of FTIR spectrometer.

4. Differential Scanning Calorimetry:

Differential Scanning Calorimetry (DSC) is a method in analytical chemistry that measures the heat flow caused by physical and chemical changes in materials as a function of temperature. It is commonly used to describe the thermal characteristics of materials, such as melting point, glass transition temperature, crystallization behavior, and reaction kinetics.

The idea of differential scanning calorimetry (DSC) is to compare the heat flow into a sample and a reference material while they are subjected to a controlled temperature program. Any energy differential between the sample and the reference material shows that a physical or chemical change has occurred in the sample. This enables the assessment of the sample's numerous thermal characteristics, including phase transitions, enthalpy changes, and heat capacity.

Thermodynamic Equations :

i. Enthalpy:- $H=\int_0^T C_p dT$

ii. Energy:- $U=\int_0^T C_v dT$

iii. Entropy:- $S=\int_0^T \frac{C_p}{T} dT$ or $S=\int_0^T \frac{C_v}{T} dT$

iv. Gibbs Free Energy:- $G = H - TS$

v. Helmothz Free Energy:- $F=U - TS$

Calorimetry is generally based on the following relationship:

$dQ = C.\Delta T = c.\ m.\ \Delta T$

In differential form assuming time independent sample mass and specific heat capacity

$$dQ = C.\Delta T = c.m.\Delta T$$

$$\frac{dQ}{dt} = \emptyset = C.\frac{dT}{dt} = c.m.\beta$$

In differential form assuming time independent sample mass and specific heat capacity where dQ is the heat exchanged ΔT is the temperature change caused by the heat exchange C is the heat capacity c=C/m is the specific heat capacity and m is the sample and β is the scan rate. DSC operates in the temperature range of $-80℃$ to $500℃$ in a nitrogenous atmosphere. In the case of a semi-crystalline polymer matrix like P(VdF-HFP), we may compute X_c, which is the proportion of crystalline phase of P(VdF-HFP) in the gel polymer electrolyte.

Working Principle:

Differential scanning calorimetry (DSC) compares the heat flow into a sample and a reference material when subjected to controlled temperature variations. Here's a thorough description of how it works:

The sample and reference materials are put in separate pans within the calorimeter. To guarantee an appropriate comparison, these pans have equal shapes and masses. The system regulates the temperature of both the sample and reference pans at the same time, usually using a programmable temperature controller. The temperature ramp might be linear or stepwise, depending on the experimental needs. As the temperature varies, heat flows into and out of the sample and reference pans. A sensor detects the amount of heat (energy) necessary to keep both pans at the same temperature. The heat flow is shown as a function of temperature and time. The heat flow into the sample is compared with that of the reference material. Any difference in heat flow between the sample and the reference suggests that a thermal event is taking place within the sample, such as melting, crystallization, phase transitions, or chemical reactions. The resultant DSC curve shows heat flow as a function of temperature. The curve's peaks and troughs correspond to endothermic (heat absorption) and exothermic (heat release) activities. Scientists may identify several thermal parameters of the sample by evaluating the form, location, and amplitude of these peaks or troughs, including melting point, glass transition temperature, enthalpy changes, and reaction kinetics. Before beginning research, the DSC equipment is calibrated using established reference materials to achieve precise temperature and heat flow data. Furthermore, validation tests are carried out to ensure the instrument's functionality and data dependability.

In summary, DSC allows for the evaluation of thermal properties and behavior of materials by monitoring the heat flow associated with temperature-induced changes, which provides vital insights into their physical and chemical characteristics.

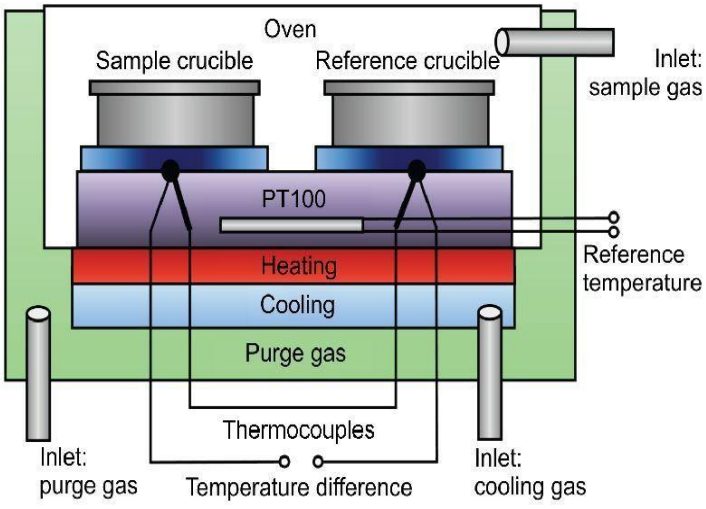


Fig 3.9 Schematic drawing of DSC measurement technique

Advantages:

- Requires a small (a few milligrams) sample size;
- Accurate measurement of temperature and magnitude of phase transitions and heat capacities;
- Clear physical meaning of test results;
- Ability to detect weak phase transitions;
- Ability to separate overlapping thermal transitions (Modulated DSC option).

Disadvantage:

- Destructive method;
- No direct structural information;
- Requires no interaction between a sample and a DSC pan.

5. Thermogravimetry Analysis (TGA):

Thermogravimetric analysis, or TGA, quantifies weight changes in an experimental material as a function of temperature in a controlled N2 environment. Figure 2.12 depicts gradually rising the temperature of an experimental sample in a furnace while its weight is monitored in an analytical balance located outside of the furnace. TGA detects mass loss when a heat event results in the loss of a volatile component. Distinct chemical processes, such as burning, cause weight loss, but distinct physical changes, such as melting, do not. The weight of the experimental sample is plotted versus temperature to show thermal transitions in the material, such as solvent and plasticizer loss in polymer electrolytes, water of hydration in inorganic materials, and degradation of the substance. Applications include determining carbon black content, decomposition temperature, moisture content of organic and inorganic materials, oxidation stability, stabilizer performance, polymer plasticizer content, low molecular weight monomers in polymers, and so forth. A TGA instrument (TA Instruments, Model: SDT Q600) was utilized to determine the range of stability of the samples in the current circumstances. At first, the sample (7-10 mg) was placed in an empty alumina pan, while Al2O3 was inserted in another pan as a comparison. The furnace temperature was raised at a rate of 10 K/min in a N_2 environment. The change in weight and heat differential provided significant information on thermal properties.

Working Principle:

A TGA instrument (TA Instruments, Model SDT Q 600) was utilized to determine the sample's stability range. The sample weighing 7-10 mg was placed in an empty alumina pan and balanced against alumina in another pan. The furnace temperature was raised at a rate of 10°C/min in N_2 atmosphere. The change in the weight and heat differential was observed for information on thermal properties.

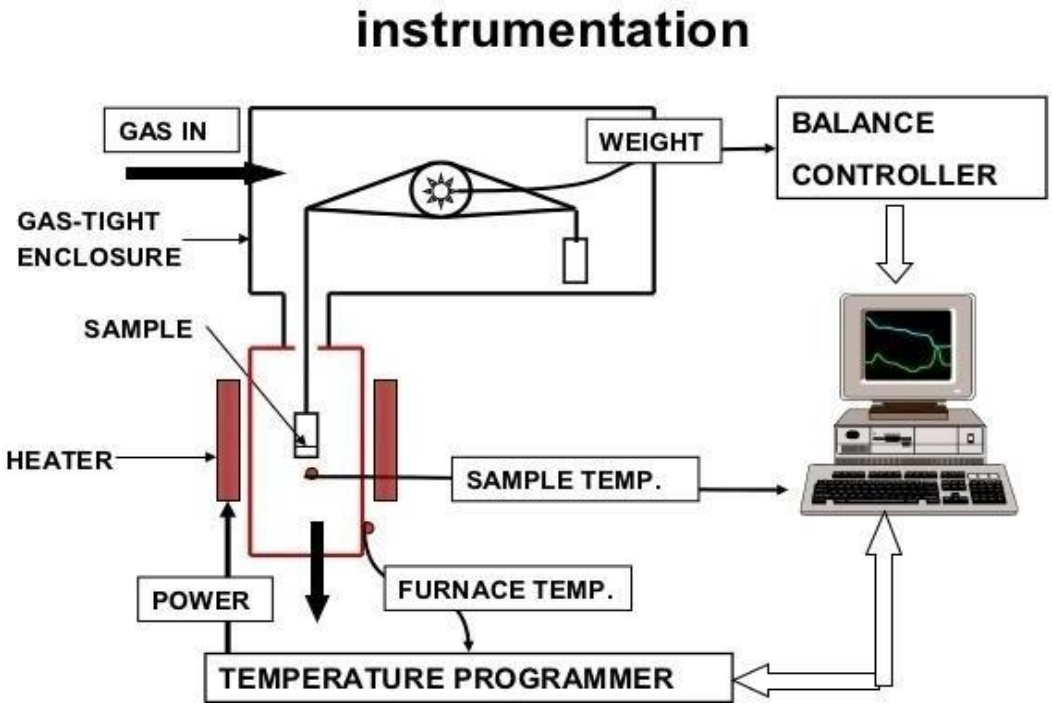


Fig 3.10 Schematic Diagram of a Thermogravimetry Analyzer

Advantages and Disadvantages of Thermogravimetry Analysis:

One of the most important advantages of thermogravimetric analysis is the **small quantity of sample required**. Even a few milligrams are, as a rule, sufficient for a reliable analysis. It is possible to analyse both **solid and liquid samples**. Also, minimal preparation of the sample is necessary.

However, TGA also has limits: it is not able to actively verify the presence of a specific substance. **Verification is only indirect** because a change in mass is explained by means of corresponding prior knowledge of the temperature-dependent behaviour of a specific substance.

Electrochemical Characterization of Devices –

For electrochemical characterization of fabricated electrochemical capacitor different techniques were adopted such as

i. Electrochemical Impedance Spectroscopy (EIS)
ii. Cyclic Voltammetry (CV)
iii. Galvanostatic Charge Discharge

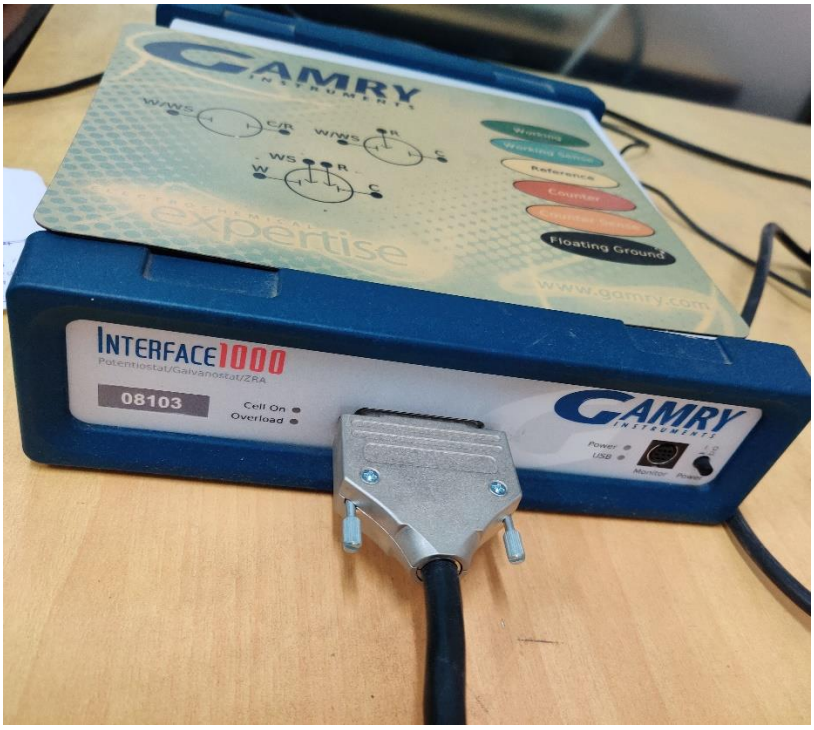


Fig 3.11 Gamry

i. Electrochemical Impedance Spectroscopy (EIS) –

Electrochemical impedance spectroscopy is a highly effective approach for investigating the electrochemical performance of electrical double layer (EDL) capacitors. Electrochemical impedance spectroscopy works by applying a small alternating current (ac) potential to an electrochemical sample over a wide range of frequencies and measuring the changes in current caused by the experimental sample's electrochemical impedance as a function of frequency. The Nyquist plot compares the imaginary impedance function (Z″) to the actual impedance function (Z′) and corresponds with system stability. The impedance pattern of an ideal capacitor exhibits a sharp rising dispersion line that overlaps with the impedance plot's imaginary axis, implying a straight line parallel to the y axis. The impedance pattern of a real capacitor is a semicircle. The equivalent series resistance (ESR) value of the electrical double layer (EDL) capacitor observed at high frequencies

is calculated using the intercept of the Nyquist plots with the actual impedance spectra axis, which is determined by R_1. The electrolyte resistance and contact resistance of the active material or current collector interface are the primary factors determining ESR value. The next intercept on the real impedance axis, indicated by R_2, indicates the charge transfer resistance (R_{ct}), which is determined as the difference between two intercepts ($R_{ct} = R_2 - R_1$). The R_{ct} value is also described as the diameter of the semicircle section of the Nyquist plot in the high frequency band, which is mostly influenced by the electron transfer process in an electrochemical sample system. The inclination line represents the electrolyte's ion diffusion behavior inside the composite electrode at intermediate frequencies. The virtually straight tail is mostly impacted by the diffusion process, which occurs in the lower frequency band.

The EIS measurements are performed with the Gamry equipment. The frequency range increases from the low frequency range of 10 mHz to 1MHz. The entire capacitance may be measured using the following relationship:

$$C_{overall}^{EIS} = -\frac{1}{2 \times \pi \times f \times Z"}$$

Where f is the frequency in Hz and Z" is the imaginary component of the total impedance measured. The specific capacitance values were calculated by multiplying the overall cell capacitance by two and dividing by the mass of a single electrode active material in g.

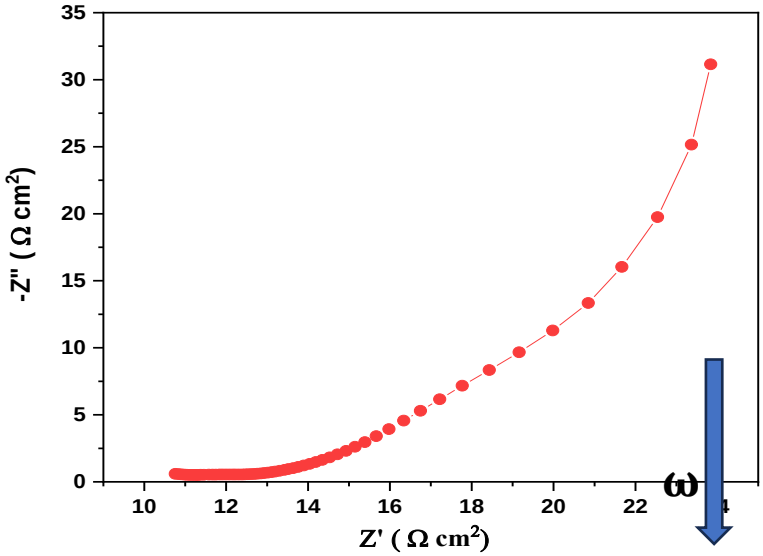


Fig 3.12 Impedance plot of a real supercapacitor

ii. Cyclic Voltammetry (CV) –

Cyclic Voltammetry is a significant probe characterization technique that applies a time-varying voltage to electrodes. The working electrode's potential is swept between two fixed positions at a constant scan rate. In CV, the initial set point is chosen so that no electrode response occurs, resulting in almost negligible current for the applied voltage. The equilibrium locations, also known as open circuit potentials, are at the start and end points. The nature of the current is revealed as a function of the scanned potential. The reversal of the potential scan rate causes a rise in the current due to the products' response. In CV, the current value climbs during the charging cycle until it reaches the extreme set point, then lowers during the discharging cycle until it is virtually zero. Thus, the forward and backward reactions occur during the charging and discharging cycles at a constant potential scan rate.

The cyclic voltammetry of an ideal capacitor with low internal resistance yields a perfect rectangular form that is scan rate dependent. Real capacitors deviate from the rectangular shape because they are a series mix of internal resistance, R, and capacitance, C.

In our investigation, all Cyclic Voltammetry measurements were acquired with Gamry Instruments (Interface 1000) and analysed using Origin Lab Software for various scan speeds at a fixed voltage range of -1 V to 1 V. The specific capacitance may be calculated using the following expression:

$$C_{Sp}^{CV} = \frac{\int I\, dV}{2 \times m \times s \times \Delta V}$$

In the following calculation, ∫ IdV represents the integrated area of the CV curve, m is the single electrode mass of the active material in g, s is the scan rate, and ΔV is the voltage range.

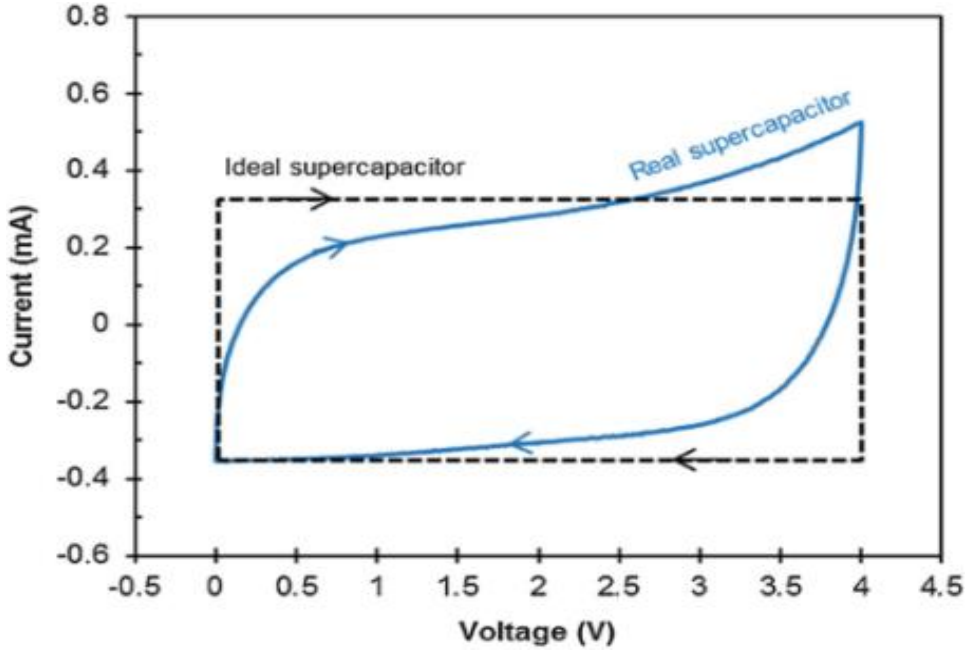


Fig 3.13 Cyclic Voltammetry of a) real supercapacitor and b) ideal supercapacitor

iii. Charge – Discharge Method

Charge-discharge methods are ways for assessing the performance of energy storage systems such batteries, supercapacitors, and fuel cells. These approaches entail charging the device to a certain amount of energy storage capacity and then discharging it under controlled settings to assess its behaviour.

- Galvanostatic Charge-Discharge –

  Galvanostatic charge-discharge involves applying a constant current to an electrochemical sample, such as a battery or capacitor, during both the charging and discharging processes. This method maintains a steady rate of charge transfer, enabling precise control and analysis of the sample's behaviour. During charge, the constant current drives the accumulation of charge carriers, storing energy in the sample. Conversely, during discharge, the constant current facilitates the release of stored energy. Monitoring voltage changes over time provides insights into the sample's electrochemical properties and performance characteristics, crucial for optimizing energy storage systems.

  When a supercapacitor cell is charged with a constant current i, the total voltage created across the cell may be represented as:

$$V = iR + \frac{\int I\, dt}{C}$$

  Since the current is constant, the expression may be written as:

$$V = i(R + \frac{t}{C_c})$$

  For a current step, the voltage across an ideal supercapacitor cell whose capacitance value increases linearly with time. After fully charging the supercapacitor to the highest permitted or desirable voltage level, it is discharged galvanostatically. The voltage decreases practically linearly with time. The voltage across the cell decreases linearly with time. When charging and draining a genuine EDL supercapacitor, a sharp decrease is noticed. An ohmic internal resistance is also known as the supercapacitor cell's equivalent series resistance. ESR is determined using the following relationship:

$$ESR = \frac{\Delta V_r}{2 \times i}$$

  The term ΔV_r refers to the internal ohmic voltage drop, whereas "i" represents the discharge current. The total capacitance of the supercapacitor cell was determined from the linear component of the discharge curve using the following relation:

$C_{cell}^{dis} = \frac{i}{m_{tam} \times \frac{\Delta V}{\Delta T}}$, where i is the discharge current m_{tam} is the total active mass in g and ΔV/Δt is the slope of the discharge characteristics after IR drop. In, symmetrical cell system, the specific capacitance referred to a single electrode (C_{sp}^{dis}) is related to overall capacitance of the cell (C_{cell}^{dis}) by the following relation:

$C_{sp}^{dis} = 4 \times C_{cell}^{dis}$. The charge-discharge experiment can be performed several times (between 4000 and 8000 cycles) to determine the cell's stability and cyclic efficiency. The charge-discharge experiment involves measuring the voltage over time with constant currents ranging from 0.5 to 5.0 mA. The ratio of discharge time to charging time, known as Coulombic Efficiency (CE), is derived using the following equation:

$$\eta\% = \frac{\Delta t_d}{\Delta t_c} \times 100\ \%$$

where , Δt_d and Δt_c are discharging and charging time obtained from charge and discharge curve respectively.

The energy density and power density are calculated from the charge discharge characteristics at different current rates using the following relations:

$$E = \frac{C_{cell}^{dis} \times (\Delta V)^2}{2} \times \frac{1000}{3600}$$

and

$$P = \frac{E \times 3600}{\Delta t}$$

Where C_{sp}^{dis} is the specific capacitance and ΔV is the cell voltage and Δt is the discharge time.

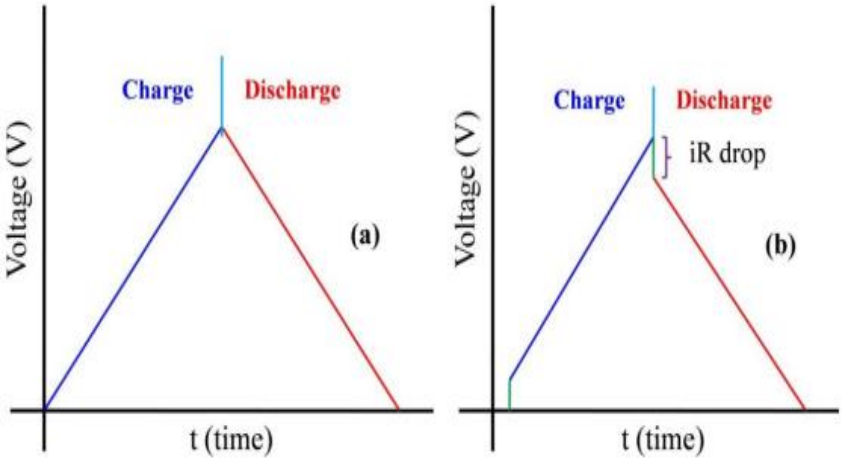


Fig 3.14 Charge discharge behaviour of a) an ideal supercapacitor and b) EDL capacitor

When a potential step is applied across a capacitor cell the capacitor charges and an exponentially decaying current is observed. The behaviour of the current I with respect to time on application of potential step V_o can be expressed as:

$$I = \frac{V_o}{R} \exp\left(-\frac{t}{\tau}\right)$$

where τ=RC is the time constant. The capacitor cell starts discharging when the operation is reversed and the pattern is like the discharge curve with reverse polarity. The charge discharge curves can be integrated to obtain the total charge stored or released. The capacitance C can be calculated as the total charge divided by the total applied voltage V_o.

CHAPTER 4:
SAMPLE PREPARATION AND FABRICATION

Synthesis of Redox Additive based Ionic Liquid based Gel Polymer Electrolytes

Polymer electrolytes have a rich history, evolving through several key phases since their inception. Here's a brief overview of their development:

The concept of polymer electrolytes was first introduced in the 1970s. Researchers began exploring the idea of incorporating salts into polymer matrices to create a material that could conduct ions. One of the pioneering works was by Fenton, Parker, and Wright in 1973, who studied the ionic conductivity in poly (ethylene oxide) (PEO) complexed with alkali metal salts. This marked the discovery of solid polymer electrolytes (SPEs). During the 1980s, significant efforts were made to enhance the ionic conductivity of polymer electrolytes. Researchers experimented with different polymers, salts, and plasticizers. The focus was on understanding the mechanisms of ion transport and the interaction between polymers and salts. Key studies demonstrated that PEO and lithium salts had favourable properties for conductivity. The development of lithium-ion batteries brought commercial interest to polymer electrolytes. Solid polymer electrolytes were seen as potential components for safer, more efficient batteries. To improve ionic conductivity and mechanical properties, gel polymer electrolytes were developed. These are essentially solid polymer electrolytes swollen with liquid electrolytes. Incorporation of nanoparticles into polymer matrices to create nanocomposite electrolytes, which offer enhanced mechanical strength and ionic conductivity. Integration of ionic liquids with polymers to create hybrid electrolytes with high ionic conductivity and thermal stability. Ongoing research focuses on solid-state batteries using advanced polymer electrolytes for higher energy density and safety. Various innovations include polymer blends, block copolymers, and single-ion conductors. Recent trends emphasize using biodegradable and environmentally friendly polymers to create greener electrolyte options.

Some polymer electrolytes have found commercial applications in consumer electronics, electric vehicles, and renewable energy storage systems. Continuous improvements in understanding the fundamental properties and performance of polymer electrolytes have led to better materials for various electrochemical applications.

Polymer electrolytes continue to be a vibrant area of research, with ongoing innovations aimed at addressing the challenges of conductivity, stability, and compatibility with modern energy storage technologies.

INTRODUCTION

Gel polymer electrolytes (GPEs) are a crucial category of ionic materials utilized in numerous applications such as supercapacitors, coin cells, batteries, dye-sensitized solar cells, and thin film transistors. GPEs are typically formed by embedding liquid electrolytes within a host polymer matrix, which offers the stability of solids and the high ionic conductivity of liquids. These quasi-solid or gel-like electrolytes address issues associated with liquid electrolytes, such as evaporation and leakage, and improve the ionic conductivity typically lacking in solid electrolytes. GPEs consist of a solvent, host polymer matrix, and salts. Essential attributes of the host polymer matrix include polarity, a low glass transition temperature, and high amorphousness. The chosen salt should be soluble in the plasticizer, possess large anions, and have low dissociation energy. The solvents or plasticizers used should have:

- A high dielectric constant to enhance salt dissociation
- Low viscosity for better ionic mobility
- A high boiling point to prevent evaporation over the desired temperature range
- A low freezing points
- Chemically active dipoles

Additionally, plasticizers should exhibit thermal and electrochemical stability, chemical compatibility, and effective plasticizing properties. Various thermoplastic polymer matrices, such as poly(methyl methacrylate) (PMMA), poly(acrylonitrile) (PAN), poly(vinylidene fluoride) (PVdF), and poly(vinylidene fluoride co-hexafluoropropylene) (PVdF-HFP), are proposed as frameworks for GPEs. This study specifically employs ionic liquid-based gel polymer electrolytes in an electric double layer supercapacitor.

Polymer Electrolyte embedded with Ionic Liquids:

Many researchers are increasingly focusing on ionic liquids as a novel electrolyte component that could enhance electrochemical performance. Unlike inorganic salts, which need to be dissolved in a solvent to dissociate into ion pairs, ionic liquids remain in a molten state at room temperature due to their bulky, asymmetric cations, and inorganic anions, eliminating the need for solvation. Integrating ionic liquids into the polymer matrix is seen as a highly promising approach to enhancing the physicochemical and electrochemical properties of polymer electrolytes. With their exceptional characteristics, ionic liquids are considered an excellent choice for achieving high electrochemical performance in various devices.

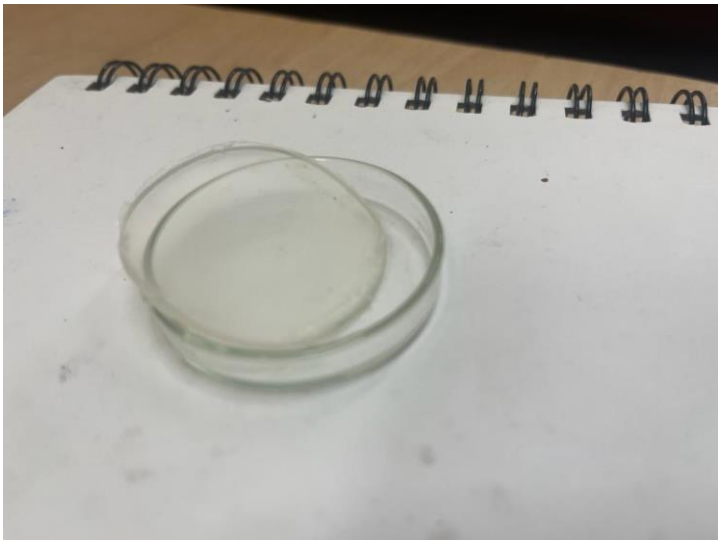


Fig 4.1 Synthesized Gel Polymer Electrolyte

Plasticized Polymer Electrolytes:

Plasticization is an essential technique to enhance the flexibility of polymer backbone chains and improve the ionic conductivity of polymer electrolytes. This is achieved by using various low molecular weight, non-volatile monomeric organic liquid plasticizers. Common plasticizers used in this process include polyethylene glycol (PEG), adiponitrile (ADN), ethylene carbonate, and propylene carbonate. Due to their small size, plasticizers can easily form strong polar interactions with the polymer backbone chains within the polymer matrix, increasing the local chain flexibility.

Experimental Section

Chemicals - All ingredients, including carbon compounds, ionic liquids, solvents and polymer matrix were utilized exactly as supplied. Adiponitrile (ADN) is utilized as a plasticizer,oly(vinylideneflouride-co-hexafluoropropylene)P(VDF-HFP), and Polyvinylidene fluoride (PVdF, powder) as a binder and ionic liquid (BMIM TFSI). Adiponitrile has a density of 0.951 g/ml, according to the Sigma Aldrich database. Aluminium foil, flexible graphite sheets with a thickness of 0.5 mm, acetone, acetylene carbon black (CB), activated carbon (AC), and redox additives (CsI, RbI, KI). Ionic liquids, like BMIM TFSI, have a density of 1.292 g/ml, according to the Sigma Aldrich database. These substances were employed without further purification. All ionic liquids were stored inside the argon gas filled glove box (mBRAUN LAB star ECO) with < 0.5 ppm H_2O and < 0.5 ppm O_2.

Preparation of Redox Active GPEs

To synthesize nonaqueous self-standing redox active gel polymer electrolyte (GPE) films via the solution casting method, a detailed process involving the preparation of specific compositions and controlled procedures is necessary. Below is a generalized methodology that can be tailored to your specific requirements:

1. GPE-IL: PVDF-HFP + ADN + BMIMTFSI + CsI (40 mg)
2. GPE-IL: PVDF-HFP + ADN + BMIMTFSI + RbI (40 mg)
3. GPE-IL: PVDF-HFP + ADN + BMIMTFSI + KI (40 mg)

Gel polymer electrolytes are produced using the cast solution method. In our procedure, we utilized PVDF-HFP (M.Wt. 455,000 g/mol) copolymer beads in a beaker with a standard stoichiometric amount. Subsequently, we incorporated Adiponitrile (ADN) plasticizers and BMIMTFSI Ionic Liquid in traditional stoichiometric ratios into the PVDF-HFP matrix placing it on a heat-top magnetic stirrer along with a magnetic bead. The weight ratio between PVDF-HFP, ionic liquid, and ADN was set at 2:3:5. Afterward, we reduce the temperature to 60°C and incorporate 40 mg of CsI (Caesium Iodide), constituting approximately 15 wt.% of the polymer matrix. The solution was then left without agitating for 1 or 2 hours before being poured into a clean petri dish to form a free-standing film with a thickness ranging from 0.25 to 0.35 mm. After being stirred for 1-2 hours, the solutions reached a viscous and homogeneous state, primarily as a result of solvent evaporation. Ultimately, the solutions were poured into a clean petri-dish to obtain the gel polymer electrolyte film through slow solvent evaporation under ambient conditions. Next, we repeat the identical procedure for other redox additives, including RbI (Rubidium Iodide) and KI (Potassium Iodide), designating them as GPE-RbI and GPE-KI, correspondingly. The self-standing gel polymer electrolytes (GPEs) were cut into various sizes according to specific measurements.

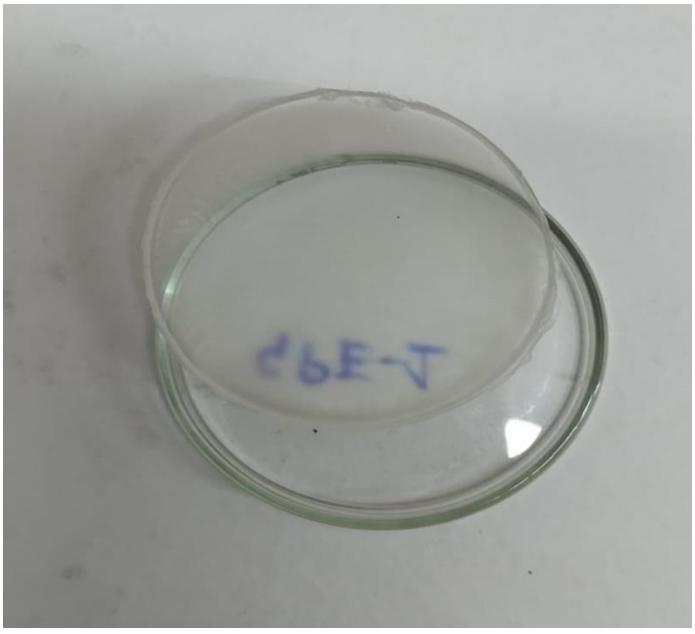
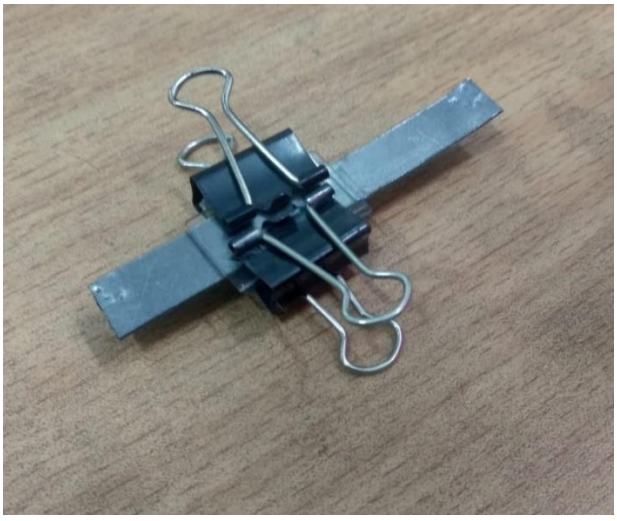
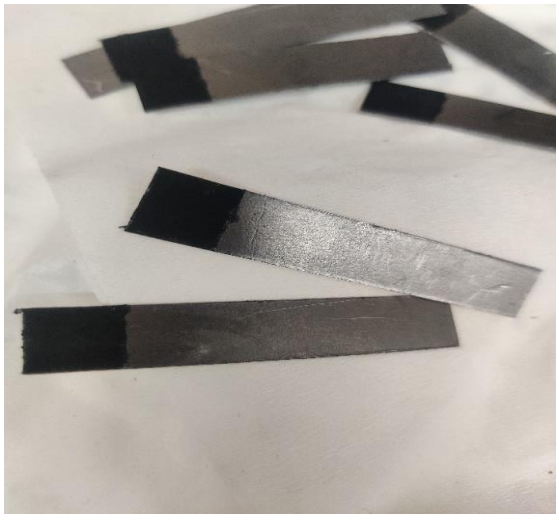


Fig 4.2 Synthesized Gel Polymer Electrolyte with Redox Additives

Electrode preparation and solid state electrochemical double layer capacitors assembly

The following is a brief description of the electrode preparation process: using a micropipette, a homogenous slurry containing activated carbon powder (AC), CB powder, P(VDF) as a binder, and dimethylformamide (DMF) as a solvent was applied to a flexible graphite sheet in a ratio of 75:10:15 (wt./wt.). The slurry was then dried in a magnetic stirrer with some heat. For a day, the carbon electrodes that were made were dried. The electrodes' average area was divided into 1×1 cm^2. By sandwiching GPE sheets between two symmetrical activated carbon electrodes and using a stainless-steel clamp to provide enough pressure, the symmetrical EDLC were put together. To prevent short circuits, the gel polymer electrolytes have a much bigger size than the electrode.





(i) EDL Capacitor *(ii) Electrodes*

Fig 4.3 (i) EDL Capacitor (ii) Electrodes

CHAPTER 5:
CHARACTERIZATION RESULTS AND DISCUSSIONS

CHARACTERIZATION OF GPEs

CHARACTERIZATION:

The X-ray diffraction (XRD) patterns of GPEs were obtained using a D8 advance Bruker AXS instrument with Cu K_α radiation (λ = 0.154 nm), a scan rate of 0.2° s^{-1}, and a step size of 0.02° over the angular range of 2θ ∼ 10−70° under ambient condition. The differential scanning calorimetry (DSC) experiment of GPEs was performed using a Q2000 TA Instruments in a N_2 atmosphere in the temperature range from −60 to 200 °C at a heating rate of 10 °C min^{-1}. The thermogravimetric analysis (TGA) was performed by using a Q600 TA Instruments from room temperature to 600 °C at a heating rate of 10 °C min^{-1}. The Fourier transform infrared (FTIR) spectra of GPEs were recorded in a FTIR spectrometer (PerkinElmer, model Spectrum100) with an attenuated total reflectance mode in the wavenumber range of 650−3500 cm^{-1} at a resolution of 1 cm^{-1}. The AC conductivity of different GPEs was measured using an LCR meter (HIOKI, model IM 3536 LCR) in the wide frequency range from 4 Hz to 8 MHz at room temperature. The GPEs were sandwiched in between two SS blocking electrodes with a diameter of about 10 mm.

The electrochemical potential window (ESW) stability was performed by a linear sweep voltammetry (LSV) technique at a 5 mV s^{-1} scan rate. The experiment for all GPEs was performed by using SS|| GPEs||Ag configuration in a VMP3 multichannel electrochemical analyzer (Bio-Logic). All the electrochemical characterizations such as electrochemical impedance spectroscopy (EIS), cyclic voltammetry (CV), and galvanostatic charge−discharge (GCD) were performed by using a VMP3 multichannel electrochemical analyser (Bio-Logic).

RESULTS AND DISCUSSIONS:

Physiochemical Properties of GPEs

1. Structural Analysis by XRD

X-ray diffraction (XRD) analysis is a technique used to determine the atomic and molecular structure of materials. It works by directing X-rays towards a sample, which then scatter off the atoms in the sample. The scattered X-rays produce a diffraction pattern that contains information about the arrangement of atoms in the material. By analyzing this diffraction pattern, researchers can determine properties such as crystal structure, lattice parameters, and phase composition of the material. XRD is widely used in various fields including materials science, chemistry, physics, and geology for characterizing crystalline materials and studying their properties.

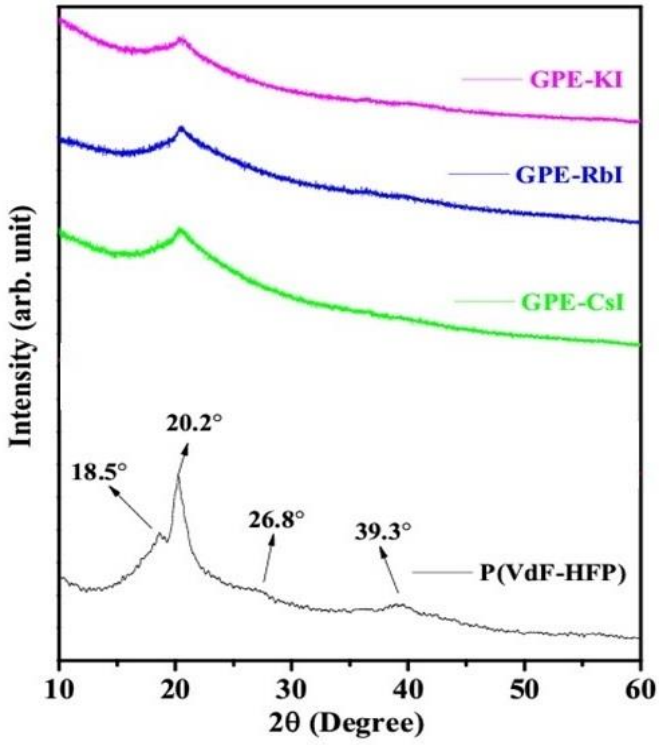


Fig 5.1 XRD patterns of P(VdF-HFP) and different GPEs

X-ray diffraction (XRD) has been employed to investigate the phase structure of the host polymer matrix poly(vinylidene fluoride-co-hexafluoropropylene) (P(VdF-HFP)) and various gel polymer electrolytes (GPEs) doped with ionic liquids (ILs). The XRD patterns of P(VdF-HFP) reveal crystalline peaks at 2θ values of approximately 18.5°, 20.2°, 26.8°, and 39.3°, indicating a semicrystalline structure. When plasticizers, ILs, and redox additives are introduced, notable changes in the structural properties of P(VdF-HFP) are observed. Several significant crystalline peaks disappear, leaving only a less intense and broader peak at around 2θ ≈ 20.2°. This suggests

that the crystalline nature of the polymer decreases gradually. Consequently, the addition of plasticizers, ILs, and redox additives plays a crucial role in enhancing the amorphous phase of the P(VdF-HFP) polymer matrix.

2. FESEM Analysis:

Field Emission Scanning Electron Microscopy (FESEM) is an advanced imaging technique that provides high-resolution images of sample surfaces. Unlike conventional scanning electron microscopy (SEM), FESEM uses a field emission gun (FEG) as its electron source, which produces a narrow, high-energy electron beam. This beam interacts with the atoms at the surface of the sample, causing the emission of secondary and backscattered electrons. These electrons are then collected by detectors to create a detailed image of the surface.FESEM is renowned for its ability to produce images with extremely high resolution, often down to the nanometer scale. This makes it an invaluable tool in various fields such as materials science, biology, nanotechnology, and semiconductor research. The technique provides detailed information about surface morphology, topography, and composition, enabling researchers to analyze the fine structure of materials and biological specimens.

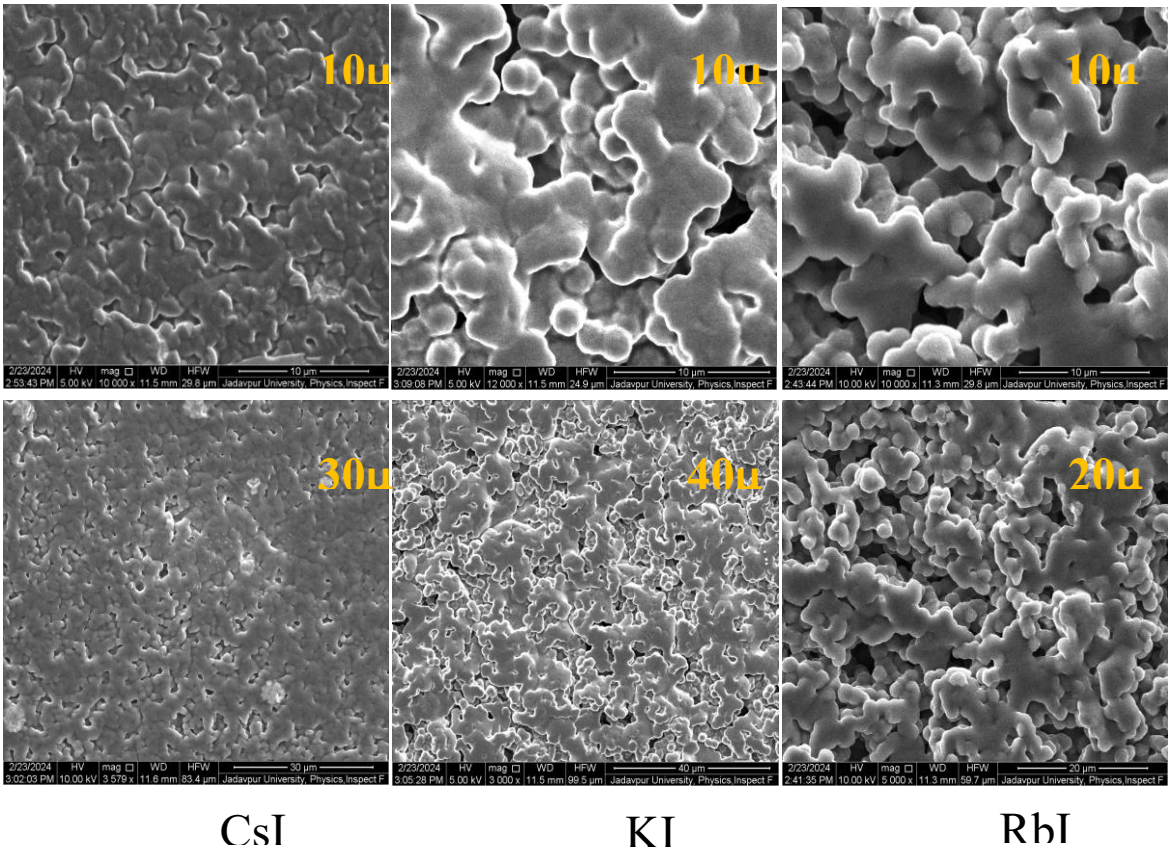


Fig 5.2 SEM Images of different GPEs (i) Cesium Iodide (CsI) (ii) Potassium Iodide (KI) (iii) Rubidium Iodide (RbI)

MORPHOLOGY

The FESEM data suggests that the Gel Polymer Electrolyte (GPE) containing various redox additives displays an irregular surface morphology characterized by interconnected granules. These granules exhibit slight variations in size. This irregular morphology could indicate non-uniform distribution of the redox additives within the gel polymer matrix. The presence of interconnected granules suggests that there might be regions of differing composition or density within the electrolyte. Understanding the morphology of the electrolyte is essential as it can influence its mechanical, electrical, and electrochemical properties, thereby impacting its performance in various applications such as energy storage devices.

3. FTIR Analysis:

Fourier Transform Infrared Spectroscopy (FTIR) is a versatile analytical technique used to investigate the chemical composition and molecular structure of materials based on their interaction with infrared radiation. It operates by directing infrared light onto a sample and measuring the absorption and transmission of this light as it interacts with the sample's molecular bonds. The resulting spectrum, known as an infrared absorption spectrum, provides valuable information about the functional groups, chemical bonds, and molecular structure present in the sample. FTIR analysis is widely applied in various fields such as chemistry, materials science, pharmaceuticals, polymers, environmental science, and forensic science for identification, characterization, and analysis of organic and inorganic substances.

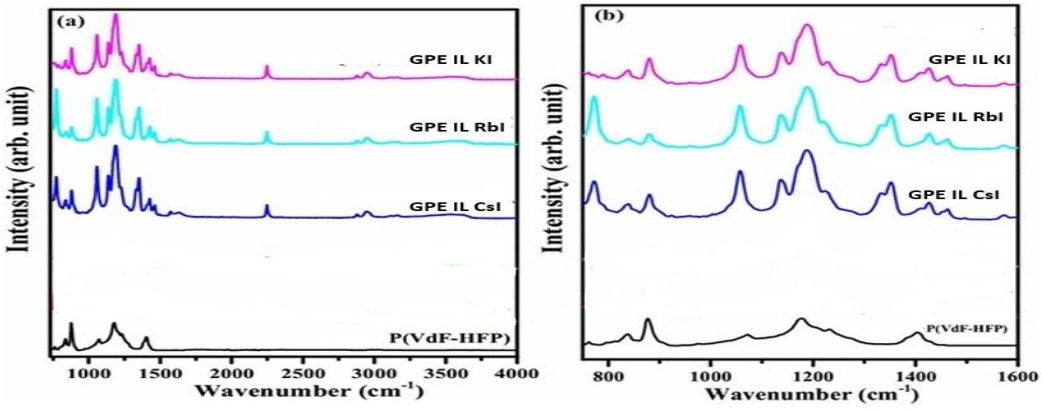


Figure 5.2 (a) FTIR spectra of P(VdF-HFP) and different GPEs in the wavenumber range of 750−4000 cm^{-1} and (b) Enlarged view of FTIR spectra of P(VdF-HFP) and different GPEs in the wavenumber range of 750−1000 cm^{-1}.

The FTIR spectra of different GPEs are presented in Figure.3(a) in the wavenumber range 750−4000 cm^{-1} to investigate the various possibilities of interactions. Figure.3(b) presents the FTIR spectra in the wavenumber range 700−1600 cm^{-1}. It is observed that the pure P(VdF-HFP) exhibits IR bands at 762, 796, and 976 cm^{-1} corresponding to CH_2 rocking, CF_3 stretching, and C−F stretching, respectively. These three bands represent the crystalline α-phase of the P(VdF-HFP) polymer matrix.

In addition, the pure P(VDF-HFP) shows peaks at 837 and 881 cm^{-1}, which correspond to CH_2 rocking and mixed mode and CF_2 and C−C symmetric stretching, respectively, due to amorphous β-phase of P(VDF-HFP). The ADN plasticizer based (GPE) polymer electrolyte shows different IR bands at wavenumbers such as 773, 837, 881, 974, 1070, 1180, 1215, 1334, 1424, 2248, 2868, and 2947 cm^{-1}.

The peaks at 837 and 881 cm^{-1} signify the existence of the amorphous phase in the GPE due to the interaction of the plasticizer with the polymer matrix. The GPE system shows that the peak intensity of the amorphous phase (881 cm^{-1}) increases, and the peak for crystalline phases (773 cm^{-1}) disappears. The peaks at 2248, 2868, and 2947 cm^{-1} arise from the addition of the plasticizer. The peaks at 2868 and 2947 cm^{-1} correspond to the C−H stretching vibration band of the GPE.

The intensity of 1070, 1180, and 1334 cm^{-1} bands increases due to redox additives and become maximum for redox additive-based GPE that confirms chemical interaction between the redox additives and the host polymer. The above observations signify that the IL and redox additives interact with the P(VdF-HFP) polymer matrix.

4. Thermogravimetric Analysis (TGA):

Thermogravimetric Analysis (TGA) is a thermal analysis technique used to study changes in the mass of a material as a function of temperature. It involves subjecting a sample to a controlled temperature increase while measuring its weight change over time. TGA provides valuable information about a material's thermal stability, decomposition kinetics, moisture content, and composition. It is widely used in various fields including materials science, chemistry, polymer science, pharmaceuticals, and environmental science for characterizing the thermal behaviour and properties of materials.

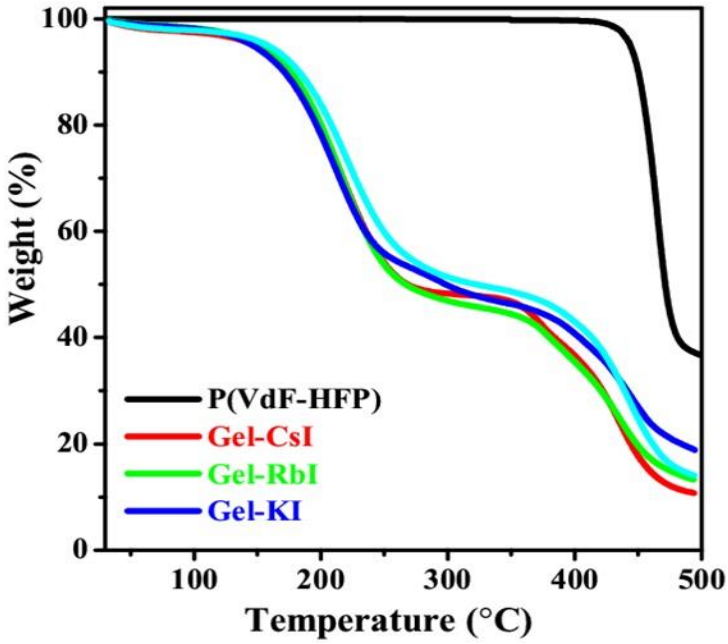


Fig 5.3 TGA thermograms of P(VdF-HFP) and different GPEs in the temperature range of 30−600 °C.

This image is a Thermogravimetric Analysis (TGA) thermogram, comparing the thermal stability and decomposition profiles of poly(vinylidene fluoride-co-hexafluoropropylene) P(VdF-HFP) and its gel polymer electrolytes (GPEs) containing different iodide salts: cesium iodide (CsI), rubidium iodide (RbI), and potassium iodide (KI).

The y-axis shows the percentage of the initial sample weight remaining as a function of temperature. It ranges from 0% to 100%. X-Axis (Temperature) indicates the temperature in degrees Celsius (°C), ranging from 0°C to 500°C.

P(VdF-HFP) represents the pure polymer matrix P(VdF-HFP). This curve shows the decomposition profile of the pure polymer, with a significant weight loss occurring at higher temperatures (around 470°C). Gel-CsI shows the thermal decomposition of the GPE containing CsI. This curve indicates an earlier onset of weight loss compared to the pure polymer, suggesting that the addition of CsI affects the thermal stability. Gel-RbI represents the GPE with RbI. This curve is similar to the CsI curve, showing an earlier decomposition onset compared to the pure polymer, but slightly later than

the CsI-containing GPE. Gel-KI for the GPE containing KI, the thermal decomposition onset is similar to that of the other GPEs, indicating that the incorporation of KI also affects the thermal stability.

The pure P(VdF-HFP) polymer shows the highest thermal stability with significant weight loss beginning around 470°C. The GPEs with different salts (CsI, RbI, KI) exhibit lower thermal stability, with decomposition starting at lower temperatures. All GPEs show a two-step decomposition process. The first weight loss step occurs between 200°C and 400°C, which can be attributed to the decomposition of the polymer-salt complex or the evaporation of any residual solvent/plasticizer in the GPE. The second step, from 400°C onwards, corresponds to the decomposition of the polymer backbone.

CsI shows the earliest onset of decomposition, indicating the least thermal stability among the GPEs tested. RbI slightly more thermally stable than the CsI-containing GPE but less stable than the KI-containing GPE. KI exhibits the highest thermal stability among the GPEs, though still less than the pure polymer.

This TGA thermogram is crucial for understanding the thermal decomposition behavior and stability of these materials, which is essential for their application in areas like solid-state batteries and other electrochemical devices where thermal stability is a key factor.

5. Differential Scanning Calorimetry (DSC)

Differential Scanning Calorimetry (DSC) is a thermal analysis technique used to investigate the heat flow associated with phase transitions and chemical reactions in materials as a function of temperature. In DSC, a sample and a reference material are subjected to identical heating or cooling profiles, and the heat flow difference between the sample and the reference is measured. This technique provides valuable information about the thermal properties of materials, including melting and crystallization temperatures, enthalpies of phase transitions, glass transition temperatures, and reaction kinetics. DSC is widely used in various fields, including materials science, chemistry, pharmaceuticals, polymers, and food science, for research, quality control, and product development purposes.

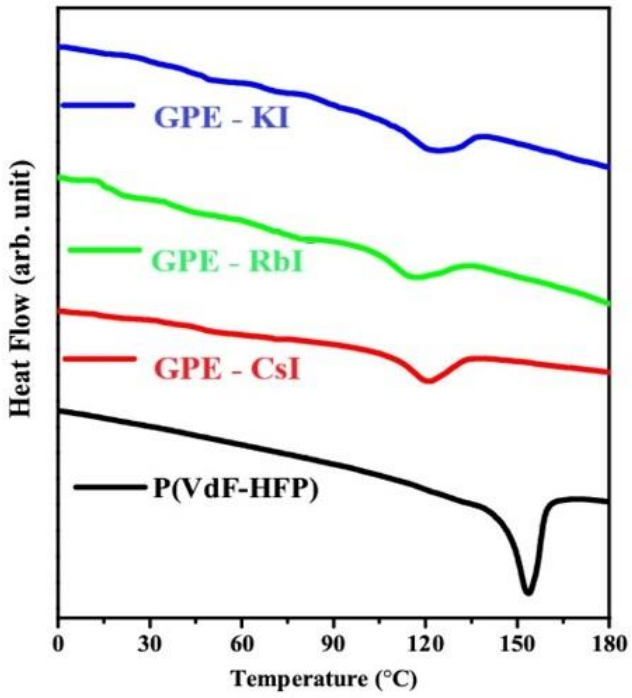


Fig.5.4 DSC Traces of P(VDF-HFP) and different GPEs

This image is a Differential Scanning Calorimetry (DSC) thermogram that compares the thermal properties of different gel polymer electrolytes (GPEs) containing potassium iodide (KI), rubidium iodide (RbI), and cesium iodide (CsI) with the polymer matrix poly(vinylidene fluoride-co-hexafluoropropylene) P(VdF-HFP).

The heat flow is plotted on the y-axis, indicating the amount of heat absorbed or released by the sample as a function of temperature. It's given in arbitrary units (arb. unit). X-Axis (Temperature) shows the temperature in degrees Celsius (°C), ranging from approximately 0°C to 180°C.

P(VdF-HFP) represents the pure polymer matrix P(VdF-HFP). The endothermic peak around 150°C indicates a phase transition, likely the melting point of the polymer. GPE – KI shows the thermal behavior of the gel polymer electrolyte containing KI. This curve seems relatively smooth with minor thermal events compared to the pure polymer. GPE – RbI represents the GPE with RbI. Similar to the KI curve, it shows minor deviations indicating the interactions between the polymer and the salt. GPE – CsI for the GPE containing CsI, this curve also follows a similar pattern, indicating modifications in thermal properties due to the inclusion of CsI.

The addition of different salts (KI, RbI, CsI) affects the thermal behavior of the base polymer. The absence of sharp endothermic peaks in the GPE curves suggests changes in crystallinity or phase transitions due to the incorporation of the salts. All GPE samples show thermal events at different temperatures, which indicate how each salt influences the polymer's thermal stability and phase transitions.

This DSC thermogram is useful for understanding how different salts impact the thermal properties of the polymer matrix, which is crucial for applications such as solid-state batteries, where thermal stability and phase behaviour are important for performance and safety.

Electrical Characterization:

Electrical characterization involves assessing the electrical properties and behaviour of materials, components, devices, or systems. It encompasses various techniques aimed at quantifying parameters like conductivity, resistivity, capacitance, impedance, and electrical response under different conditions. This process provides valuable insights into the electrical performance, reliability, and functionality of the subject being studied. Common techniques include current-voltage measurements, impedance spectroscopy, Hall effect measurements, dielectric spectroscopy, sheet resistance measurements, breakdown voltage measurements, and capacitance-voltage measurements. Electrical characterization is crucial in fields such as semiconductor manufacturing, telecommunications, energy storage, and consumer electronics for optimizing and ensuring the quality of electronic materials and devices.

i. AC Conductivity:

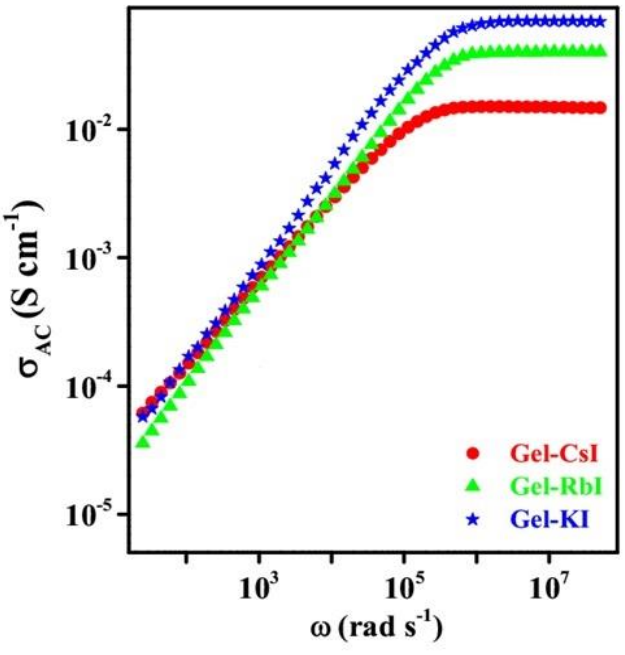


Fig 5.5 AC conductivity spectra for different GPEs at room temperature.

This graph displays the AC conductivity spectra for different gel polymer electrolytes (GPEs) at room temperature. The x-axis represents the angular frequency (ω) in radians per second (rad s^{-1}), and the y-axis represents the AC conductivity (σ AC) in siemens per centimetre (S cm^{-1}).

All three GPEs show an increase in AC conductivity with increasing frequency. At lower frequencies (around 10^3 rad s^{-1}), the conductivities are relatively similar, starting around 10^{-5} S cm^{-1}. As the frequency increases, the differences in conductivity among the GPEs become more pronounced.

Gel-KI exhibits the highest AC conductivity across all frequencies. At the highest frequencies (~10^7 rad s^{-1}), it reaches around 10^{-2} S cm^{-1}. Gel-RbI shows intermediate AC conductivity, higher than Gel-CsI but lower than Gel-KI. It reaches a maximum of about 10^{-3} S cm^{-1} at the highest frequencies. Gel-CsI demonstrates the lowest AC conductivity among the three GPEs. At the highest frequencies, it approaches around 10^{-3} S cm^{-1} but remains consistently lower than both Gel-RbI and Gel-KI.

The conductivity increases with frequency for all GPEs, which is typical behavior due to the increased mobility of charge carriers at higher frequencies. The different slopes and maximum values indicate variations in how each GPE facilitates ionic movement under alternating current conditions.

Gel-KI shows superior ionic conductivity, making it potentially the best candidate for applications requiring high conductivity, such as in high-performance batteries or supercapacitors. Gel-RbI also performs well but is slightly less conductive than Gel-KI, suggesting it could be used where moderately high conductivity is sufficient or where the specific properties of RbI are advantageous. Gel-CsI has the lowest conductivity, indicating it may be less suitable for applications where high ionic conductivity is critical but could be used in scenarios where lower conductivity is acceptable or where CsI offers other beneficial properties.

This AC conductivity spectra analysis highlights the differences in ionic conductivity for Gel-CsI, Gel-RbI, and Gel-KI at room temperature. Gel-KI demonstrates the highest conductivity, making it highly suitable for energy storage applications requiring efficient ion transport. Gel-RbI also performs well but with slightly lower conductivity, while Gel-CsI shows the least conductivity among the three, suggesting different potential application niches for each material based on their electrochemical performance.

Electrochemical Performance studies of solid-state EDL capacitors –

We have successfully fabricated solid-state EDL capacitors using gel polymer electrolytes, which exhibit excellent physicochemical properties such as high thermal stability, high ionic conductivity at room temperature, and a wide working potential window. These attributes directly enhance the specific capacitance and energy density of the devices. Additionally, we have thoroughly investigated the electrochemical performance of these EDL capacitors.

1. Cyclic Voltammetry

Cyclic voltammetry is a technique used in electrochemistry to study the behaviour of electrochemical systems, particularly redox reactions. In cyclic voltammetry, a voltage is applied to an electrochemical cell while measuring the resulting current. The voltage is typically varied linearly with time, first increasing in one direction and then reversing direction. This creates a cyclic pattern in the recorded current, hence the name.

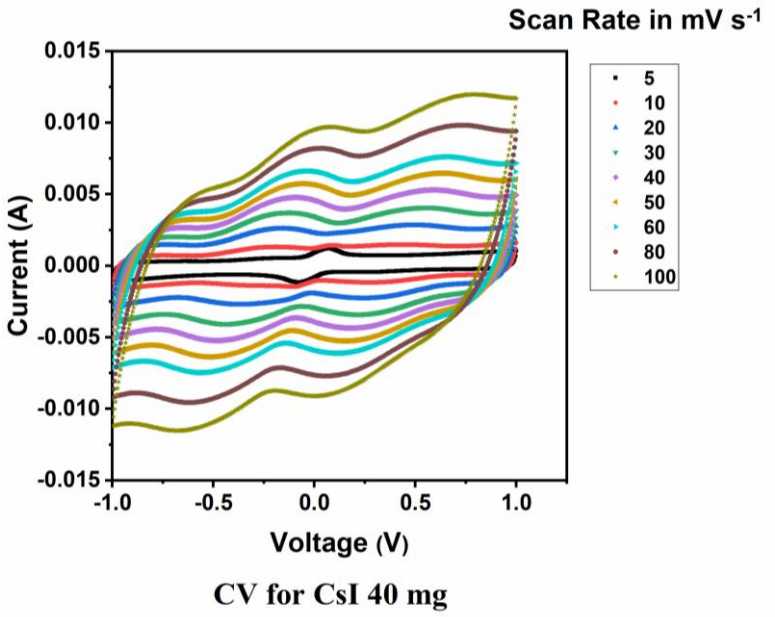


Fig 5.6 (a) Cyclic Voltammetry of different EDL Capacitor cell GPE – CsI

Fig.5.6 (a) graph is a cyclic voltammetry (CV) plot for a sample of CsI (cesium iodide) weighing 40 mg. The plot displays the current (in amperes, A) on the y-axis versus the voltage (in volts, V) on the x-axis for various scan rates, which are indicated in millivolts per second (mVs^{-1}). The CV curves are plotted for scan rates ranging from 5 mVs^{-1} to 100 mVs^{-1}

As the scan rate increases, the current response generally becomes larger. This is a typical behaviour in cyclic voltammetry, as faster scan rates result in higher current peaks due to the increased rate of the redox reactions occurring at the electrode surface. The shape of the CV curves provides information about the electrochemical reversibility of the redox processes. The quasi-rectangular shape suggests a capacitive behaviour, typical of materials with pseudocapacitive properties or double-layer capacitance. The symmetry of the curves around the y-axis indicates the presence of

both oxidation and reduction processes. The nearly symmetrical nature implies that the redox reactions are reversible. As the scan rate increases, the oxidation and reduction peaks shift slightly, which is a common observation. This shift can be attributed to the increased overpotential needed to drive the reaction at higher scan rates. The data from these curves can be analysed to determine various electrochemical parameters such as the diffusion coefficient, the rate of electron transfer, and the specific capacitance of the material.

Overall, this CV plot indicates the electrochemical behaviour of CsI under different scan rates, providing insight into its potential use in electrochemical applications such as batteries, capacitors, or sensors.

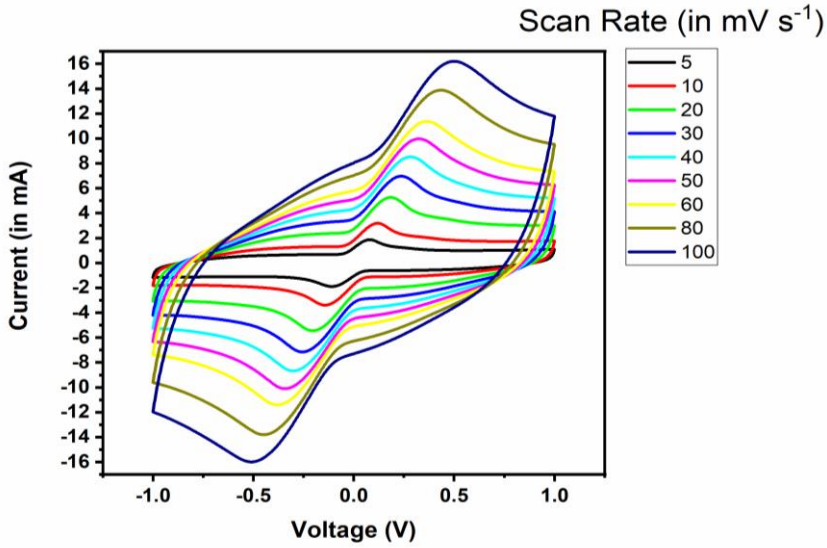


Fig 5.6 (b)Cyclic Voltammetry of different EDL Capacitor cell GPE – RbI

Fig 5.6 (b) graph is a cyclic voltammetry (CV) plot for a sample of RbI (rubidium iodide) weighing 40 mg. The plot displays the current (in amperes, A) on the y-axis versus the voltage (in volts, V) on the x-axis for various scan rates, which are indicated in millivolts per second (mV/s). The CV curves are plotted for scan rates ranging from 5 mVs^{-1} to 100 mVs^{-1}.

As the scan rate increases, the current response generally becomes larger. This is typical in cyclic voltammetry, as faster scan rates result in higher current peaks due to the increased rate of the redox reactions occurring at the electrode surface. The shape of the CV curves provides information about the electrochemical reversibility of the redox processes. The quasi-rectangular shape suggests a capacitive behaviour, which is typical of materials with pseudocapacitive properties or double-layer capacitance. The symmetry of the curves around the y-axis indicates the presence of both oxidation and reduction processes. The nearly symmetrical nature implies that the redox reactions are reversible. As the scan rate increases, the oxidation and reduction peaks shift slightly, which is a common observation. This shift can be attributed to the increased overpotential needed to drive the reaction at higher scan rates. The data from these curves can be analysed to determine various

electrochemical parameters such as the diffusion coefficient, the rate of electron transfer, and the specific capacitance of the material.

The CV plot indicates the electrochemical behaviour of RbI under different scan rates, providing insight into its potential use in electrochemical applications such as batteries, capacitors, or sensors. The material exhibits capacitive behaviour with reversible redox processes, suggesting it could be suitable for energy storage applications.

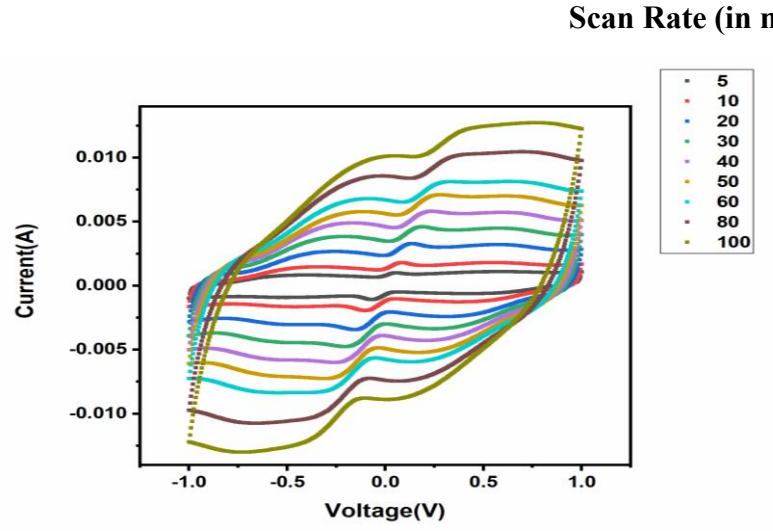


Fig 5.6 (c) Cyclic Voltammetry of different EDL Capacitor cell GPE - KI

Fig. 5.6 (c) graph is a cyclic voltammetry (CV) graph displays the electrochemical behaviour of a 40 mg sample of rubidium iodide (RbI) at various scan rates, ranging from 5 mV s^{-1} to 100 mV s^{-1}. Here is a detailed analysis:

As the scan rate increases, the peak currents also increase, which is typical in CV measurements. This relationship is often described by the Randles-Sevcik equation for a reversible redox system, where the peak current is proportional to the square root of the scan rate. The CV curves are symmetric around the origin, indicating a reversible redox process, likely due to the RbI in the sample. Peak separation and shape can provide insights into the kinetics of the redox process. Increased peak separation at higher scan rates may indicate kinetic limitations or quasi-reversibility. The observed peaks represent oxidation and reduction reactions of rubidium iodide. The forward scan (increasing voltage) typically shows oxidation, while the reverse scan (decreasing voltage) shows reduction. The current response's increase with scan rate suggests the electrochemical reactions are diffusion-controlled, and the analyte has fast electron transfer kinetics.

Such CV studies help in understanding the electrochemical properties of materials. For RbI, this can provide insights into its redox behaviour, reaction kinetics, and potential applications in various electrochemical devices.

By examining these CV curves, we can gain valuable information on the electrochemical characteristics and behaviour of rubidium iodide under varying conditions.

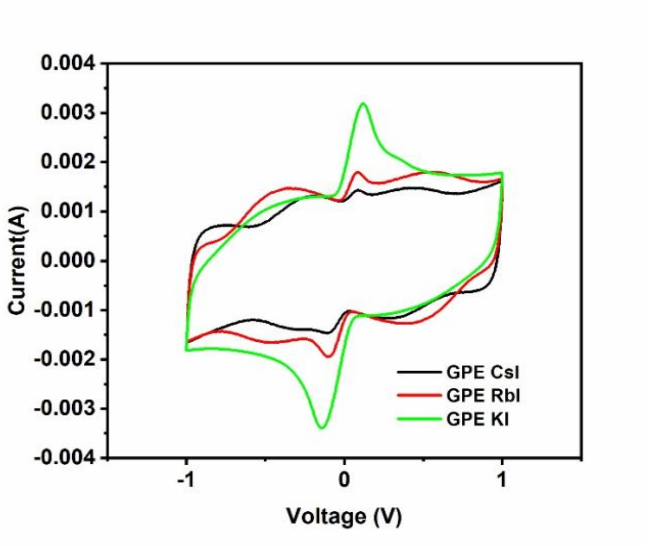


Fig 5.6 (d) Common CV at constant scan rate 10 mV s^{-1}

Fig 5.6 (d) This cyclic voltammetry (CV) data at a constant scan rate of 10 mV s^{-1} shows the electrochemical behaviour of three different gel polymers (GPE containing: GPE CsI, GPE RbI, GPE KI. All three GPEs exhibit peaks and troughs, indicative of redox processes occurring during the voltage sweep. The presence of these peaks suggests reversible electrochemical reactions where oxidation and reduction occur**.**

GPE KI Shows the highest current response among the three electrolytes, indicating either higher ionic conductivity or more active redox sites**.** It exhibits the highest peak currents among the three, especially in the positive potential region. The sharp and high peaks suggest that KI provides the best electrochemical performance in terms of current response. The higher currents can be attributed to better ion transport properties or higher ion mobility in the GPE KI.

GPE RbI exhibits moderate current responses, higher than CsI but lower than KI.

GPE CsI displays the lowest current response, suggesting lower ionic conductivity or fewer active redox sites.

The significantly higher current response of GPE KI suggests that potassium iodide imparts higher ionic conductivity to the gel polymer electrolyte. This makes GPE KI a superior candidate for applications requiring efficient ion transport, such as batteries or supercapacitors. The variation in peak heights and shapes among the three GPEs provides valuable information on their electrochemical performance. GPE KI demonstrates superior performance, while GPE RbI and GPE CsI show progressively lower performance. The differences in the CV curve shapes indicate variations in the nature and kinetics of the electrochemical reactions occurring within each GPE. GPE KI's sharp peaks suggest more rapid and perhaps more reversible reactions, while the more subdued peaks of GPE CsI indicate slower, less efficient reactions.

The shape and symmetry of the CV curves can provide insights into the electrochemical behaviour of each electrolyte. GPE KI's sharp and high peaks imply more efficient ion transport and possibly

faster redox kinetics. GPE RbI and GPE CsI have more moderate and symmetric peaks, indicating less efficient ion transport and slower redox kinetics compared to GPE KI**.**

This CV data is crucial for understanding the electrochemical properties of different electrolytes in gel polymer electrolytes. The higher current response and distinctive curve shape of GPE KI highlight its potential for applications requiring high ionic conductivity and efficient electrochemical performance. The analysis of such CV data aids in selecting appropriate electrolytes for specific applications in energy storage and conversion technologies.

Specific Capacitance of CV

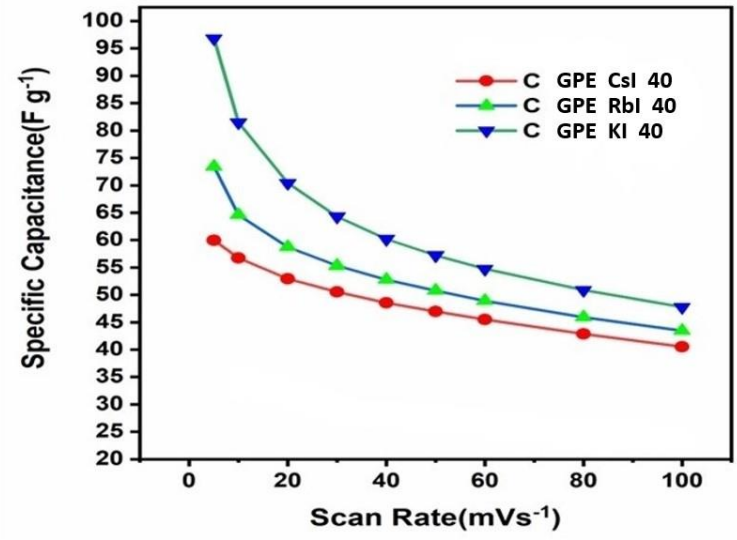


Fig 5.7 Specific Capacitance of CV

The provided graph shows the specific capacitance as a function of scan rate for three different gel polymer electrolytes (GPE) containing cesium iodide (CsI), rubidium iodide (RbI), and potassium iodide (KI). The specific capacitance is measured in farads per gram (F/g), and the scan rate ranges from 0 to 100 mV s^{-1}. For all three GPEs, the specific capacitance decreases as the scan rate increases. This is a typical behaviour in electrochemical capacitors where higher scan rates lead to reduced capacitance due to insufficient time for the electrolyte ions to penetrate into the deeper pores of the electrode material.

GPE KI Shows the highest specific capacitance across all scan rates, indicating superior electrochemical performance. The specific capacitance starts above 90 F/g at the lowest scan rate and gradually decreases to about 50 F/g at the highest scan rate. GPE RbI exhibits moderate specific capacitance values, higher than GPE CsI but lower than GPE KI. It starts around 75 F/g and decreases to about 45 F/g. GPE CsI displays the lowest specific capacitance among the three, starting around 65 F/g and dropping to about 40 F/g at the highest scan rate.

At low scan rates, the specific capacitance is higher for all GPEs, indicating efficient charge storage and good ion accessibility to the electrode material. GPE KI demonstrates the best performance, suggesting it has the most effective ionic transport and highest capacitance storage capability. As the scan rate increases, the specific capacitance decreases for all GPEs. However, GPE KI still maintains the highest specific capacitance compared to GPE RbI and GPE CsI, even at higher scan rates. This suggests that GPE KI has better rate capability, which is important for high-power applications. The superior performance of GPE KI across various scan rates indicates its higher ionic conductivity and better electrochemical stability. This makes it a promising candidate for use in supercapacitors and other energy storage devices where high capacitance and good rate performance are crucial.

The specific capacitance data clearly show that GPE KI outperforms GPE RbI and GPE CsI across all scan rates. The high specific capacitance and better rate capability of GPE KI make it a highly effective electrolyte for applications requiring efficient energy storage and rapid charge-discharge cycles. This data is valuable for designing and optimizing gel polymer electrolytes for supercapacitors and other electrochemical energy storage systems.

2. Electrochemical Impedance Spectroscopy (EIS)

Electrochemical Impedance Spectroscopy (EIS) is a powerful and versatile technique used to study the electrochemical properties of materials and interfaces. I t involves applying a small AC voltage to an electrochemical cell and measuring the resulting current to analyse the impedance of the system over a range of frequencies. EIS is widely used in various fields including battery research, corrosion studies, fuel cells and biosensors.

The Nyquist plots for the fabricated electrochemical double-layer capacitors are taken at room temperature in the frequency range from 10 MHz to 1 MHz with a 30 mV AC signal. The impedance behavior of an ideal electrochemical capacitor is typically parallel to the imaginary Z axis, indicating a purely capacitive response. However, you observed a steep rising behavior at low frequencies and a semicircular arc at high frequencies.

By analyzing the Nyquist plots, you can extract information about the capacitive performance, bulk resistance, and charge transfer resistance of the electrochemical double-layer capacitors. The shape and characteristics of the plots can provide insights into the overall impedance behavior of the cells and help optimize their design for specific applications.

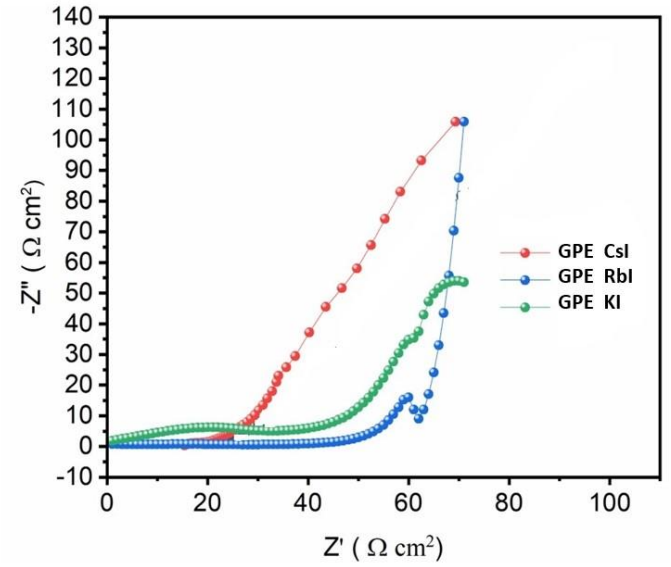


Fig 5.8 Common Nyquist plot

The provided graph is a Nyquist plot displaying the impedance spectra for three different samples: GPE CsI 40, GPE RbI 40, and GPE KI 40.

The graph provided is a Nyquist plot, which is commonly used in electrochemical impedance spectroscopy (EIS) to represent the impedance of a system. The plot shows the imaginary part of the impedance (Z'') versus the real part of the impedance (Z') for three different gel polymer electrolytes (GPE): GPE-CsI, GPE-RbI, and GPE-KI.

GPE-CsI Shows a higher real part of impedance (Z') with a steep rise in the imaginary part (Z''). The curve starts around 10 cm^2 for (Z') and reaches approximately 100 cm^2 the highest point. This indicates higher resistance in the system compared to the other GPEs.

GPE-RbI Shows a lower real part of impedance compared to GPE-CsI. The curve starts around 5 cm^2 for (Z') and extends up to approximately 80 cm^2 at the highest point. Indicates lower resistance compared to GPE-CsI but higher than GPE-KI.

GPE-KI exhibits the lowest real part of impedance among the three samples. The curve starts around 0 cm^2 for (Z') and extends up to around 70 cm^2 at the highest point. This suggests that GPE-KI has the lowest resistance and possibly the best ionic conductivity among the three GPEs.

The Nyquist plot typically consists of a semicircle at high frequencies followed by a straight line at low frequencies. Here, the high-frequency semicircle part is evident, which is related to the charge transfer resistance and the double-layer capacitance.

GPE-CsI shows the largest semicircle, indicating the highest charge transfer resistance. GPE-RbI and GPE-KI have smaller semicircles, indicating lower charge transfer resistance with GPE-KI being the lowest. The intercept of the curves on the real axis (Z') gives an indication of the bulk resistance of the electrolyte.

- GPE-KI appears to have the lowest resistance and the best electrochemical performance among the three GPEs, which is consistent with its higher AC conductivity observed in the previous graph.
- GPE-CsI shows the highest resistance, indicating lower ionic conductivity compared to the other two GPEs.

These characteristics are crucial for selecting appropriate gel polymer electrolytes for applications such as batteries, supercapacitors, and other electrochemical devices where ionic conductivity and resistance play key roles in performance.

3. Electrochemical Potential Stability Window (EPSW)

The electrochemical potential stability window, also known simply as the stability window or electrochemical stability window, refers to the range of electrochemical potentials over which a material remains stable when subjected to a specific environment, typically an electrolyte solution. This concept is particularly relevant in fields such as electrochemistry, battery technology, corrosion science, and materials science.

In practical terms, the stability window defines the maximum and minimum potentials at which a material can operate without undergoing undesirable chemical reactions, such as oxidation, reduction, or dissolution. For example, in the context of battery technology, the stability window of an electrolyte determines the maximum voltage that a battery can reach without causing unwanted side reactions, such as electrolyte decomposition or electrode degradation.

Understanding and controlling the stability window is crucial for designing and optimizing electrochemical devices, such as batteries, fuel cells, sensors, and corrosion-resistant materials. It involves a combination of experimental measurements, theoretical modelling, and material selection to ensure that the operating conditions remain within the safe range for the intended application.

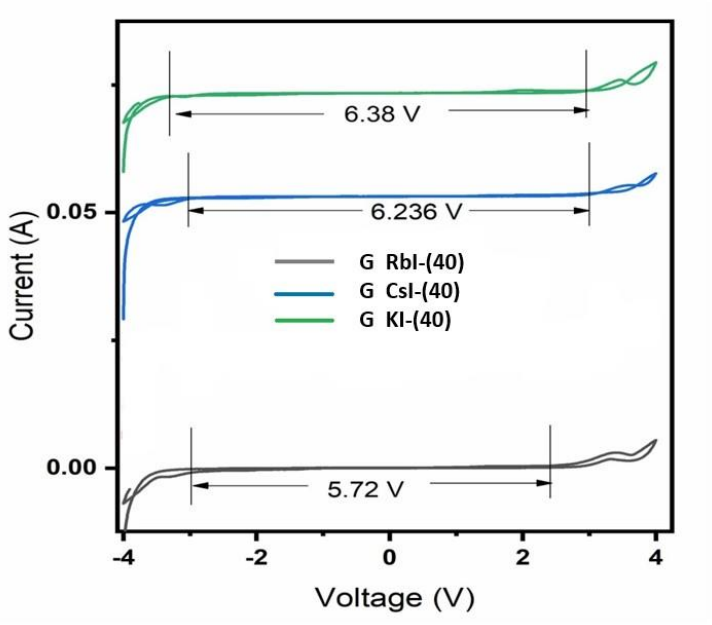


Fig 5.9 Electrochemical Stability Potential Window

The provided graph shows the electrochemical stability potential window (ESPW) for three different gel polymer electrolytes (GPE) doped with various iodide salts: rubidium iodide (RbI), cesium iodide (CsI), and potassium iodide (KI). The current (A) is plotted against the voltage (V) for each GPE, and the stability windows are indicated by the potential ranges within which the electrolytes remain stable without significant current increase, indicating decomposition.

GPE KI exhibits the widest ESPW, with a range of approximately 6.38 V. This indicates that GPE KI can withstand higher voltages before decomposing, suggesting excellent electrochemical stability. GPE CsI shows a slightly narrower ESPW compared to GPE KI, with a range of around 6.236 V. This still represents good electrochemical stability, though slightly less than GPE KI. GPE RbI displays the narrowest ESPW, with a range of about 5.72 V. This suggests that GPE RbI has the lowest electrochemical stability among the three GPEs.

The ESPW is a crucial parameter for determining the suitability of electrolytes in high-voltage applications. A wider ESPW means the electrolyte can operate safely at higher voltages without undergoing decomposition. GPE KI, with the widest ESPW, is the most stable and therefore the best candidate for high-voltage applications. It can tolerate higher voltages, which is advantageous for increasing the energy density of devices such as batteries and supercapacitors.

The performance of GPE KI superior electrochemical stability (6.38 V) suggests it has a robust ionic liquid framework that resists breakdown under high voltage, making it highly suitable for advanced energy storage applications. While GPE CsI with good stability (6.236 V), it is also a viable candidate for many applications, though slightly less effective than GPE KI and GPE RbI is the least stable (5.72 V), it is less suitable for high-voltage applications but might still be useful where lower voltage operations are sufficient or preferred.

The wide ESPWs of GPE KI and GPE CsI highlight their potential use in next-generation electrochemical devices where high voltage operation is desired. These materials can contribute to the development of more efficient and longer-lasting energy storage solutions, aligning with the growing demand for high-performance batteries and supercapacitors.

The electrochemical stability potential window analysis demonstrates that GPEs doped with potassium iodide (KI) and cesium iodide (CsI) show superior stability compared to rubidium iodide (RbI). GPE KI, with the broadest ESPW, is particularly promising for high-voltage applications, offering excellent electrochemical stability and enhancing the performance and safety of energy storage devices.

4. Galvanostatic Charge Discharge (GCD)

Galvanostatic charge-discharge (GCD) is a technique commonly used in electrochemistry and battery research to characterize the performance of batteries and other electrochemical systems. In GCD, the battery is charged or discharged at a constant current rate, known as the galvanostatic current. This allows researchers to study various electrochemical properties of the battery, such as its capacity, energy efficiency, charge and discharge rates, and voltage profiles.

During the charge process, a constant current is applied to the battery, causing it to accumulate charge and store energy. As a result, the battery voltage increases over time. Once the battery reaches its maximum voltage or a predetermined endpoint, the charging process is stopped.

During the discharge process, the battery is connected to an external load, and the stored energy is released as electric current flows out of the battery. The discharge current is also held constant throughout this process. As the battery discharges, its voltage gradually decreases until it reaches its minimum voltage or another predetermined endpoint, at which point the discharge process is halted.

By analysing the voltage and current profiles during both the charge and discharge processes, researchers can extract valuable information about the battery's electrochemical behaviour, including its capacity, efficiency, and rate capabilities. This information is essential for optimizing battery performance and designing new battery technologies for various applications.

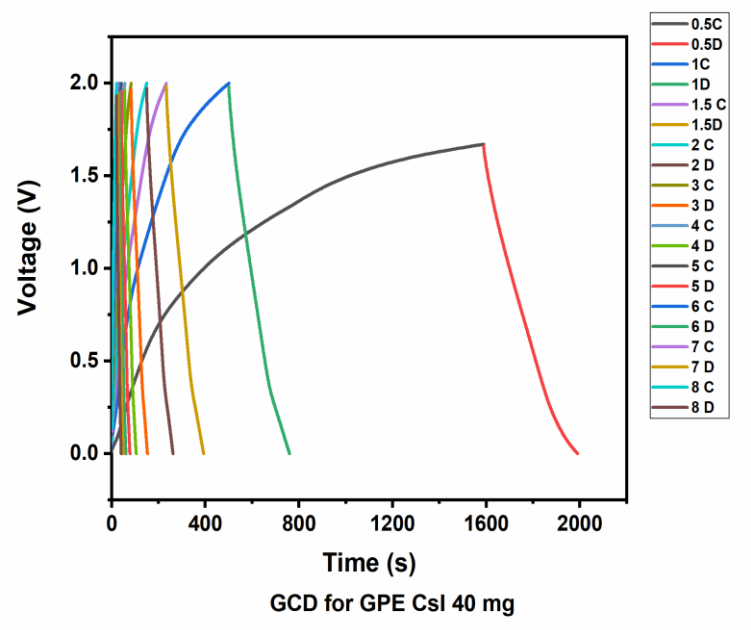


Fig 5.10(a) GCD for GPE CsI 40 mg

The provided graph displays Galvanostatic Charge-Discharge (GCD) curves for the sample GPE CsI 40 mg at various current densities or C-rates (0.5C, 0.5D, 1C, etc.). The curves generally show a typical charging and discharging behaviour. For lower current densities (e.g., 0.5C, 0.5D), the curves show a longer discharge time, which is expected as the lower current densities allow the device to

discharge more slowly. For higher current densities (e.g., 7C, 8C), the curves indicate a quicker discharge, demonstrating that the device discharges more rapidly under higher current loads. The charge and discharge processes are evident from the slopes of the curves. At higher current densities, the voltage drops faster, which may indicate higher internal resistance or faster depletion of the stored charge. The longest discharge time appears to be for 1D or 1.5D with a very extended time span up to around 2000 seconds. The shortest discharge times are observed at higher C-rates, such as 7C and 8C, where the discharge completes in a much shorter timeframe. The area under each curve is indicative of the total energy delivered by the system. A larger area under the curve at lower current densities suggests better energy storage performance under these conditions.

This graph effectively illustrates the performance characteristics of the GPE CsI 40 mg sample under various charge-discharge conditions, highlighting how different current densities impact the discharge times and overall energy delivery.

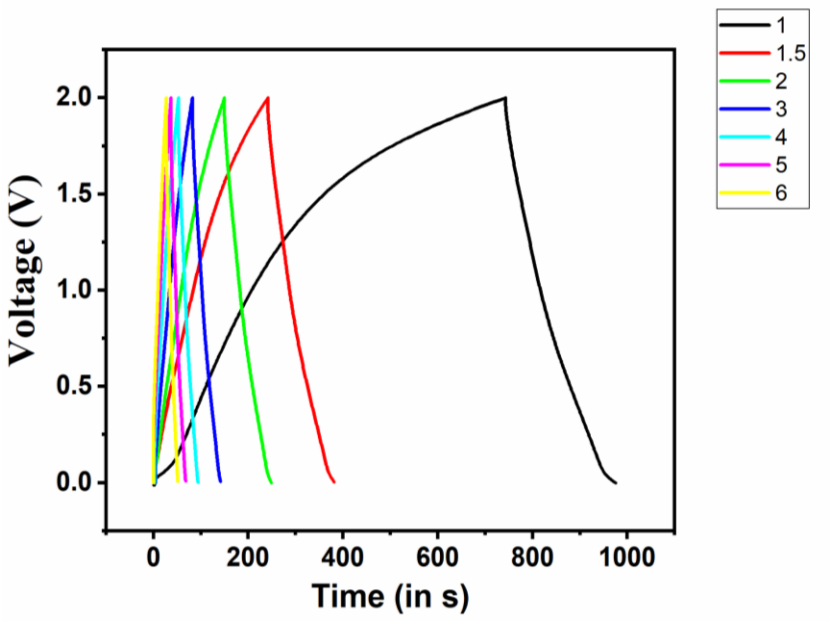


Fig 5.10(b) GCD for GPE KI 40 mg

The provided graph depicts the Galvanostatic Charge-Discharge (GCD) curves for a sample labelled "KI 40 mg" at various current densities or C-rates (1, 1.5, 2, 3, 4, 5, and 6). Here are the key observations and interpretations:

Lower C-rates (1, 1.5, 2) show longer discharge times, indicating that the sample discharges more slowly under lower current densities. Higher C-rates (4, 5, 6) show shorter discharge times, indicating rapid discharge under higher current densities. For higher current densities, the voltage drops rapidly, indicating higher internal resistance or quicker depletion of stored charge. The curves exhibit a characteristic charging plateau followed by a discharge slope.The longest discharge time is observed for the C-rate labeled "1," reaching up to around 1000 seconds. The shortest discharge

times are seen at higher C-rates, particularly "6," where discharge completes in less than 200 seconds. The area under each curve represents the total energy delivered by the sample. Larger areas under the curves for lower C-rates suggest better energy storage performance under these conditions.

Similar to the CsI 40 mg sample, the KI 40 mg sample shows typical charge-discharge behaviour where lower current densities result in longer discharge times. The curves for the KI 40 mg sample are relatively closer together in terms of discharge time span compared to the CsI 40 mg sample, indicating potentially different electrochemical properties and performance characteristics.

Overall, this graph illustrates the performance of the KI 40 mg sample under different charge-discharge conditions, showing how the sample's energy delivery varies with current density. Lower current densities allow for extended discharge times, while higher current densities lead to rapid discharge, which is crucial for applications requiring quick energy release.

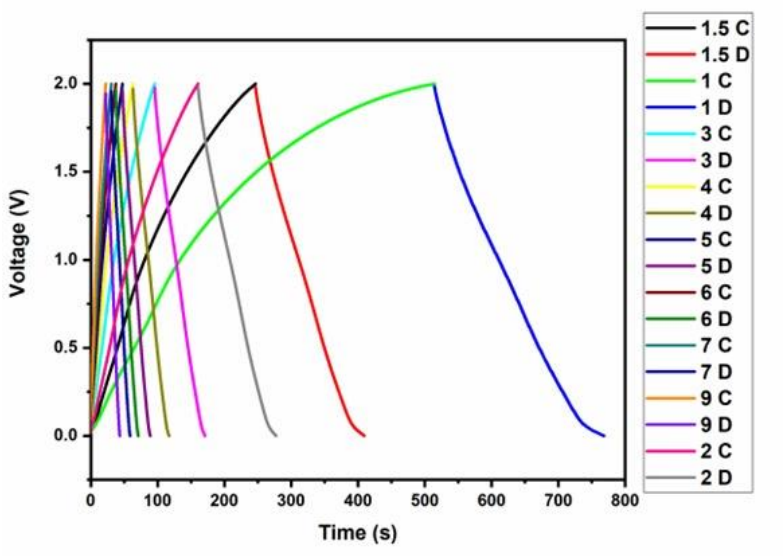


Fig 5.10(c) GCD for RbI 40 mg

This graph depicts the galvanostatic charge-discharge (GCD) curves for a sample with 40 mg of RbI (Rubidium Iodide) at various current densities, represented as C-rates (C) and D-rates (D). The x-axis represents the time in seconds, while the y-axis represents the voltage in volts (V). Here's a detailed analysis of the graph:

The initial voltage for all the curves starts from around 0 V.

The maximum voltage reaches up to about 2.0 V for some curves.

C-rates (charge rates) and D-rates (discharge rates) are used to describe the charging and discharging speeds relative to the battery capacity. The different curves represent various C-rates and D-rates as indicated in the legend.

The curves labelled with D-rates (discharge) generally show a rapid increase in voltage followed by a relatively quick drop back to 0 V, indicating faster discharge cycles. The curves labelled with C-

rates (charge) show a slower, more gradual increase and a sustained voltage before eventually dropping, indicating longer charge cycles.

Higher C-rates (e.g., 9 C) indicate a faster charging process but typically result in shorter times until the voltage drops back to 0 V. Lower C-rates (e.g., 1 C) demonstrate a more prolonged charging time, indicating slower but potentially more stable charging processes. The longest duration for maintaining voltage is observed for the 2 C charge rate, which sustains voltage up to about 700 seconds.

This type of analysis is crucial for understanding the performance of battery materials in energy storage applications. It helps in identifying optimal charging and discharging rates that maximize the efficiency and lifespan of the battery.

In summary, this GCD graph is an essential tool for evaluating the electrochemical performance of RbI in energy storage, helping researchers and engineers determine the most effective charge-discharge rates for practical applications.

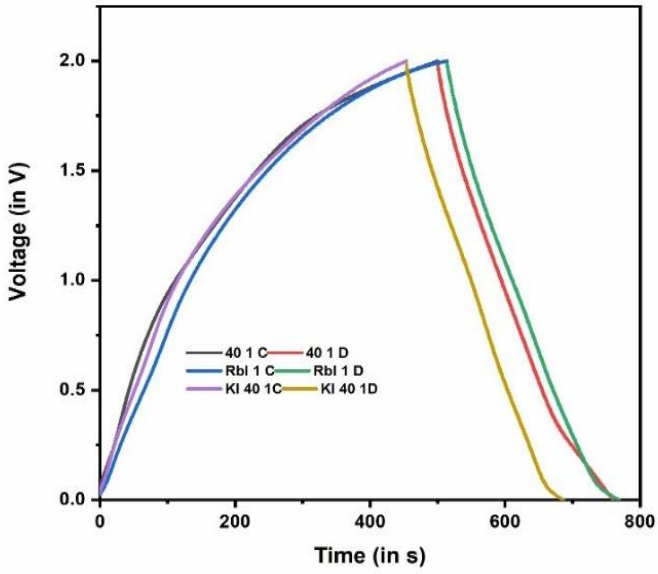


Fig 5.10(d) Common GCD

This graph shows the galvanostatic charge-discharge (GCD) curves comparing different materials and conditions. The x-axis represents time in seconds (s), and the y-axis represents voltage in volts (V). The curves represent the charge (C) and discharge (D) profiles for different materials at a rate of 1 C.

All the charge curves show a similar pattern of gradual increase in voltage, reaching approximately 2.0 V around 400 seconds. 40 mg sample and RbI closely overlap, indicating similar charge behavior. KI) also follows a similar trend but might show slight variations, suggesting some differences in charge efficiency or capacity.

The discharge curves all initially maintain the high voltage reached during charging before sharply decreasing back to 0 V. 40 mg sample and RbI curves are quite similar, indicating comparable

discharge behaviours. KI shows a slightly different discharge pattern, with a potentially faster voltage drop, suggesting differences in discharge characteristics between KI and the other materials. All materials show efficient charge retention up to 2.0 V, indicating good capacity for energy storage. The similar charging behaviour suggests that both RbI and KI have comparable charge efficiency when used in similar quantities. The red and green curves indicate that RbI and the 40 mg sample have similar discharge efficiencies and rates. The faster drop in the yellow curve (KI) could imply that KI might have a quicker discharge rate or lower retention, which might affect its performance in prolonged usage.

This GCD graph effectively compares the charging and discharging characteristics of RbI and KI, along with a general 40 mg sample. The data suggest that RbI and the 40 mg sample exhibit very similar electrochemical behaviours, while KI shows some differences, particularly in its discharge profile. This information is valuable for selecting appropriate materials for specific applications in energy storage devices, considering both charge retention and discharge rates.

Specific Capacitance from GCD

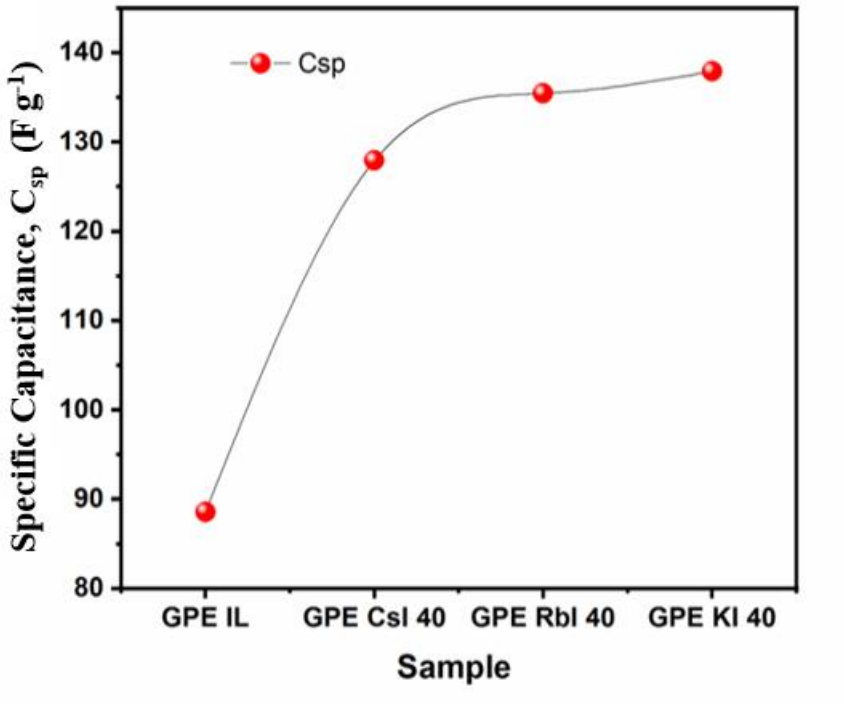


Fig 5.11 Specific Capacitance of GCD

The graph shows the specific capacitance (C_{sp}) of various gel polymer electrolytes (GPEs) obtained from galvanostatic charge-discharge (GCD) measurements. The samples include GPE IL, GPE CsI 40, GPE RbI 40, and GPE KI 40. Here's a detailed analysis of the data presented in the graph:

The base GPE IL has the lowest specific capacitance, indicating the least efficient charge storage. Doping the GPE with CsI (40) results in a substantial increase in specific capacitance, suggesting

improved ionic conductivity and better electrode-electrolyte interaction. Further improvement is observed with RbI (40) doping, which increases the specific capacitance to a higher level than CsI. KI (40) doping results in the highest specific capacitance among the samples tested, indicating the most significant enhancement in electrochemical performance.

The overall Performance shows a clear improvement in specific capacitance with the introduction of different dopants, with the order of increasing specific capacitance being GPE IL < GPE CsI 40 < GPE RbI 40 < GPE KI 40. This suggests that doping with KI (40) provides the best enhancement in capacitive properties, followed closely by RbI (40) and then CsI (40).

The specific capacitance values obtained from the GCD measurements demonstrate that doping the GPE with CsI, RbI, and KI significantly improves the charge storage capability of the material. GPE KI 40 exhibits the highest specific capacitance, indicating that KI is the most effective dopant among those tested in enhancing the electrochemical performance of the GPE. This improvement can be attributed to better ionic conductivity and enhanced interaction between the electrolyte and the electrodes.

5. Ragone Plot

A Ragone plot is a graphical representation commonly used in the field of energy storage to compare the energy density and power density of different energy storage systems, such as batteries, capacitors, and fuel cells

In a Ragone plot, the energy density of an energy storage system is typically plotted on the y-axis, while the power density is plotted on the x-axis. Energy density refers to the amount of energy that can be stored per unit volume or mass of the storage device, usually measured in watt-hours per litre (Wh/L) or watt-hours per kilogram (Wh/kg). Power density, on the other hand, refers to the rate at which the energy can be delivered from the storage device, usually measured in watts per litre (W/L) or watts per kilogram (W/kg).

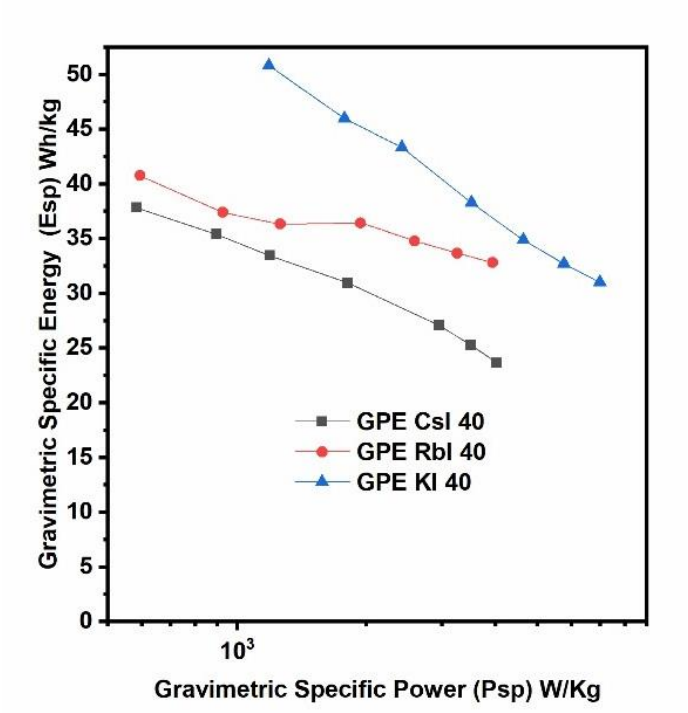


Fig 5.12 Ragone Plot

This plot is a Ragone plot, commonly used to compare the performance of energy storage devices. It shows the relationship between gravimetric specific energy (Esp, in Wh/kg) and gravimetric specific power (Psp, in W/kg). In this plot, three different gel polymer electrolytes (GPEs) with different salts (CsI, RbI, KI) are compared, each at a concentration of 40%.

GPE KI 40 exhibits the highest gravimetric specific energy across all levels of specific power, indicating that KI-based electrolytes provide the best energy storage performance in this comparison. GPE RbI 40 shows intermediate performance, with gravimetric specific energy values between those of GPE KI 40 and GPE CsI 40. GPE CsI 40 demonstrates the lowest gravimetric specific energy, indicating that CsI-based electrolytes are the least effective among the three tested for energy storage.

As specific power increases, the specific energy decreases for all three electrolytes, which is typical behaviour in energy storage devices due to the trade-off between energy and power density. This relationship highlights the balance that must be struck between energy capacity and power delivery rate in the design and selection of electrolytes for specific applications.

To calculate the power density (P) and energy density (E) from the given Ragone plot, we can use the data points for each electrolyte. The Ragone plot provides gravimetric specific energy (E_{sp}) in Wh/kg and gravimetric specific power (P_{sp}) in W/kg.

Here are the steps to convert specific energy and specific power into power density and energy density:

Power Density (P): Given directly on the x-axis in W/kg.

Energy Density (E): Given directly on the y-axis in Wh/kg.

To illustrate the calculation, let's take a few data points from the plot:

GPE KI 40

1. At P_{sp} = 1000 W/kg:
   - $E_{sp} \approx$ 45 Wh/kg
   - Power Density (P) = 1000 W/kg
   - Energy Density (E) = 45 Wh/kg

2. At P_{sp} = 2000 W/kg:
   - $E_{sp} \approx$ 40 Wh/kg
   - Power Density (P) = 2000 W/kg
   - Energy Density (E) = 40 Wh/kg

GPE RbI 40

1. At P_{sp} = 1000 W/kg:
   - $E_{sp} \approx$ 37 Wh/kg
   - Power Density (P) = 1000 W/kg
   - Energy Density (E) = 37 Wh/kg

2. At P_{sp} = 2000 W/kg:
   - $E_{sp} \approx$ 33 Wh/kg
   - Power Density (P) = 2000 W/kg
   - Energy Density (E) = 33 Wh/kg

GPE CsI 40

1. At P_{sp} = 1000 W/kg:
   - E_{sp} ≈ 35 Wh/kg
   - Power Density (P) = 1000 W/kg
   - Energy Density (E) = 35 Wh/kg

2. At P_{sp} = 2000 W/kg:
   - E_{sp} ≈ 30 Wh/kg
   - Power Density (P) = 2000 W/kg
   - Energy Density (E) = 30 Wh/kg

To generalize, the power density and energy density values are the same as the specific power and specific energy values given on the plot. This plot essentially provides the direct relationship between these two metrics for the different gel polymer electrolytes (GPEs) tested with different salts.

Summary Table

GPE Type	P_{sp} (W/kg)	E_{sp} (Wh/kg)
GPE KI 40	1000	45
GPE KI 40	2000	40
GPE RbI 40	1000	37
GPE RbI 40	2000	33
GPE CsI 40	1000	35
GPE CsI 40	2000	30

These calculations demonstrate the performance characteristics of each electrolyte, illustrating how power density and energy density change with different specific powers.

References

1. Gupta, H.; Shalu, S.; Balo, L.; Singh, V. K.; Chaurasia, S. K.; Singh, R. K. Effect of phosphonium based ionic liquid on structural, electrochemical and thermal behaviour of polymer poly (ethylene oxide) containing salt lithium bis (trifluoromethylsulfonyl) imide. RSC Adv. 2016, 6 (91), 87878−87887.
2. Pal, P.; Ghosh, A. Solid-state gel polymer electrolytes based on ionic liquids containing imidazolium cations and tetrafluoroborate anions for electrochemical double layer capacitors: Influence of cations size and viscosity of ionic liquids. J. Power Sources 2018, 406, 128−140.
3. Bhat, M. Y.; Yadav, N.; Hashmi, S. A. Gel Polymer Electrolyte Composition Incorporating Adiponitrile as a Solvent for High Performance Electrical Double-Layer Capacitor. ACS Appl. Energy Mater. 2020, 3 (11), 10642−10652.
4. Kolthoff, I.; Sarver, L. Properties of diphenylamine and diphenylbenzidine as oxidation-reduction indicators. J. Am. Chem. Soc. 1930, 52 (11), 4179−4191.
5. Akinwolemiwa, B.; Peng, C.; Chen, G. Z. Redox Electrolytes in Supercapacitors. J. Electrochem. Soc. 2015, 162 (5), A5054−A5059.
6. Senthilkumar, S.; Selvan, R. K.; Melo, J. Redox additive/active electrolytes: a novel approach to enhance the performance of supercapacitors. J. Mater. Chem. A 2013, 1 (40), 12386−12394.
7. Ganesan, S.; Muthuraaman, B.; Mathew, V.; Madhavan, J.; Maruthamuthu, P.; Austin Suthanthiraraj, S. Performance of a new polymer electrolyte incorporated with diphenylamine in nanocrystalline dye-sensitized solar cell. Sol. Energy Mater. Sol. Cells 2008, 92 (12), 1718−1722.
8. Ivanishchev, A. V.; Ivanishcheva, I. A. Ion Transport in Lithium Electrochemical Systems: Problems and Solutions. Russ. J. Electrochem. 2020, 56 (11), 907−928.
9. Ivanishchev, A. V.; Churikov, A. V.; Ushakov, A. V. Lithium transport processes in electrodes on the basis of Li3V2(PO4)3 by constant current chronopotentiometry, cyclic voltammetry and pulse chronoamperometry. Electrochim. Acta 2014, 122, 187−196.
10. Pandey, K.; Yadav, P.; Mukhopadhyay, I. Elucidating the effect of copper as a redox additive and dopant on the performance of a PANI based supercapacitor. Phys. Chem. Chem. Phys. 2015, 17 (2), 878−887.
11. Lim, C.-S.; Teoh, K. H.; Liew, C.-W.; Ramesh, S. Electric double layer capacitor based on activated carbon electrode and biodegradable composite polymer electrolyte. Ionics 2014, 20 (2), 251−258.

12. Roldán, S.; Barreda, D.; Granda, M.; Menéndez, R.; Santamaría, R.; Blanco, C. An approach to classification and capacitance expressions in electrochemical capacitors technology. Phys. Chem. Chem. Phys. 2015, 17 (2), 1084−1092.

13. Zhang, J.; Jiang, J.; Li, H.; Zhao, X. A high-performance asymmetric supercapacitor fabricated with graphene-based electrodes. Energy Environ. Sci. 2011, 4 (10), 4009−4015.

14. Ghamouss, F.; Brugere,` A.; Jacquemin, J. Physicochemical Investigation of Adiponitrile-Based Electrolytes for Electrical Double Layer Capacitor. J. Phys. Chem. C 2014, 118 (26), 14107−14123.

15. Pameté, E.; Köps, L.; Kreth, F. A.; Pohlmann, S.; Varzi, A.; Brousse, T.; Balducci, A.; Presser, V. The Many Deaths of Supercapacitors: Degradation, Aging, and Performance Fading. Adv. Energy Mater. 2023, 13 (29), 2301008.

16. Ivanishcheva, I. A.; Ivanishchev, A. V.; Chang, J. H.; Song, J.-H.; Lee, S.-H.; Kim, J.-J.; Kim, Y. J.; Nam, S.-C. Illustration of Capacity Fading Factors on the Example of La2(Li0.5Ni0.5)O4-Modified High Nickel Layered Oxide Material. Batteries Supercaps 2023, 6 (3), No. e202200466.

17. Yadav, N.; Singh, M. K.; Yadav, N.; Hashmi, S. A. High performance quasi-solid-state supercapacitors with peanut-shellderived porous carbon. J. Power Sources 2018, 402, 133−146.

18. Fan, L.-Q.; Zhong, J.; Wu, J.-H.; Lin, J.-M.; Huang, Y.-F. Improving the energy density of quasi-solid-state electric double-layer capacitors by introducing redox additives into gel polymer electrolytes. J. Mater. Chem. A 2014, 2 (24), 9011−9014.

CHAPTER 6:
CONCLUSION AND FUTURE SCOPE OF WORK

Conclusion and Future Scope of Work

Conclusion

The redox active gel polymer electrolytes (GPEs) were developed using a standard solution casting method for the creation of high-capacitance symmetrical carbon supercapacitors (SCs). These dual redox active GPEs were synthesized by incorporating P(VdF-HFP) as the host polymer, ADN as the plasticizer, BMIMTFSI as the ionic liquid, and Caesium Iodide (CsI), Rubidium Iodide (RbI), and Potassium Iodide (KI) as redox additives. This formulation of GPEs achieved the highest ionic conductivity and a broad electrochemical stability potential window of approximately 6.4 V at room temperature. Additionally, these GPEs demonstrated enhanced thermal stability, remaining stable up to around 200 °C. The addition of dual redox additives increased the amorphous phase of the polymer by enhancing the β-fraction in P(VDF-HFP). Nonlinear cyclic voltammetry (CV) curves confirmed the occurrence of reversible redox reactions during oxidation and reduction cycles. Symmetrical carbon SCs were fabricated utilizing these high-conductivity, electrochemically stable dual redox active GPEs. The galvanostatic charge-discharge (GCD) curves indicated that the charging and discharging times reached their peak values in the redox active-based SC, due to pseudocapacitive redox reactions at the interface between the electrode and electrolyte. This redox contribution significantly enhanced the specific capacitance and specific energy density of the SC cells. The ionic conductivity of electrolytes increases with the decrease of cation size ($KI^+ > RbI^+ > CsI^+$). Furthermore, the redox-based SC demonstrated excellent cycle stability, with an initial capacity fading of approximately 34% and a Coulombic efficiency of around 100% over 5000 cycles. Consequently, the redox-based SCs achieved high specific capacitance, energy density, and long-term cycle stability.

Scope for Future

In order to obtain high voltage and high energy density batteries for the current study, more dual ion battery research can be conducted. Furthermore, free volume measurement using Positron Annihilation Spectroscopy (PALS) can be performed to investigate further, opening the door to additional research on gel polymer-based electrolyte. The experimental method known as Positron Annihilation Spectroscopy (PAS) is used to examine the electronic structure and imperfections in materials. Gel polymer supercapacitors, often referred to as gel polymer electrolyte-based supercapacitors, have drawn a lot of interest lately because of their potential to overcome the drawbacks of traditional supercapacitors. The capacity of gel polymer supercapacitors to attain higher energy densities in comparison to conventional supercapacitors is one of their primary advantages. This is because the gel polymer electrolyte has special qualities that enable higher operating voltages and improved charge storage capacities. In order to further increase energy

density, research is still being done on creating new polymer materials and improving the electrode-electrolyte interface. Compared to liquid electrolytes used in traditional supercapacitors, gel polymer electrolytes are non-flammable and offer superior thermal stability. This increases the safety and dependability of gel polymer supercapacitors, especially in applications where safety is a major concern, like electric cars and portable electronics, which may be a use for the study discussed in this article. The polymer electrolyte's gel-like properties enable the creation of flexible, even wearable, supercapacitors. The studies described in this paper may have relevance in the development of sealable, portable electronics that are affordable. The polymer electrolyte's gel-like properties enable the creation of flexible, even wearable, supercapacitors. Scientists are trying to create scalable and reasonably priced manufacturing techniques for gel polymer supercapacitors. This includes investigating substitute materials, refining electrode designs, and enhancing fabrication methods. Gel polymer supercapacitors must be made affordable and scalable in order to be widely used in a variety of sectors. Gel polymer supercapacitors and batteries combined in hybrid energy storage systems provide the ability to deliver high power density and high energy density at the same time. While gel polymer supercapacitors have demonstrated encouraging results in laboratory settings, more research and development efforts are required to overcome challenges related to material optimization, manufacturing processes, and system integration before they can be widely commercialized. These hybrid systems can find applications in electric vehicles, renewable energy storage, and other areas where both high power and high energy are required. Nonetheless, the material sample's gel polymer supercapacitors' potential advantages—such as increased energy density, safety, and flexibility—make them a desirable subject for further research in energy storage technology.